Ife Journal of Technology, Vol. 18(2), 1-4, 2009

Full paper

BIODIESEL PRODUCTION BY TRANSMETHYLATION OF NIGERIAN PALM KERNEL OIL

A.S. Shote
Department of Mechanical Engineering
Obafemi Awolowo University, Ile-Ife, Osun State, Nigeria

E. Betiku
Biochemical Engineering Laboratory
Department of Chemical Engineering
Obafemi Awolowo University, Ile-Ife, Osun State, Nigeria
ebetiku@oauife.edu.ng

A.A. Asere
Department of Mechanical Engineering
Obafemi Awolowo University, Ile-Ife, Osun State, Nigeria

ABSTRACT

The need for this study arose from the recent energy crisis coupled with the huge potential that Nigeria has for the production of Palm Kernel Oil (PKO). Locally produced PKO was chemically modified (methanolysis) to produce PKO-based biodiesel. The reaction temperature and the catalyst loading were maintained at 60°C and 1.0% weight of oil, respectively. The methanol to oil molar ratio was kept at 6:1. The production of PKO-based biodiesel (at 60°C for 1.5 hours) by transmethylation process in the presence of NaOH as catalyst yielded crude products, Glycerol and biodiesel. Subsequently, PKO (parent oil), automotive gas oil (AGO) and PKO methyl esters transesterified were characterized to determine their properties and suitability as fuels in Compression Ignition Engine (CIE). Results of the transmethylated PKO showed that properties such as viscosity (3.359 cSt), specific gravity (0.8728), water content (nil) and flash point (100°C) conformed to standards (ASTM, BIS). Properties of the PKO biodiesel were comparable with properties of AGO. Emissions assessment showed that CO concentration was reduced by 30% when PKO biodiesel was used in CIE compared with AGO. Hence, PKO-based biodiesel has a promising prospect for partial or total replacement for petro-diesel in CIE.

Keywords: Palm Kernel Oil, transmethylation, alkali catalyst, emissions

1. INTRODUCTION

The ever increasing energy demand around the globe, the depletion of fossil fuels, the fluctuation of crude oil price in the international market as well as greater recognition of the unfavourable environmental consequences of fossil fuels have made renewable biofuels an attractive alternative to conventional petro-fuels. Biodiesel (fatty acid methyl esters; FAMEs and fatty acid ethyl esters; FAEEs) produced from vegetable oils, animal fats and waste oils can substitute petro-diesel. This is because of the properties of biodiesel; especially flash point, cetane number as well as volumetric heating value, which have been shown to be comparable to those of petro-diesel (Ma and Hanna, 1999; Lang et al, 2001; Usta, 2005; Jeong et al, 2006). Biodiesel has some marked advantages over petro-diesel which include non-toxicity, biodegradability CO_2 recycling over short period and environmentally-friendly, that is, it shows a decrease in the emission of CO_2, SO_x and unburned hydrocarbons during the combustion process (Graboski and McCormick, 1998; Antolin et al, 2002).

Previously reported feedstocks employed in the biodiesel production include vegetable oils - edible (soybean), non-edible (Jatropha), animal fats (tallow, lard), and waste oil (canola). Palm kernel oil (PKO) is one of the non edible oils that Nigeria has in abundance (Table 1). Palm fruits; *Elaeis guineensis* contain about 45% PKO which is rich in lauric acid, $C_{12:0}$ (48.3%), myristic, $C_{14:0}$ (15.6%) but also contains other fatty acids like palmitic acid $C_{16:0}$ (7.5%) and oleic acids, $C_{18:1}$ (Rossell, 1985; Goh, 1993; Omar et al, 1998). These fatty acid triglycerides give the fats a solid consistency at ambient temperature that melts below 30°C. World production of PKO was 3236 metric tons in 2003 among which Malaysia produced 1644 metric tons of PKO (MPOB, 2003). Extraction of PKO requires relatively high pressure and temperatures for separation from palm kernel as palm kernel is hard and compact, and has an intricate honeycombed pericarp (Hassan et al, Hassan 2000; Rahman et al, 2001; Zaidul et al, 2006). Separation of PKO from palm kernel using supercritical CO_2 afford development of clean separation process (Bharath et al, 1992) and may require high pressure (>30 MPa).

Table 1: Profile of some vegetable oils in Nigeria

Commodity	Quantity (tons)	% Share
Palm Oil	800,000	50
PKO	270,000	17
Others: peanuts, Cottonseed, Soybean	260,000	16
Imports	270,000	17
National Requirement	1,600,000	100

Source: David (2007)

Methods employed in biodiesel production are hydrotreatment, transesterification, esterification and oleaginous microorganisms. In the transesterification of different types of oils or fat, triglycerides react with an alcohol, generally methanol or ethanol, to produce esters and glycerol. The presence of a catalyst accelerates the conversion. Alkali (NaOH or KOH), acid (H_2SO_4) and enzyme (lipases) are the catalysts that have reported in transesterification. Alkali catalyst is preferred than acid catalyst in the industries. This is because alkali process is more efficient and less corrosive than the acid process. Although, enzyme catalyst has some advantages, however, it also has some disadvantages, among which are: lost of some initial activity due to volume of the oil molecule, number of support enzyme is not uniform and biocatalyst is more expensive that the natural enzyme.

This study investigated Palm Kernel Oil (PKO) as a possible feedstock in transesterification in biodiesel production for use in a diesel engine, to discover its physical and chemical properties and emission characteristics using a Compression Ignition Engine (CIE).

2. MATERIALS AND METHODS

2.1. Reagents and Materials

Chemicals used for the experiment include methanol (CH_3OH), Sodium Hydroxide (NaOH), and Calcium Chloride ($CaCl_2$). They are all of analytical grades. Automotive Gas Oil (AGO) was purchased from Total Service Station at Iyana Ife, Ife-Ibadan Express Way, Ibadan, Nigeria.

2.2. Equipment

The various items of major equipment used include: Magnetic Stirrer and the Hot plates, Water bath, Pensky Marten Closed Cup (PMCC) Tester, Canon Fenske Viscometers, Pour and Cloud Point Tester, Separating Funnel, Seta Lovibond Colour Comparator. Other essential equipment used include: Sensitive Weighing Balance, The Combustion Analyzer, Compression Ignition Engine, Measuring Cylinders, Beakers, Distillation Set Up (including Heating Mantle and Condenser), Oven, Timer, Pump, Pyrex Flasks (flat bottom and conical), Pet Bottles, Thermometers, Safety Wears (Overall, Hand Gloves), Funnel and Sieve.

2.3 Transmethylation Process of PKO-Based Biodiesel

2.3.1 Background to the production of PKO-based biodiesel

Transesterification is an equilibrium reaction in which excess alcohol is required to drive the reaction close to completion. The transesterification reaction (Fig. 2) requires 3-moles of alcohol per one mole of triglyceride to give 3-moles of fatty esters and 1-mloe of glycerol. It is consequential to use excess alcohol or remove one of the products from the reaction mixture to shift the reaction to the right as stated by Le Châtelier's Principle. The latter option is preferred for the reaction to proceed to completion. A reaction temperature near the boiling point of the alcohol (60°C for methanol) and a molar ratio of 6:1 of alcohol to vegetable oil are recommended (Freedman et al, 1984; Noureddini and Zhu, 1997). A catalyst concentration in the range of 0.5 – 1% (w/w) has been found to yield 94 – 99% conversion to vegetable oil esters (Feuge and Gros, 1949; Saka and Dadan, 2001). Additional catalyst will not affect the conversion but only leads to increase in cost because it will be washed away at the end of the reaction (Barnwal and Sharma, 2005).

2.3.2. Production of PKO-biodiesel

It should be noted that the composition of solid or liquid fuel is usually expressed by weight whereas the composition of a gaseous fuel is given by volume. Production trials were done at the Chemical Engineering Department, Obafemi Awolowo University, Ile-Ife, Nigeria. Empirically, 300ml of PKO was measured in a conical flask and it was preheated to 50°C on the Hot Plate with magnetic stirrer. Methanol (100ml) was also measured with the aid of a measuring cylinder and poured into a pet bottle. NaOH (2.8 g) was quickly added and agitated for dissolution of the catalyst. Table 2 showed the synopsis of the measurements taken. The resulting methoxide was turned into the preheated PKO on the Hot Plate.

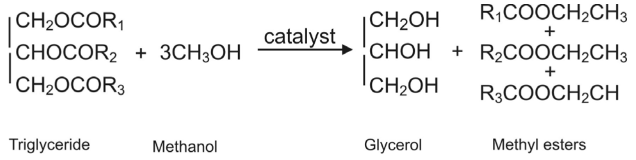

Fig. 2: General equation for transesterification of triglycerides

The Hot Plate temperature Probe was then put back into the oil with the aid of the probe holder, temperature preset to 60°C and lid was secured tightly. Phase separation was noticed, hence, stirring was introduced at 800 rpm, and the reaction was left for 90 min. At the end of the reaction time, the product was poured into a Separating Funnel separation under gravity. The glycerol was tapped off the bottom of the Separating Funnel. The crude biodiesel left in the Separating Funnel was washed with distilled water (preheated to 50°C) to remove the residual catalyst. Settling of the water was performed within 3 min. The water was later tapped off the bottom of the Separating Funnel. This process was repeated until the water was clear. Drying was done with $CaCl_2$ (fused gran) to remove the water content.

Table 2: Transmethylation process parameters

S/N	Production variables	Values for production runs
1	PKO quantity (ml)	300
2	Methanol quantity (ml)	100
3	NaOH catalyst (g)	2.8
4	Reaction temperature (°C)	60 (140°F)

2.4. Characterization of PKO-Based Biodiesel; AGO and PKO

Essentially, the following tests were performed to ascertain the compatibility of PKO-based biodiesel with Internal Combustion Engine (ICE). Specific gravity was measured with the aid of the specific gravity bottle and viscosity was determined with the aid of Canon Fensky Viscometer. Colour was determined with the aid of Seta Lovibond Colour Comparator. Pensky Martens Apparatus was used as recommended by ASTM D-93 to determine the flash point. Pour/Cloud point cabinet was used according to ASTM D-97 to obtain the temperature cloud haze and eventually when it seizes to flow (pour point). Crackle test was also carried out to determine whether there was water content in the oil. Water is not desirable since it will affect its combustion in the CIE and may also cause hydrolytic degradation of the PKO biodiesel most especially when stored over a long period of time.

2.5. Assessment of Emissions

In order to test the suitability of the PKO biodiesel produced in CI engines as well as compare the emissions with that of AGO, 100% AGO and 100% PKO-biodiesel were burnt in a CIE in succession and emissions such CO, NO_2 and NO_x were measured with the aid of the Gas Analyzer.

3. RESULTS AND DISCUSSION

3.1 Prospects of Nigerian PKO and Production of PKO-Based Biodiesel

PKO is in abundance since it took a share of 17% from the significantly available vegetable oils. This percentage can also be increased if resources are channel towards increasing the agricultural output. Transmethylation method used for the PKO Biodiesel production gave excellent results. The glycerol was separated under gravity with the aid of the Separating funnel within few hours (7 – 24 h). Additional time of separation is insignificant. It can be seen that glycerol settles at the bottom, this is an indication that the by-product (Propan-1, 2, 3-triol) is denser than the crude PKO biodiesel. During the washing process to remove the residual catalyst, the water separates out within few minutes (1 – 5). The density of water is higher than that of the biodiesel, hence, it settles at the bottom and the water was tapped off. Clear water was observed after the fifth washing was done. After washing, the biodiesel was heated up to temperature above that of the water by which significant washing-water in the biodiesel was vaporized before it was finally dried with calcium chloride.

3.2 Properties of The PKO-Based Biodiesel Produced

Table 3 showed the characteristics of the biodiesel produced. It also contained the characteristics of the petro-based AGO and the parent PKO used. It can be seen that the specific gravity and viscosity of the parent oil: PKO has been reduced from 0.9208, 32.381 cSt to 0.8728, 3.359cSt, respectively. The kinematic viscosity showed a reduction of about 90% after the PKO has undergone transesterification (alcoholysis) process. Viscosity of vegetable oil (PKO) at 32 cSt may trigger severe problem in the fuel filter and the engine. Knothe (2005) reported that high viscosity of untransesterified oils and fats leads to operational problems in the diesel engine such as deposits on various engine parts. Cold starting may also be very difficult since 'cloud haze' would have been noticed at 23°C (Gautier, 1933). This is evidenced from the results tabulated in Table 3.

Comparison of automotive gas oil (AGO) and PKO methyl esters showed that both of them have very close physical properties like viscosity and specific gravity, hence, both can be blended in ratios. There is also the possibility of using the PKO methyl esters produced 100% since both have similar properties. However, the higher flash point recorded for the PKO methyl esters will be helpful in handling and storage logistics.

Table 3: Properties of AGO; PKO–Biodiesel and PKO

Properties	AGO	PKO-Biodiesel	PKO
Specific Gravity @ 15°C	0.8600	0.8728	0.9208
Viscosity @ 40°C (cSt)	3.073	3.359	32.381
Colour	3.5	0.5	1.0
Flash Point (°C)	71 (159.8°F)	100 (212°F)	190(374°F)
Pour Point (°C)	-16 (3.2°F)	-3 (26.6°F)	18 (64.4°F)
Crackle Test	-ve	-ve	-ve
H_2O Content (% vol)	Nil	Nil	Nil
Cloud point (°C)	-12 (10.4 °F)	3 (37.4 °F)	23 (73.4°F)
Density @ 15°C (kg/m^3)	860	873	921

Essentially, the characteristics of the PKO biodiesel produced conformed to standards. Besides, the pour point (-3°C) is also very good result for the cold starting of the engine. The viscosity (3.359 cSt) is within the standards (ASTM D -445; IS: 1400 – 1974). Crackle test showed no sign of water content. This observation is good for long time storage and the engine performance in general (Knothe, 2005; Gerpen, 2005). Results of emissions assessment are presented in Table 4.

Table 4: Emissions from combustion of biodiesel/diesel in CIE

Fuel Type	CO (ppm)	NO_2 (ppm)	NO_x (ppm)
PKO Biodiesel	278.3	28.3	153.7
AGO	390.0	35.0	159.0

It was observed that CO concentration was reduced by 30% when 100% PKO biodiesel was used in CIE compared with AGO. Both NO_2 and NO_x concentrations were slightly lower when PKO biodiesel was used than in the case of AGO. It has been reported that biodiesel is more environmentally friendly than petro-diesel (Graboski and McCormick, 1998; Antolin et al, 2002).

4. CONCLUSIONS

A number of studies have shown that vegetable oils and animal fats hold great promise as alternative fuels for the Compression Ignition (CI) engines. PKO is not an exception to this. There is colossal potential to be realised from Nigerian PKO since it is also produced in large quantity. The results (viscosity, specific gravity, flash point and density) of the characterisation of PKO-based biodiesel satisfied most international standards. This work will also contribute to appropriating the PKO-based biodiesel as a supplement or total replacement of conventional petroleum based diesel fuel particularly in compression ignition engine.

5. ACKNOWLEDGEMENT

The authors gratefully acknowledged the technical assistance offered by Mr. Akano Adesina of Conoil Nigeria Plc. Equipment donation by World University Service, Germany is acknowledged by E. Betiku.

REFERENCES

Antolin, G., Tinaut, F.V., Briceno, Y., Castano, V., Perez, C. and Ramiez, A.I. Optimisation of biodiesel production by sunflower oil transesterification. *Bioresource Technology*, 83: 111–114, 2002.

Barnwal, B.K. and Sharma, M.P. Prospects of biodiesel production from vegetable oils in India, *Renewable and Sustainable Energy Reviews*, 9: 363–378, 2005.

Bharath, R., Inomata, H., Adschiri, T. and Arai, K. Phase equilibrium study for the separation and fractionation of fatty oil components using supercritical carbon dioxide. *Fluid Phase Equilibra*, 81: 307-320, 1992.

David, A.M. Nigeria Oilseeds and Products, *Annual 2006 USDA: Lagos*, 1-9, 2007.

Feuge, R.O. and Gros, A.T. Modification of vegetable oils. VII Alkali catalysed interesterification of pea-nut oil with ethanol. *Journal of the American Oil Chemists' Society*, 26(3): 97-102, 1949.

Freedman, B. Pryde, E.H. and Mounts, T.L. Variables affecting the yields of fatty esters from transesterified vegetable oils. *Journal of the American Oil Chemists' Society*, 61(10): 1638–1643, 1984.

Gautier, M. Use of Vegetable Oils in Diesel Engines, *Rev. Combust. Liq.* 11, 19–24, 1933.

Gerpen, J.V. The History of Vegetable Oil-Based Diesel Fuels, In: G. Knothe, J.V. Gerpen & J. Krahl (eds.), The Biodiesel Handbook, AOCS Press, 2005.

Goh, E.M. Specially fats from palm and palm kernel oils, in selected readings on palm oil and its uses, *Palm Oil Research Institute of Malaysia (PORIM), Malaysia*, 1993.

Graboski, M.S. and McCormick, R.L.Combustion of fat and vegetable oil derived fuels in diesel engines, *Progress Energy Combustion Science* 24: 125–164, 1998.

Hassan, M.N., Rahman, N.A.N., Anuar, B.O., Ibrahim, M.H. and Omar, A.K.M. Simple fractionation through the supercritical carbon dioxide extraction of palm kernel oil, *Separation and Purification Technology*, 19: 113-120, 2000.

Jeong, G.T. , Oh, Y.T. and Park, D.H. Emission profile of rapeseed methyl ester and its blend in a diesel engine, *Applied Biochemistry and Biotechnology*, 129-132: 165–178, 2006.

Knothe, G. What is Biodiesel? In: Knothe, G., Gerpen, J.V. and Krahl, J. (eds.), The Biodiesel Handbook, AOCS Press, 2005.

Lang, X., Dalai, A.K., Bakhshi, N.N. Reaney, M.J. and Hertz, P.B. Preparation and characterization of bio-diesels from various bio-oils, *Bioresource Technology* 80: 53–62, 2001.

Ma, F. and Hanna, M.A. Biodiesel production: a review, *Bioresource* Technology, 70: 1–15, 1999.

MPOB, Report of Malaysia palm oil research board, *Palm Oil Research Board of Malaysia*, 2003.Noureddini, H. and Zhu, D. Kinetics of transesterification of soybean oil. *Journal of the American Oil Chemists' Society*, 74: 1457-1463, 1997.

Omar, A.K.M., Rahman, N.A.N. and Hassan, M.N. Process for a simultaneous extraction and fractionation of palm kernel oil using supercritical carbon dioxide as a solvent, *Malaysia Patent* (P19805730), 1998.

Rahman, N.A.N., Hassan, M.N., Anuar, B.O., Ibrahim, M.H. and Omar, A. K. M. The effect of dehulling on supercritical extraction of palm kernel oil. *Journal of Chemical Engineering of Japan*, 34(3): 407-410, 2001.

Rossell, J.B. Fractionation of lauric oils. *Journal of the American Oil Chemists' Society*, 62: 485-490, 1985.

Saka, S. and Dadan, K. Biodiesel fuel from rapeseed oil as prepared in supercritical methanol. *Fuel*, 80: 225-231, 2001.

Usta, N. Use of tobacco seed oil methyl ester in a turbocharged indirect injection diesel engine, *Biomass Bioenergy*, 28 (1): 77–86, 2005.

Zaidul, I.S.M., Norulaini, N.N.A., Omar, A.K.M. and Smith, R. L. Jr. Supercritical carbon dioxide (SC-CO_2) extraction and fractionation of palm kernel as cocoa butter replacers blend, *Journal of Food Engineering*, 73(3): 210-216, 2006.

Ife Journal of Technology, Vol. 18(2), 5-10, 2009

Full Paper

SIMULATION OF GROUNDWATER CONTAMINANT TRANSPORT IN THE AMEKI AQUIFER DOMAIN OF ANAMBRA STATE, SOUTH EASTERN NIGERIA

A.A. Adegbola
Department of Civil Engineering
Ladoke Akintola University of Technology
Ogbomoso, Nigeria
dayomos2002@yahoo.com

O. A. Agbede
Department of Civil Engineering
University of Ibadan, Ibadan, Nigeria

ABSTRACT

About 95% of water schemes located within the Ameki aquifer domain of Anambra State depend on groundwater exploitation. Provision of potable water to the generality of communities within the domain was grossly inadequate, based on reliable community population statistics. Dependence on untreated surface water in some places gave rise to water borne diseases. Groundwater flow and contaminant transport models were developed to evaluate the movement of hypothetical contaminants within the Ameki aquifer in Anambra State. Hypothetical particle-tracking simulations revealed that water high in dissolved solids concentration moved from the designed contaminant source, Ogbakuba community in Ogbaru Local Government Area, toward the nearest pumped well situated at Nza Community in Ekwusigo Local Government Area. Introduced contaminant particles moved a distance of 950m from 1979 to 1999. Results of the hypothetical simulation for the 1979-2050 period showed that by 2050 most of the particles introduced in Ogbakuba Community would have moved about 1200m, reaching the nearest well at Nza Community. The results indicated that with continued pumping the hypothetical contaminant particles will eventually extend to reach more production wells as cone of depression of well fields increases. The paper preliminarily assessed the implication of exploiting groundwater reserve, without recourse to the effects of sustained pumping on the aquifer system. Other factors governing the transport of solute in groundwater such as dispersion and chemical reaction were not considered.

KEYWORDS: Groundwater flow, simulation, contaminant transport, particle-tracking

1. INTRODUCTION

The project area covering the Ameki domain in Anambra State is situated within latitudes $6^{0}15^{1}$N and $5^{0}40^{1}$N and longitudes $6^{0}35^{1}$E and $6^{0}55^{1}$E. The problem domain is situated within the South Eastern part of the Anambra Basin. The domain has a boundary with the famous Niger River on its entire Western borderline. Figure 1 depicts the map of Nigeria with the boundaries of Anambra State indicated.

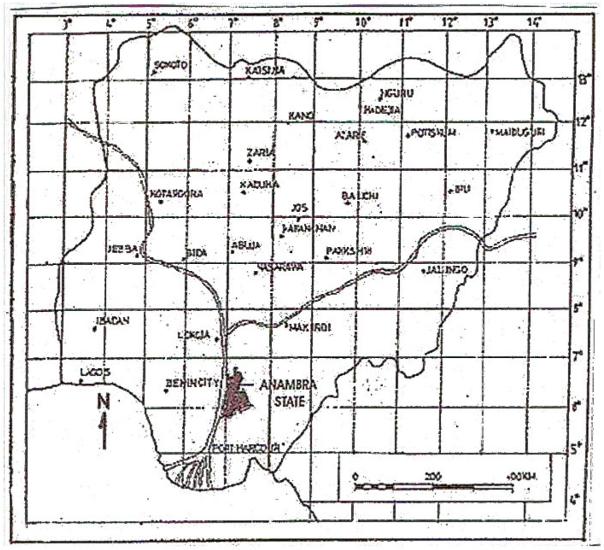

Figure 1: Map of Nigeria with the boundaries of Anambra State indicated

The problem domain is drained mainly by the Anambra River and its main tributaries such as Oyi, Ezochie and Igbariam. Most of the rivers traversing the entire project area have small catchments which are highly seasonal. The basin climate is tropical wet and dry seasons, with less than 5^{0}C temperature range. The average annual precipitation is about 200.5cm (Tokun, 2003). Offodile, 1992, described generally the climate in the entire Anambra Basin area as hot and humid, with mean annual rainfall of 152.4cm to 203.2cm in the Enugu area to 101.6cm to 228.6cm in Idah area to the north of the Basin. The dry season is relatively short from about November to March. Maximum temperature is 34^{0}C.

According to literatures (Ezeigbo, 1987; Nwakwor and Eche, 1987), the most important aquiferous formation within the project area are the Ameki, Alluvium and Nanka. A small portion of the Ajalli Formation extends to parts of Ayamelum Local Government Area (LGA) of Anambra State.

2. HYDROGEOLOGY

The generalized geological map of the Anambra Basin is presented in Figure 2. The geological map of Anambra State, with the location of the problem domain, is shown in Figure 3. The existing water supply system in Anambra State comprises mainly boreholes – both shallow and deep, and in some places fully reticulated to serve the residents/villages within the catchment area; hand dug wells – mostly provided through communal efforts and fully developed impounded lakes.

The peculiar geology of the Anambra State has not made open wells feasible in most of the LGA's or communities, except in the riverine areas and a few upland communities (Emenike, 2001). The water bearing aquifer within the study area is the Ameki. Overlying the Imo Shale to the south eastern part of the study area, according to Offodile, 1992 and Ezeigbo, 1987, lies the Ameki Formation. This extends far south beyond the boundaries of Anambra State, up to Okigwe. The Ameki Formation, which is the main aquifer covering Onitsha, Ogbaru, Nnewi and Nnobi areas, is underlain by a series of sandstones interbedded with shales and thin limestones.

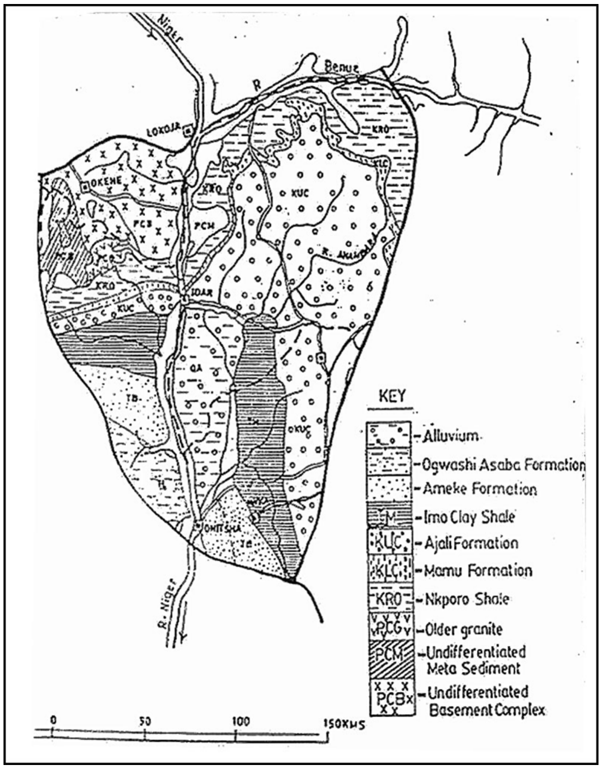

Figure 2: The generalized geological map of the Anambra Basin (after Offodile, 1992)

3. METHODOLOGY

The Ameki model was represented by a rectangular finite difference grid discretized into rows and columns that formed model cells where the ground-water flow equation was solved numerically at nodes at the center of each cell. The Ameki aquifer problem domain was discretized into a finite difference grid of 20 rows and 15 columns, with the origin at the upper left corner. The origin of the grid (that is, the upper left corner of the grid; row 1, column 1) is at a coordinate of 6035'E and 6017'N (Figure 4). The Ameki domain is idealized as a water table aquifer with an average bottom elevation of 50m below sea level. All the model cells formed by the grid for the Ameki domain have dimensions of 26,000m by 26,000m along the x and y axes respectively. The boundaries of the Ameki aquifer, in each case, are approximated in a stepwise fashion, making some of the nodes within the model grid to be outside the aquifer areas. By assigning zero transmissivities to such nodes outside the boundaries, they are excluded from the calculations. The governing equation for the three-dimensional movement of ground water of constant density through the study area was described by the partial-differential equation:

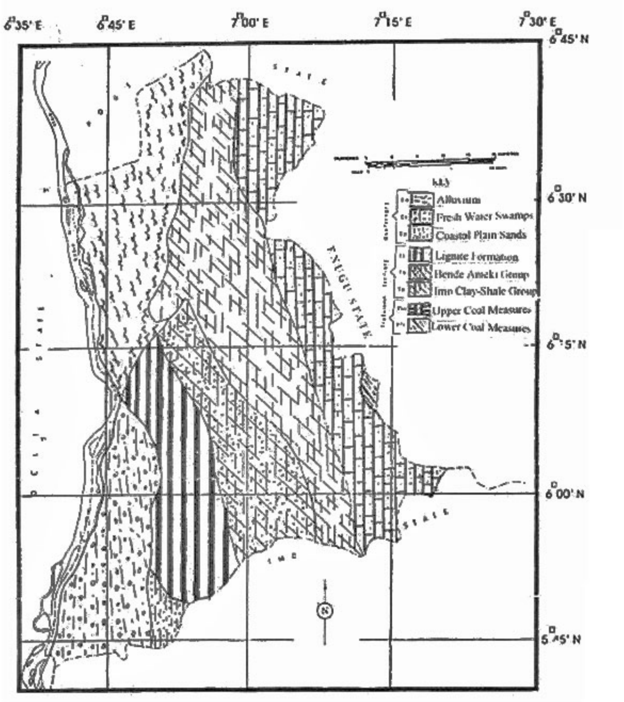

Figure 3: The geological map of Anambra State with the location of the problem domain (after Badafash Nig. Ltd., 1994)

$$\frac{\partial}{\partial x}\left\{K_{xx}\frac{\partial h}{\partial x}\right\}+\frac{\partial}{\partial y}\left\{K_{yy}\frac{\partial h}{\partial y}\right\}+\frac{\partial}{\partial z}\left\{K_{zz}\frac{\partial h}{\partial z}\right\}-W=S_s\frac{\partial h}{\partial t} \tag{1}$$

where:

K_{xx}, K_{yy} and K_{zz} are values of hydraulic conductivity along the x, y, and z coordinate axes, which are assumed to be parallel to the major axes of hydraulic conductivity (LT^{1}); h is the potentiometric head (L); W is a volumetric flux per unit volume and represents sources and/or sinks of water (T^{-1}); S_s is the specific storage of the porous material (L^{-1}); and t is time (T).

The MODFLOW codes used in this model included Basic (BAS), Block-Centered Flow (BCF), Well (WEL), River (RIV), Recharge (RCH), Discretization (DIS), and Strongly Implicit Procedure (SIP) [BAS, BCF, WEL, RIV, RCH, DIS and SIP] by (McDonald and Harbaugh, 2004; Pollock, 1994; Ahlfeld, 2005; Smith et al, 1996; Guiger and Franz, 2003). The model boundaries for the Ameki aquifer domain was determined from the hydrogeological map of Anambra State part of the Anambra Basin, and cross-sections

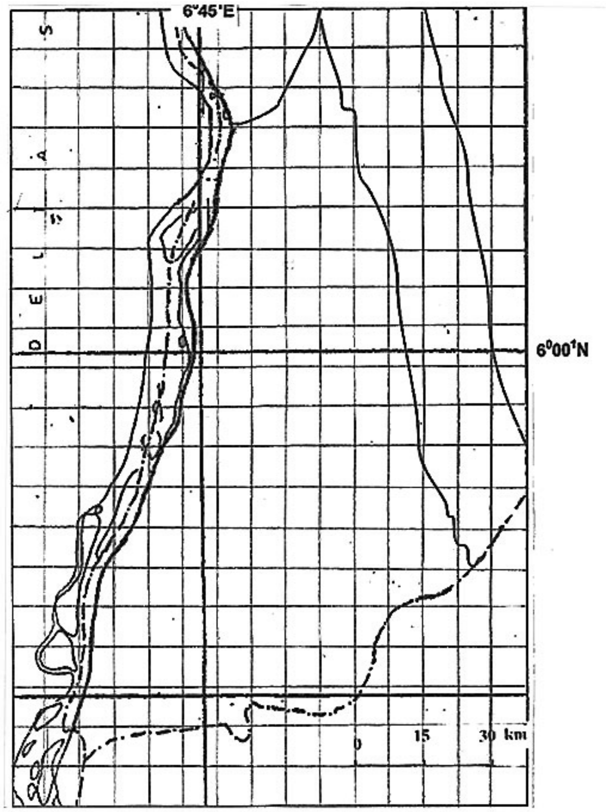

Figure 4: Model grid of the Ameki Aquifer domain

through the aquifer domains. The top boundary of the model, the water table, was simulated in each case as a free-surface boundary (unconfined) to allow it to move vertically in response to changes between inflow and outflow. No-flow boundaries were used below the modeled area to represent contact with aquicludes and ground-water divides.

The surface area of each model array as initially generated had the form of a rectangular box. Where the limits of the study area (problem domain) did not coincide with this rectangular shape, inactive cells were used to delete portions of the model array which fell outside the aquifer boundaries. Out of the many rivers and streams traversing the model domain, only Rivers Niger and Anambra were considered as contributing water to the ground-water system or draining water from it, depending on the head gradient between the river and the ground-water regime. Others were identified and treated as dry washes having relevance mostly at the peak of the wet season. The calibrated ground water flow model was used to preliminarily simulate groundwater flow direction and traveltimes for hypothetical contaminants introduced in the Ogbaru Local Government Area (LGA). Advection by the ground water flow system is one of the main processes controlling the fate and transport of solutes in groundwater. The partial differential equation describing conservation of mass in the Ameki steady-state, three dimensional ground-water flow system was expressed as:

$$\frac{\partial}{\partial \mathrm{x}}\{\mathrm{nv_x}\}+\frac{\partial}{\partial \mathrm{y}}\{\mathrm{nv_y}\}+\frac{\partial}{\partial \mathrm{z}}\{\mathrm{nv_z}\}=\mathrm{W} \qquad \ldots\ldots(2)$$

where: vx, vy, and vz are the principal components of the average linear ground-water velocity vector; n is porosity and W is the volume rate of water created or consumed by internal sources and sinks per unit volume of aquifer.

Equation 2 expressed the conservation of mass for an infinitesimally small volume of the aquifer domain. The finite difference approximation of Equation 2 presented a mass balance equation for a finite-sized cell of the Ameki aquifer that accounted for water flowing into and out of the cell, and for water generated or consumed within the cell. Figure 5 shows a finite-sized cell of aquifer and the components of inflow and outflow across its six faces. The six cell faces were referred to as x_1, x_2, y_1, y_2, z_1, and z_2. Face x_1 is the face perpendicular to the x direction at x-x_1. Similar definitions hold for the other five faces. The average linear velocity component across each face in cell (i, j, k) was obtained by dividing the volume flow rate across the face by the cross sectional area of the face and the porosity of the material in the cell, as follows:

$$v_{x_1}=\frac{Q_{x_1}}{(n\Delta y\Delta z)}\ ,\qquad v_{x_2}=\frac{Q_{x_2}}{(n\Delta y\Delta z)} \qquad (3)$$

$$v_{y_1}=\frac{Q_{y_1}}{(n\Delta x\Delta z)}\ ,\qquad v_{y_2}=\frac{Q_{y_2}}{(n\Delta x\Delta z)} \qquad (4)$$

$$v_{z_1}=\frac{Q_{z_1}}{(n\Delta x\Delta y)}\ ,\qquad v_{z_2}=\frac{Q_{z_2}}{(n\Delta x\Delta y)} \qquad (5)$$

where Q is a volume flow rate across a cell face, and Δx□□ Δy, and Δz are the dimensions of the cell in the respective coordinate directions. If flow to internal sources or sinks within the cell is specified as Qs, the following mass balance equation for the cell is:

$$\frac{(nv_{x_2}-nv_{x_1})}{\Delta x}+\frac{(nv_{y_2}-nv_{y_1})}{\Delta y}+\frac{(nv_{z_2}-nv_{z_1})}{\Delta z}=\frac{Q_s}{(\Delta x\Delta y\Delta z)} \qquad (6)$$

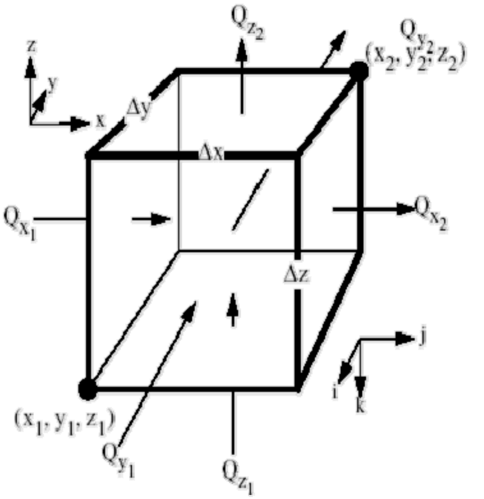

Figure 5: Finite-difference Cell showing definitions of x-y-z and i-j-k.

The left side of equation 6 represented the net volume rate of outflow per unit volume of the cell, and the right side represented the net volume rate of production per unit volume due to internal sources and sinks. Substitution of Darcy's law for each of the flow terms in equation 6 resulted in a set of algebraic equations expressed in terms of heads at nodes located at the cell centers. The solution of that set of algebraic equations yielded the values of head at the node points. Once the head solution had been obtained, the inter-cell flow rates was computed from Darcy's law using the values of head at the node points. The U. S. Geological Survey modular three-dimensional finite-difference ground-water flow model, (MODFLOW), would then solve for head and calculate inter-cell flow rates. In order to compute path lines, a method was established to compute values of the principal components of the velocity vector at every point in the flow field based on the inter-cell flow rates from the finite difference model.

Linear interpolation was used to compute the principal velocity components at points within a cell. Using simple linear interpolation, the principal velocity components was expressed in the form:

$$v_x = A_x(x - x_1) + v_{x_1} \qquad (7)$$

$$v_y = A_y(y - y_1) + v_{y_1} \qquad (8)$$

$$v_z = A_z(z - z_1) + v_{z_1} \qquad (9)$$

where A_x, A_y, and A_z are constants that corresponded to the components of the

velocity gradient within the cell:

$$A_x = \frac{(v_{x_2} - v_{x_1})}{\Delta x} \qquad (10)$$

$$A_y = \frac{(v_{y_2} - v_{y_1})}{\Delta y} \qquad (11)$$

$$A_z = \frac{(v_{z_2} - v_{z_1})}{\Delta z} \qquad (12)$$

Linear interpolation produced a continuous velocity vector field within each individual cell that identically satisfied the differential conservation of mass equation (equation 2) everywhere within the cell. In considering the movement of a particle, p, through a three-dimensional finite-difference cell, the rate of change in the particle's x-component of velocity as it moved through the cell would be given by:

$$\left\{\frac{dv_x}{dt}\right\}_p = \left\{\frac{dv_x}{dx}\right\} \left\{{}_z\frac{dx}{dt}\right\}_p \qquad (13)$$

To simplify notation, the subscript, p, was used to indicate that a term was evaluated at the location of the particle [denoted by the x-y-z coordinates (x_p, y_p, z_p)]. For example, the term, $(dv_x/dt)_p$ is the time rate of change in the x-component of velocity evaluated at the location of the particle. In equation (13), the term $(dx/dt)_p$ is the time rate of change of the x-location of the particle. By definition,

$$v_{x_p} = \left\{\frac{dx}{dt}\right\}_p \qquad (14)$$

where is the x-component of velocity for the particle. Differentiating equation (7) with respect to x yields the additional relation:

$$\left\{\frac{dv_x}{dx}\right\} = A_x \qquad (15)$$

Substituting equations (14) and (15) into equation (13) gives,

$$\left\{\frac{dv_x}{dt}\right\}_p = A_x v_{x_p} \qquad (16)$$

Analogous equations are obtained for the y and z directions,

$$\left\{\frac{dv_y}{dt}\right\}_p = A_y v_{y_p} \qquad (17)$$

$$\left\{\frac{dv_z}{dt}\right\}_p = A_z v_{z_p} \qquad (18)$$

Equations (16) through (18) can be rearranged to the form,

$$\left\{\frac{1}{v_{x_p}}\right\} d(v_{x_p}) = A_x dt \qquad (19)$$

Equation (19) can be integrated and evaluated between times t_1 and t_2, (t_1 and t_2) to give,

$$\ln\left\{\frac{v_{x_p}(t_2)}{v_{x_p}(t_1)}\right\} = A_x \Delta t \qquad (20)$$

where $\Delta t = t_2 - t_1$. By taking the exponential of each side of equation (20), substituting equation (7) for $v_{Xp}(t_2)$, and rearranging, we obtain,

$$x_p(t_2) = x_1 + \left\{\frac{1}{A_x}\right\} \left\{v_{x_p}(t_1)\exp(A_x \Delta t) - v_{x_1}\right\} \qquad (21)$$

Analogous equations can be developed for the y and z directions, as:

$$y_p(t_2) = y_1 + \left\{\frac{1}{A_y}\right\} \left\{v_{y_p}(t_1)\exp(A_y \Delta t) - v_{y_1}\right\} \qquad (22)$$

$$z_p(t_2) = z_1 + \left\{\frac{1}{A_z}\right\} \left\{v_{z_p}(t_1)\exp(A_z \Delta t) - v_{z_1}\right\} \qquad (23)$$

The velocity components of the particle at time t_1 are known functions of the particle's coordinates. Consequently, the coordinates of the particle at any future time (t_2) could be computed directly from equations (21) through (23). For the steady-state flow, the direct integration method described above was imbedded in a simple algorithm that allowed a particle's exit point from a cell to be determined directly given any known starting location within the cell. Transient finite-difference flow simulations consist of a series of discrete time steps during which flow rates are constant and storage changes within cells contribute an additional component to the internal source/sink term on the right side of equation 6. The particle tracking algorithm described previously for steady-state flow systems was extended to transient finite-difference simulations by taking advantage of the fact that transient simulations behave as a series of steady state flow periods. For each time step, particle paths were computed just as for the steady state case until the end of the time step was reached. A new velocity distribution was then calculated for the next time step and the computation of particle paths was resumed. The computation of paths forward or backward, boundary conditions, and the path line termination criteria were handled the same as for steady state flow.

The computer code MODPATH, developed by Pollock, 1994, was used to simulate advective transport for this research work. Modpath used particle-tracking techniques to compute path lines and travel times based on the results of MODFLOW simulations (McDonald and Harbaugh, 2004). Results of the calibrated simulations of the ground water flow model developed for the Ameki model domain were used in the application of MODPATH. Other processes controlling the fate and transport of solutes in ground water, for example dispersion, diffusion, adsorption and chemical reactions were not included in the MODPATH simulation exercise.

The effect of pumping on ground water flow and travel times were demonstrated by introducing hypothetical particles into mode cells under transient (1979-99) ground water conditions. The particles tracking simulations were used to assess the potential for poor quality water to migrate into the main pumping areas. Ground water flow direction and distances traveled were shown by tracking particles through time. Particles were introduced in the Ogbakuba community in Ogbaru Local Government Area. Particles were released to the top face for a single time period, 1979, assumed to be the base year representing the state of predevelopment in the Ameki aquifer domain. MODPATH simulated the path along which the particles were advected under the transient conditions (1979-1999), and the predictive conditions (1979 – 2050).

4. RESULTS AND DISCUSSION

The study area map and topographical elevations for the Ameki domain is presented in Figure 6. The contours represent the Natural Ground Level (N.G.L.), Above Mean Sea Level (A.M.S.L.), while the locations represent the positions of observation wells in the aquifer domain. The idealization exercise is similar to that developed by Agbede, 1989; Bear and Verruijt, 1992; Harbaugh and McDonald, 1996; Bouwer, 1999; Olowofela and Akinyemi, 2001; Asiwaju-Bello and Oladeji, 2001; Agbede and Adegbola, 2005; and Bexfield and McAda, 2003, for simplification of model aquifer domains prior to numerical simulation. The values of initial and final transmissivities in m^2/sec for the Ameki ground water flow model domain are 1.5 x 10^{-4} and 1.25 x 10^{-4} , while the storage coefficients have initial and final values of 1.0 x 10^{-4} and 4.5 x 10^{-3} . The procedure for deriving the final hydraulic parameter is consistent with the approach adopted by Carrera and Neuman, 1986; Busari and Agbede, 1992; Christensen, 1997; Cooley, 1979; and D'Agnese et al, 1996.

The calibrated transient state model for the Ameki Domain was used to carry out a preliminary assessment of the movement of hypothetical contaminants within the aquifer. Hypothetical particle-tracking simulations revealed that water high in dissolved solids concentration moved from the designed contaminant source (Ogbakuba community in Ogbaru LGA) toward the nearest pumped well situated at Nza Community in Ekwusigo Local Government Area (Figure 7). Hypothetical contaminant particles introduced in the Ogbakuba community in Ogbaru LGA moved a distance of 950m between 1979 and 1999.

Results of the hypothetical simulation for the 1979-2050 period showed that by 2050 most of the particles introduced in Ogbakuba Community in Ogbaru LGA would have moved about 1200m, reaching the nearest well at Nza Community in Ekwusigo LGA. The results indicated that with continued pumping the hypothetical contaminant particles will eventually extend to reach more production wells as cone of depression of well fields increases. The exercise was carried out purely to assess and demonstrate the application of the Ameki calibrated model to analyse transport of contaminants in groundwater flow within a domain.

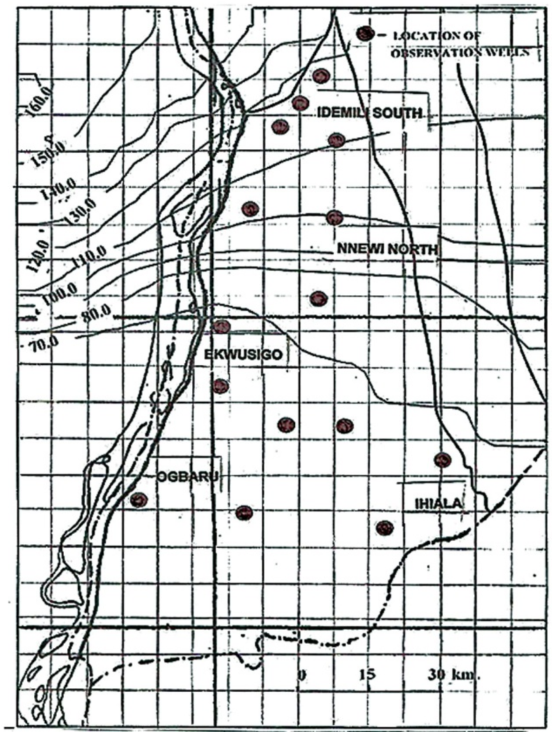

Figure 6: Study Area Map showing positions of observation wells and topographical elevations of the Ameki Domain

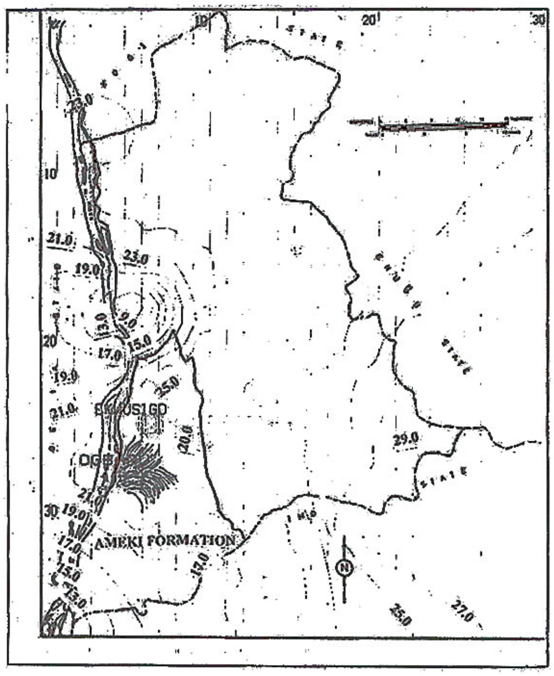

Figure 7: Location Map of the Ameki Aquifer Contaminant Transport Domain with contours of static water levels in observation wells

5. CONCLUSIONS

Preliminary particle tracking simulation was carried out within the Ameki aquifer domain to demonstrate the potentials of the calibrated model to investigate advective transport of contaminants in groundwater. Introduction of hypothetical contaminants in the Ogbakuba Community in Ogbaru LGA moved a distance of 950m between 1979-99 while results of the hypothetical simulation for the 1979-2050 showed a movement of about 1,200m, reaching the nearest well at Nza community in Ekwusigo LGA. Other factors governing the fate of transport of solutes in groundwater such as dispersion and chemical reaction were not considered in the present study. The accuracy of the Ameki ground water model is limited by the assumptions made in formulating the governing flow equations and in the assumptions made during model construction. The model was also limited by the availability of data and the interpolations and extrapolations of available data. In future, with the availability of additional data, further refinement of the model should be carried out, which could improve the accuracy of model prediction of the effects of additional stresses on the aquifer system, such as increased withdrawals or drought.

REFERENCES

Agbede, O. A. and Adegbola, A. A. Modelling Groundwater Flow in the Sokoto Basin using the Finite Difference Technique. Journal of Research Information in Civil Engineering (RICE). 2(1) : 26-33, 2005.

Agbede, O. A. Model as a Management Tool in Water Resources. Modelling, Simulation and Control C, AMSE Press. 19(1) : 1-10, 1989.

Ahlfeld, D. A. Barlow P. M. and Mulligan, A. E. GWM – A Ground-Water Management Process for the U.S. Geological Survey, Modular ground water model (MODFLOW – 2000). Open file report, 1072. 124p, 2005.

Asiwaju-Bello, Y. A. and Oladeji, O. S. Numerical Modelling of Groundwater Flow Patterns within Lagos Metropolis, Nigeria. Journal of Mining and Geology. 37(2) : 185-194, 2001.

Badafash (Nig.) Ltd, Federal Ministry of Water Resources and Rural Development, Abuja. Final Report for Borehole Data Inventory and Pumping test Analysis for Groundwater Development in Nigeria (Phase II), 1994.

Bear, J. and Verruijt, A. Modelling Groundwater Flow and Pollution. D. Reidel Publishing Company. Dordrecht/Boston/Lancaster/Tokyo, 1992.

Bexfield, L. M. and McAda, D. P. Simulated Effects of Ground-Water Management Scenarios on the Santa Fe Group Aquifer System, Middle Rio Grande Basin, New Mexico, 2001-40, 2003.

Bouwer, H. Gro-Buxton, H. T. and Smolensky, D. A. Simulation of the Effects of Development of the Ground-Water Flow System of Long Island, New York: U.S. Geological Survey Water-Resources Investigations Report 98-4069, 57 p., 1999.

Busari, M. A. O. and Agbede, O. A. Modelling of Groundwater Flow and Pollution. A Technical Paper presented at the National Workshop on Development of Groundwater Resources held at the Conference Centre, U.I., Ibadan between 24th and 31st July, 1992.

Carrera, J. and Neuman, S. P. Estimation of Aquifer Parameters under Transient and Steady-State Conditions: Water Resources Research, 22(2) : 199-242, 1986.

Christensen, S. On the Strategy of Estimating Regional-Scale Transmissivity Fields: Ground Water, 35(1) : 131-139, 1997.

Cooley, R. L. A Method for Estimating Parameters and Assessing Reliability for Models of Steady State Groundwater Flow 2. Application of Statistical Analysis: Water Resources Research, 15(3) : 603-617, 1979.

D'Agnese, F. A. Faunt, C. C. Hill, M. C. and Turner, A. K. Death Valley Regional Ground-Water Flow Model Calibration using Optimal Parameter Estimation Methods and Geoscientific Information Systems: in Kovar, Karel and van der Heidje, Paul, eds., Calibration and Reliability in Groundwater Modeling, Proceedings of the 1996 Model CARE Conference, Golden, Colorado, September, 1996: International Association of Hydrologic Sciences, Publ. 237, p. 41-52, 1996.

Emenike, E. A. Geophysical Exploration for Groundwater in a Sedimentary Environment: A Case Study from Nanka over Nanka formation in Anambra basin, South-eastern Nigeria. Published in the Global Journal of Pure and Applied Sciences, 7(1), 2001.

Ezeigbo, T. Quality of Water Resources in Anambra State Nigeria, Published by Nigeria Journal of Mining and Geology, 23(1 & 2), 1987.

Guiger, N. and Franz, T. Visual Modflow. Waterloo, Hydrogeologic, Inc. Waterloo Ontario, 2003.

Harbaugh, A. W. and McDonald, M. G. User's documentation for MODFLOW-96, an update to the U.S. Geological Survey Modular Finite Difference Ground-Water Flow Model: U.S. Geological Survey Open-File Report 96-485, 56 p, 1996.

McDonald, M. G. and Harbaugh, A. W. A Modular Three-Dimensional Finite Difference Flow Model. V.S. Geological survey Techniques of Water Resources investigations, book 6, chap. A2, 286 pp., 2004.

Nwakwor, G. I. and Eche, B. S. Hydrogeological Evaluation of the Greater Onitsha Water Scheme Anambra State, Nigeria: Journal of Mining and Geology 26(2), 1980.

Offodile, M. E. An Approach to Groundwater Study and Development in Nigeria. Published by MECON Services Ltd. P. O. Box 6022, Jos, 1992.

Olowofela, J. A. and Akinyemi, O. D. A Numerical Model for the Migration and Fate of Contaminants in Groundwater. Nigerian Journal of Science. 35(1) : 87-93, 2001.

Pollock, D. W. User's Guide for MODPATH/MODPATH-PLOT, Version 3: A Particle Tracking Post-Processing Package for MODFLOW, the U.S. Geological Survey finite-difference ground-water flow model: U.S. Geological Survey Open-File Report, 94-464, 1994.

Smith, D. Wall, W. Cheng, Z. and Barnes, R. Surfer (Win 32) Surface Mapping System. Golden Software, Inc. Golden Colorado, 1996.

Tokun, A. Planning and Performance Comparison of Rural and Urban Water Development in Nigeria. Osot Associates Consulting Engineers Bi-Monthly Seminar, Prost Building, Opposite The Polytechnic South Campus, Sango-Eleyele Road, Ibadan, 2003.

Ife Journal of Technology, Vol. 18 (2), 11-14, 2009

Full Paper

CORRELATIONS FOR NUSSELT NUMBER IN A STAGGERED CROSS-FLOW TUBE-TYPE HEAT EXCHANGER

D. A. Fadare
Department of Mechanical Engineering,
University of Ibadan
Ibadan, Nigeria.
fadareda@yahoo.com

ABSTRACT

Empirical correlations for Nusselt number (Nu) in a staggered multi-row multi-column cross-flow tube-type heat exchanger is presented in this paper. In the experiment, air at ambient temperature was drawn by a centrifugal fan perpendicularly over banks of cylindrical rods arranged in staggered configuration of 5 rows by 4 columns. A test element consisting of a tube of pure copper with length, internal and external diameters of 0.125, 0.0115 and 0.0125 m was heated to a maximum temperature of about 90^{0}C and inserted into the air stream in the working section. Rate of cooling was measured by thermocouple embedded at the centre, via a digital multimeter which was connected to a computer for monitoring temperature data. A semi-logarithms plot of the data was used to calculate the heat transfer coefficient (h) between the copper element and air, and hence the Nusselt number. The heat transfer coefficient at the centre of each of the four columns at ten different flow rates with throttle valve openings ranging from 10 - 100% were investigated. Results showed that the Nusselt number increased exponentially with increase in air flow rate and also increased in successive columns in the direction of flow at a diminishing rate. Correlations of Nusselt number with Reynolds number (Re) were developed for preliminary design and performance assessment of staggered multi-row multi-column cross-flow tube-type heat exchanger.

KEYWORDS: Staggered cross-flow, heat exchanger, Nusselt number, Reynolds number

Nomenclature:

$\dot{q}$	rate of heat transfer to air (J/s)
μ	viscosity of air (kg/ms)
A	surface area of element (m^2)
A_1	effective surface area of element (m^2)
c	specific heat of copper element (J/kg ^{0}C)
c_p	specific heat of air at constant pressure (J/Kg ^{o}C)
D	outside diameter of element (m)
d	inside diameter of element (m)
h	coefficient of heat transfer (J/m^{2}s ^{0}K)
k	thermal conductivity of air (J/ms ^{0}C)
l	length of copper element (m)
l_1	effective length of element (m)
M	slope of cooling curve
m	mass of element (kg)
Nu	Nusselt Number
p_A	barometric pressure (N/m^2)
Re	Reynolds Number
t	time (s)
T	temperature of element (^{o}K)
T_A	temperature of air (^{o}K)
V	mean velocity past element (m/s)
ρ	density of air (kg/m^3)

1. INTRODUCTION

Heat transfer over a bank of tubes in cross flow is of numerous applications in heat exchanger, such as steam generator in a boiler or air cooling in the coil of an air conditioner. In these applications, one fluid moves over the tubes, while a second fluid at a different temperature passes through the tubes and hence, heat is exchanged between the fluids based on the convective heat transfer coefficient. Heat transfer analysis for different configurations of tube-type cross-flow heat exchangers has been investigated by Kays and London (1964) and McAdams (1954).

For cross-flow heat exchangers, the tubes are either arranged in staggered or aligned configuration. The experiment of Incropera and Dewih (2002) has shown that the flow conditions within the bank are dominated by boundary layer separation effects and by wake interactions, which in turn influence the convection heat transfer. Hence, the heat transfer coefficient associated with a tube is determined by its configuration and position of the bank. The heat transfer coefficient of staggered configuration has been reported to be higher than that of aligned (Incropera and Dewih, 2002). Also, for a given configuration, the heat transfer coefficient in the first column from the air intake was found to be lower than that associated with tubes of inner columns. In most configurations, however, heat transfer conditions stabilize, such that little change occurs in the convection coefficient for tube beyond the fourth or fifth column (Incropera and Dewih, 2002; Plint and Partners, 1981).

Analysis of the relationships between the heat transfer, flow rate and configuration of the system has been the concern of many researchers over the years. Different analytical models have been developed and applied for modeling this relationship (Zhukauskas, 1972). However, the applicability of these analytical models is limited to a confined range of flow conditions due to the complexity of the relationships. In this sense, therefore, other methods based on numerical techniques have been applied in the analysis such as: artificial neural networks (Pacheco-Vega *et al.*, 2001a; Pacheco-Vega *et al.*, 2001b; Fadare and Fatona, 2008; Fatona, 2008; Islamoglu, 2003), finite element method (Ranganayakulu and Seetharamu, 1999a; Ranganayakulu and Seetharamu, 1999b). However, these numerical methods are approximate solutions, which in most cases, required validation based on empirical data. Different forms of empirical correlations have been proposed for airflow across tube bank with different geometry and configurations (McAdams, 1954; Mwaba et al., 2006).

The aim of this study was to develop empirical correlations for fully developed Nusselt number and Reynolds number of air flowing over a bank of copper tubes at centre of each of the four columns of a staggered cross-flow tube-type heat exchanger.

2. MATERIALS AND METHODS

2.1 Experimentation

The cross-flow heat exchanger apparatus (Plint Engineers, Model TE.93/A, England) was used in this study for purpose of data gathering as shown in Figure 1. The nominal dimensions of the working section and the configuration of the tube bank are shown in Figure 2. Air at ambient temperature was drawn by a centrifugal fan over bank of cylindrical Perspex rods arranged in staggered configuration of 5 rows by 4 columns in Perspex working section. The centrifugal fan was driven by a 1.0 hp induction electric motor at a constant speed of 2,500 rpm. The fan inlet was connected to the downstream of working section and the outlet was connected to a graduated throttle valve by which air velocity through the apparatus was regulated.

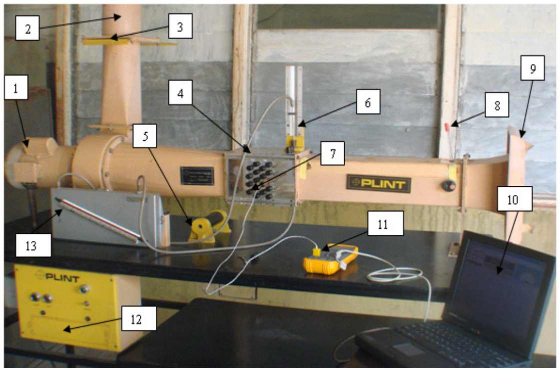

1. Fan, 2. Air outlet, 3. Throttle opening, 4. Working section, 5. Electric heater, 6. Total head tube, 7. Test element, 8. Thermometer, 9. Air inflow, 10. Computer, 11. Digital multimeter, 12. Control panel, 13. Inclined water manometer.

Fig. 1: The experimental setup

Detailed experimental procedures, the nominal dimensions, properties of the copper tube and air have been reported elsewhere (Fadare and Fatona, 2008; Fatona, 2008). A thermocouple (K type) of 0.2 mm diameter was imbedded at the centre of the tube to measure its temperature. The thermocouple voltage output is wired to digital multimeter (Mastech®, MAS-345), which was connected to Pentium 4 Laptop computer with DMM View software to record the measured temperature. The ambient temperature of the air was measured with a mercury–in–glass thermometer at the air inlet.

The copper tube was then inserted into the spaces provided in the working section at middle points of each of the 4 columns of the tube bank. For each column position, the rate of cooling of the tube as indicated by a thermocouple embedded at its centre was recorded at the rate of 1 data per second by the computer for 10 different flow rates with throttle openings ranging between 10 - 100%. The velocity distribution upstream and downstream of the tube bank was measured with a total head tube connected to an inclined water manometer.

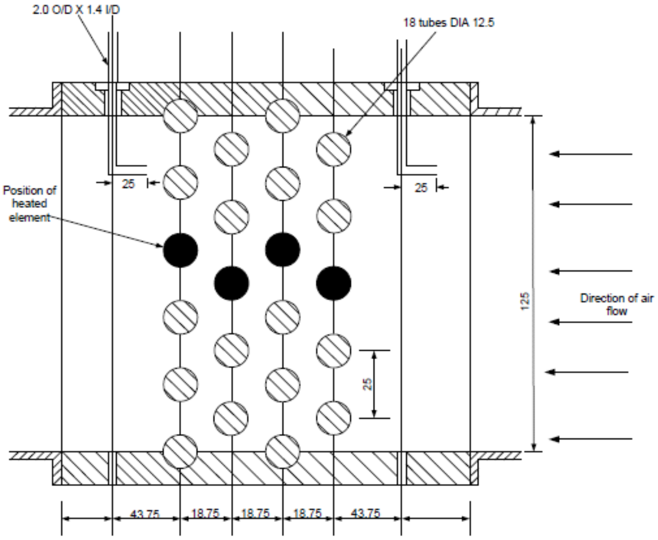

Fig. 2: Nominal dimensions of the working section with staggered tube arrangement

2.2 Data analysis

The air flow rate was measured in terms of the Reynolds number as:

$$\mathrm{Re} = \frac{\rho V D}{\mu} \qquad (1)$$

where (ρ) is the density of air, (V) is the mean velocity, (D) is the outside diameter of tube, and (μ) is the viscosity of air.

For the purpose of estimating the heat transfer coefficient, it was assumed that the whole of the heat lost from the tube is transferred to the air flowing past it. It was also assumed that temperature gradient within the tube thickness was negligible, so that the thermocouple embedded at the centre in the inner diameter gives a true indication of the effective surface temperature of the tube. The rate of heat loss from tube to air is given by:

$$\dot{q} = hA_1(T - T_A) \qquad (2)$$

where h is the heat transfer coefficient, (A_1) is the effective surface area of tube, (T) is the temperature of tube, and (T_A) is the temperature of air.

In a period of time dt the temperature drop dT is given as:

$$-\dot{q}dt = mcdT \qquad (3)$$

where (m) is the mass of tube, and (c)is the specific heat of copper tube.

Combining equations (2) and (3) and eliminating $\dot{q}$ gives:

$$\frac{-dT}{(T - T_A)} = \frac{hA_1}{mc}dt \qquad (4)$$

Integrating equation (4) gives:

$$\log_e(T - T_A) - \log_e(T_0 - T_A) = -\frac{hA_1 t}{mc} \qquad (5)$$

where T_0 is the tube temperature at $t = 0$.

Hence, the plot of $\log_e(T-T_A)$ against t yields a straight line of slope:

$$M = -\frac{hA_1}{mc} \qquad (6)$$

From this the heat transfer coefficient h can be calculated as:

$$h = -\frac{mc}{A_1} M \qquad (7)$$

The fully developed Nusselt number (Nu) is evaluated by

$$Nu = \frac{hD}{k} \qquad (8)$$

where (k) is the thermal conductivity of air and (D) is the outside diameter of tube.

Microsoft® Excel 2003 curve fitting algorithm was used to develop the correlations for Nu and Re at the centre of the four columns of the heat exchanger in the form:

$$Nu = A\,\mathrm{Re}^{b} \qquad (9)$$

where A and b are constants.

3. RESULTS AND DISCUSSION

Figures 3 and 4 show typical cooling curve and corresponding semi-log plot obtained for the copper tube positioned at the centre of column 1 with 100% throttle opening with corresponding calculated Reynolds number of 20.9 x 10^3. In Figure 3, it can be seen that temperature of the copper tube decreased exponentially from 90 - 28°C (ambient) within 100 seconds. In Figure 4, the fitted linear model showed that the equation for the cooling curve was $\log_e (T-T_A) = -0.0352t + 4.2462$ with a high coefficient of determination (R^2-value) of 0.9934. It can be observed that the slope (M) of the linearized cooling curve was equal to -0.0352. The negative sign simply indicated a reduction in temperature of the copper tube with respect to time.

The measured velocity head (H_1), Reynolds number (Re), slope of cooling curve (M) and Nusselt number (Nu) for the copper tube at different column position and throttle openings are given in Table 1. It can be seen that H_1, Re, M and the associated heat transfer property (Nu) increased with increase in throttle opening from 10 – 100% and also increased from column position number 1 – 4. The increase in H_1, Re, M and the associated heat transfer property (Nu) with throttle opening for all the column position can be attributed to the increase in flow rate of the air over the copper tube. As the flow increased from laminar to turbulent flow and thus enhancing the convective heat transfer. The increase in Nu due to the change in position of the copper tube from the outer column 1 to the inner columns can be attributed to the effects of boundary layer separation and wake formation caused by the turbulence of the air over the successive columns of tubes. As the number of column is increased, the boundary layer separation and wake formation tend to reduce after the fourth column. Hence, the heat transfer conditions stabilize, such that little change occurs in the convection coefficient for tube beyond the fourth column.

The plot of Re against Nu for different column positions of the copper tube at different throttle openings (10 – 100%) and the fitted power law model are shown in Figure 5. The Nu increased with increase in Re and increased from column position 1 – 4, though at diminishing rate. Similar observation has been reported by Incropera and Dewih (2002) and Plint and Partners (1981). The correlations between the Nu and Re for the different column positions and the coefficients of determination (R^2-values) between the correlations and experimental data are shown in Table 2. The correlation models gave very high predictive accuracies with R^2-values ranging between 0.9275 and 0.9649.

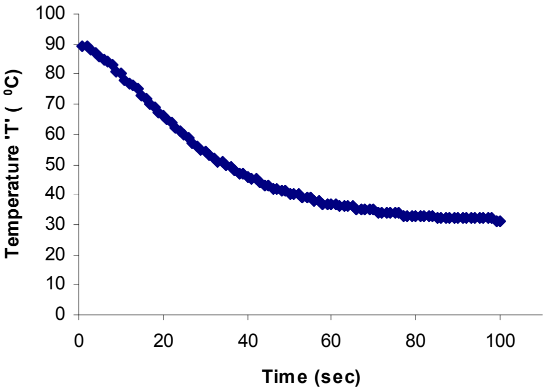

Fig. 3: Typical cooling curve of the heated test element at the centre of column 1 with 100% throttle opening.

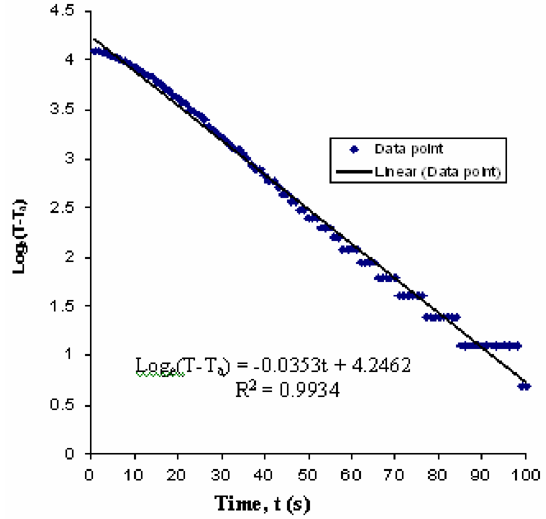

Fig. 4: Typical semi-log plot of the cooling curve of the copper tube at centre of column 1 (100% throttle opening).

4. CONCLUSIONS

Empirical correlations for fully developed Nusselt number with Reynolds number for air flowing over a bank of copper tubes at centre of the four columns of a staggered cross-flow tube-type heat exchanger have been developed. The convective heat transfer property measured in terms of Nusselt number increased exponentially with increase in flow rate of the air. Nu increased, though at diminishing rate as the copper tube position is moved from the outer column position 1 to the inner columns. The optimum number of column was found to be four columns for this configuration. The proposed models are useful for preliminary design and performance assessment of staggered multi-row multi-column cross-flow tube-type heat exchanger.

REFERENCES

Fadare, D.A. and Fatona, A.S. Artificial neural network modeling of heat transfer in a staggered cross-flow tube-type heat exchanger, Pacific Journal of Science and Technology, 9(2):317-323, 2008.

Fatona, A.S. Heat transfer analysis of air flowing over cylindrical tubes using artificial neural networks. M.Sc. Dissertation of Department of Mechanical Engineering. University of Ibadan, Ibadan, Nigeria, 2008.

Table 1: The velocity head, Reynolds number, gradient of curve and Nusselt number at different throttle openings

			Column position of test element							
			1		2		3		4	
% Throttle opening	H_1	Re X(10^3)	M	Nu	M	Nu	M	Nu	M	Nu
10	0.03	3.53	-0.0173	13.4452	-0.0209	16.2430	-0.0225	17.4866	-0.0275	21.3724
20	0.05	4.56	-0.0207	16.0876	-0.0241	18.7301	-0.0282	21.8388	-0.0290	22.5382
30	0.1	6.44	-0.0244	18.9632	-0.0276	21.4501	-0.0321	24.9475	-0.0332	25.8023
40	0.15	7.89	-0.0274	21.2947	-0.0312	24.2410	-0.0352	27.3567	-0.0365	28.3670
50	0.25	10.2	-0.0295	22.9269	-0.0326	25.3360	-0.0368	28.6002	-0.0424	32.9524
60	0.45	13.7	-0.0315	24.4812	-0.0348	27.0458	-0.0384	29.8437	-0.0440	34.1959
70	0.65	16.4	-0.0322	25.0252	-0.0378	29.3774	-0.0417	32.4084	-0.0459	35.6725
80	0.8	18.2	-0.0333	25.8801	-0.0368	28.6002	-0.0433	33.6519	-0.0459	35.6725
90	0.95	19.9	-0.0352	27.3567	-0.0382	29.6882	-0.0425	33.0301	-0.0460	35.7502
100	1.05	20.9	-0.0352	27.3567	-0.0388	30.1545	-0.0417	32.4084	-0.0471	36.6051

H1 = velocity head; Re = Reynolds number; M= slope of cooling curve; Nu = Nusselt number

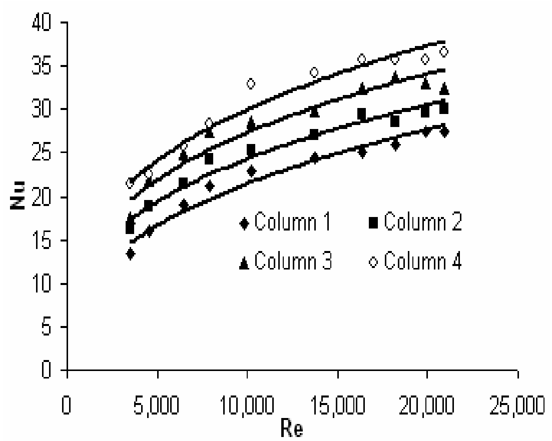

Fig. 5: Plot of Re against Nu for the copper tube at different column positions.

Table 2: Correlation parameters for the copper tube at different column positions

Column position No.	Correlation Model	R^2-value
1	$Nu = 0.7330Re^{0.3667}$	0.9583
2	$Nu = 1.1925Re^{0.3274}$	0.9649
3	$Nu = 1.4340Re^{0.3200}$	0.9275
4	$Nu = 1.6461Re^{0.3152}$	0.9625

Incropera, F.P. and Dewih, D.P. Fundamental of heat and mass transfer, Replika Pub. Ltd, 2002.

Islamoglu, Y. A new approach for the prediction of the heat transfer rate of the wire-on-tube type heat exchanger––use of an artificial neural network model, Applied Thermal Engineering, 23: 243-249, 2003.

Kays, W.M. and London, A.L. Compact heat exchanger, McGraw-Hill, New York, 1964.

McAdams,W.H. Heat transmission, McGraw-Hill, New York, 1954.

Mwaba, M.G., Golriz, M.R. and Gu, J. A semi-empirical correlation for crystallization fouling on heat exchange surfaces, Applied Thermal Engineering, 26(4): 440-447, 2006.

Pacheco-Vega, A., Sen, M., Yang, K.T. and McClain, R.L Neural network analysis of fin-tube refrigerating heat exchanger with limited experimental data, Int. J. Heat and Mass Transfer. 44: 763-770, 2001b.

Pacheco-Vega, A., Sen, M., Yang, K.T. and McClain, R.L. Heat rate predictions in humid air-water heat exchangers using correlations and neural networks, J. Heat Transfer, 123: 348-354, 2001a.

Plint and Partners Ltd. Manual for cross flow heat exchanger-Model TE93/A, England, 1981.

Ranganayakulu, C.H. and Seetharamu, K.N. The combined effects of wall longitudinal heat conduction, inlet fluid flow nonuniformity and temperature nonuniformity in compact tube-fin heat exchangers: a finite element method, Int. J. Heat Mass Transfer, 42(2): 263-273, 1999a.

Ranganayakulu, C.H. and Seetharamu, K.N. The combined effects of longitudinal heat conduction, flow nonuniformity and temperature nonuniformity in crossflow plate-fin heat exchangers, Int. Commun. Heat Mass Transfer, 26(5): 669-678, 1999b.

Zhukauskas, A. Heat transfer from tubes in cross flow, In J.P. Hartnett & T.F. Irvine Jr., Eds., advances in heat transfer, Vol. 8. Academic Press, New York, 1972.

Ife Journal of Technology, Vol. 18 (2), 15-18, 2009

Full Paper

POTENTIAL OF DIKA NUT OIL AS LUBRICANT FOR SUSTAINABLE TECHNOLOGICAL GROWTH

O. A. Abidakun
Department of Mechanical Engineering,
Obafemi Awolowo University, Ile-Ife, Nigeria
dejabonline@yahoo.com

O. A. Koya
Department of Mechanical Engineering,
Obafemi Awolowo University, Ile-Ife, Nigeria

ABSTRACT

The paper presents a report on the physico-chemical properties and lubricity grade of refined Dika nut oil for use as lubricant, in consonance with sustainable technological development for vision 20:2020. Chemical properties such as iodine, acid and saponification values of the oil were evaluated. The physical properties of the oil were characterized in terms of its density, viscosity at 40 and 100°C, flash and pour points. The lubricity of the oil was estimated on the basis of its viscosity, comparing with Society for Automotive Engineering (SAE) oil grades. Test results showed that the oil has the following physical properties: viscosity of 57.57 cSt at 40°C and 6.78 cSt at 100°C; viscosity index of 71; flash point of 296°C; cloud point of 37°C; pour point of 32°C; and specific gravity of 0.928 at 15°C. The chemical properties in terms of its oxidative stability, saponification, acid and iodine values were 250 hours, 199.72 mgKOH/g, 0.3 mgKOH/g and 0.518%, respectively. The viscosity of the oil at 40 and 100°C ranked between SAE 20 and 30 lubricating oil at both temperatures. The oil, thus, shows a strong potential for use as lubricant.

Keywords: Biodegradable, lubricant, Dika nut, lubricity, oiliness

1. INTRODUCTION

The key goal of vision 20:2020 is to make Nigeria one of the 20 largest economies in the world, to consolidate her leadership role in Africa and establish her as a significant player in the global economic and political arena (Nigeria Vision 2020, 2009). This expectation suggests a definite need for increase in technological growth in the exploitation of the vast natural resources of the country. This will ultimately lead to a diversification of the economy, to relieve the country's over reliance on crude oil. The projection (Iseghohi, 2008) of a Gross Domestic Product of between $500 and $800 could then be feasible.

The expected technological growth implies that more machines and vehicles will be put to use and, there will be increasing demands for lubricants in the maintenance of the machines. It is also well known that without the improvement in lubricant technology, the advancement achieved in other branches of engineering such as design and manufacturing of machineries would have been impossible (Dara, 2007). Currently, nearly all lubricants in use in the country are petroleum based, with the attendant risk of environmental degradation when disposed because mineral oils are non-biodegradable. Researchers (Oseni et al., 2006; Marth, 2007; Petlyuk and Adams, 2004) have therefore focused on the development of straight and blended vegetable oil-based lubricants, which are non-toxic and are biodegradable. This is strictly important, because about 60% of spent lubricants end up in the soil and water, constituting environmental hazard if non-biodegradable.

A data bank of classification of available vegetable oil lubricants is therefore essential, to provide viable alternatives to the mineral oils, in the anticipated technological growth. Vegetable oils are renewable and are also preferred in certain applications where mineral oil contamination is inadmissible (Honary, 2004). Increased use of the oil-seeds will also stimulate new challenges in crop production and bioengineering, to contribute further to attaining the vision 20:2020.

In this regard, many oil seeds such as, linseed with 35 to 44% oil content (Willem et al., 2008; Ibrahim and Onwualu, 2005); groundnut, 38 to 50% (Ibrahim and Onwualu, 2005; Adeeko and Ajibola, 1990) and palm kernel, 46 to 57% (Akinoso et al., 2006; Faborode and Favier, 1996) have been exploited. However, the Dika kernel which contains about 60% oil, large quantity of saturated fatty acid, small quantity of unsaturated fatty acid and similar chemical constituents when compared with palm kernel, remains unexploited for its lubricity (Leakey and Tchoundjeu, 2001; Ogunsina et al., 2008; Atangana et al., 2002). In addition, the Dika tree has been identified as the most important tree for domestication in West and Central Africa, because of its termite resistant wood (Leakey et al., 2004). A corresponding effort in the increased exploitation of the crop is therefore worthwhile as it would add to the needed impetus for its cultivation.

Consequently, the goal in this work was to determine the suitability of Dika nut oil as lubricant. However, impurities are not desirable in lubricants, so that, the refined Dika nut oil was used. Also, because the lubricity of oil depends on its physico-chemical properties, the main objectives of this work, therefore, were to:

(a) determine the physical properties such as viscosity, pour and flash points, and density of refined Dika nut oil;
(b) evaluate chemical properties of the oil; and
(c) obtain the lubricity grade of the oil.

2. MATERIALS AND METHODS

2.1. Materials Preparation

Based on a preliminary experiment (Abidakun, 2009) coarsely ground Dika kernel (particle size of between 1.4 and 2.8 mm) at 6% moisture content (w.b.) was preheated at 100oC for 10 minutes and pressed in a hydraulic press to extract the oil. The oil was then refined by adding 3% by volume of water to the expressed oil. The mixture was agitated mechanically for 60 minutes at 70°C, to hydrate the phospholipids and gums. The oil was filtered and 1% concentrated alkali solution (Sodium hydroxide) was added to neutralize the free fatty acids. The alkali solution was added to the oil, heated to 40oC in an oven and was properly mixed for 35 minutes. The temperature was then increased rapidly to 60oC, to break the emulsion. Temperature was monitored by using a thermocouple with digital readout. After breaking the emulsion, the heat was turned off and the solution was allowed to settle for 4 hours before it was filtered. Distilled water, 10% by volume preheated to 50oC was added to the neutralized oil and then heated to 95oC for 4 hours in order to evaporate the water. This was followed by drying with Silica gel to obtain the refined oil.

2.2. Determination of Chemical Characteristics

2.2.1 Neutralisation value

A measure of 5 g of refined Dika nut oil was weighed into a dried 250 mL flask, using a digital electronic balance, Mettler PL 1200, with precision of 0.001 g. A quantity of 50 mL of solution made up of equal volume of 95% ethanol and diethyl ether was added and then gently mixed to dissolve the oil. The mixture was heated at 40°C to bring mixture to complete solution. The mixture was then titrated with 0.1 N Methanoic potassium hydroxide (KOH), using 1 mL of phenolphthalein indicator, until a slight pink colour persisted for 15 seconds. The acid value was computed (Fasina, 1988) using Equation 1.

$$\text{Acid value} = \frac{\mathrm{V}\times\mathrm{F}\times 56.1}{\mathrm{m}} \quad \ldots \quad (1)$$

where, V is sample titre value in mL; F is Normality for Me-KOH and m is the sample mass in g.

2.2.2 Saponification value

A measure of 2 g of Dika nut oil was weighed into a conical flask, and 25 mL of 0.5 alcoholic KOH was added to the oil in the flask. A long air condenser was attached and the flask was heated until the solution became homogenous (saponification was completed). The boiling, accompanied by agitating the content occasionally, was done for 30 minutes at such rate as to prevent loss of alcohol from the air condenser. The solution was allowed to cool and 1 mL of phenolphthalein indicator was added; while the excess alkali was titrated with 0.5 N HCl. A blank determination at the same time and under the same conditions using the same quantity of KOH solution was carried out. The saponification value was obtained (Fasina, 1988) as follows

$$\text{Saponification Value} = \frac{56.1\times\mathrm{N}\times(\mathrm{V}-\mathrm{U})}{\mathrm{W}} \quad \ldots \quad (2)$$

where, V is the blank level in mL; U is the titration volume for sample in mL; W is the mass of sample in g; N is the normality HCl solution; and 56.1 is the concentration conversion coefficient for the potassium hydroxide used. The 56.1 is the equivalent mass of potassium hydroxide.

2.2.3 Iodine value

A quantity of 0.25 g of dika nut oil was weighed into a 300 mL glass stoppered bottle and 10 ml chloroform was added to dissolve the oil. Hanus iodine solution of 30 mL was then added from a pipette and was stirred by swirling the content of the stoppered flask. The bottle was allowed to stand for 30 minutes to complete the halogenation. Thereafter, 20 mL of 15% potassium iodide and 100 mL of distilled water were added to separate the chloroform from the solution. The solution was then titrated with Sodium thiosulphate solution using 2 mL of starch indicator solution. A blank containing all the components except Dika nut oil was carried out following the same procedure as stated above and the iodine value was determined (Fasina, 1988) using Equation 3.

$$\text{Iodine value} = \frac{(T_b - T_s)\times N\times 12.69}{W} \quad \ldots \quad (3)$$

where, T_b is mL of thiosulphate solution for blank titration; T_s is mL of thiosulphate solution for sample; N is normality of sodium thiosulphate; W mass of sample in g; and 12.69 is the equivalent mass of iodine.

2.3. Determination of Physical Properties

2.3.1 Viscosity

The refined oil was sucked into one arm of a viscometer using its auxiliary pump. The viscometer was then placed inside the thermostatic oil bath which had been pre-heated to the required temperature. The viscometer containing the oil was placed inside the bath for 30 minutes, to adjust the temperature of the oil to that at which the viscosity was to be taken. The oil was sucked into the second arm of the viscometer and the time taken in seconds for the oil to flow through an orifice at this temperature was noted. The kinematic viscosity of the oil was derived following the procedure by the viscometer manufacturer. The viscosity of the oil was taken at 40 and 100°C.

2.3.2 Cloud and pour points

The cloud and pour point were determined by placing a quantity of the heated oil inside a test tube, and introducing it into a cold bath. The test tube was swirled gently but steadily in the bath to facilitate even dissipation of heat. The cooling continued until the oil became solidified. The temperature of the oil at which the first cloudy oil was noticed was taken as the cloud point; while, the temperature at which there was no movement of oil when the test tube was bent horizontally was taken as the pour point.

2.3.3 Flash point

The Penken Martens close cup flash point tester was used for determining the oil's flash point. The cup was filled to a specified point with the refine oil and placed inside the holder so as to heat it over a flame. As the heating continued, the flame placed at a distance from the oil's surface travels across the surface of the oil. This continued until a spark was notice on the surface of the oil. The temperature at which the spark occurred was taken as the flash point.

2.3.4 Oxidative stability

The oxidative stability of the oil was determined following the ASTM D943 method (Petlyuk and Adams, 2004). One percent by volume of water was added to 200 mL of oil placed inside a container with metallic copper as catalyst to the oxidation reaction. This combination was heated at 150°C in the open air so as to provide the oxygen required for the oxidation. The neutralization number of the heated oil was tested at intervals of fifty hours in order to determine the time at which the oil's neutralization number was up to 2 mgKOH/g of the oil.

2.3.5 Specific gravity

The oil was heated and poured into a 1000 mL measuring cylinder to permit the determination of the specific gravity. Graduated glass hydrometers were dropped inside in turns until the one where the reading could be made was achieved. The value of the specific gravity was then read off the graduated stem of the glass hydrometer. The specific gravity was determined at 36°C and was converted to specific gravity at 15°C by using the relationship (Godfrey and Herguth, 1996) in Equation 4.

$$S.G_{@15/15} = [(T - 15^{o}C) \times 0.00061] + Y \quad \ldots \qquad (4)$$

where, T is the temperature at which the specific gravity was determined using the hydrometer and Y is the observed specific gravity at temperature T.

2.4. Assessment of Lubricity Grade

In order to determine the lubricity grade, the refined oil was charted against the SAE viscosity chart (Hamrock et al., 1998) using the value of the kinematic viscosity obtained at 40 and 100°C. The chart was then used to obtain the range within which the oil was ranked on SAE scale. The refined Dika nut oil was also compared with commercial grade lubricants: biodegradable hydraulic oil SAE 10W (ISO VG 46); engine oil, SAE 10W-40; and way lubricant ISO 68.

3. RESULTS AND DISCUSSION

A summary of the physico-chemical properties of oil is shown in Table 1. The oil exhibited an iodine value of 0.518% which indicates a tendency of high viscosity. High iodine value is undesirable because it lowers the viscosity of oil, and increases the oil's rate of oxygen absorption from the air at ordinary temperature. Oxygen absorption causes polymerization of the acid and renders the oil unfit for lubrication due to rapid sludge formation (Akbar et al., 2009).

A high saponification value of 199.72 mgKOH/g shows that the oil has high molecular weight fatty acids, which is an indication of high antifriction property. The importance of high saponification value is further reiterated by the addition of fatty additives to certain lubricants such as worm gear oils, steam cylinder oils, machine tool way lubricants, and pneumatic tool oils so as to improve their antifriction properties (Akbar et al., 2009). Also, the refined oil has an acid value of 0.3 mgKOH/g, which is relatively low enough to make it suitable for use as a lubricant. An ideal lubricant should be free from acids which cause corrosion of the metals in the system and results in the oil's poor oxidative stability (Bongardt, 1995).

The kinematic viscosity of the oil is 57.57 cSt at a temperature of 40°C, 6.78 cSt at 100°C, yielding a viscosity index of 71. On the basis of the viscosity, refined Dika nut oil lies between SAE 20 and 30 lubricating oil at 40°C and 100°C (Fig. 1). The viscosity index which shows how much the viscosity of the oil changes with temperature, falls within the range of 55 and 100, where the viscosity index of most industrial mineral lubricating oils lie (Godfrey and. Herguth, 1996). The low viscosity index shows that the oil's viscosity will change rapidly with temperature. However, the viscosity index can be enhanced by adding some viscosity index improver.

The observed flash point of 296°C for refined Dika nut oil is higher than 165°C and 146°C required for turbine and insulating oil, respectively (Demirbas, 2008). This shows that the oil can be used as lubricant without fear of fire hazard. The value of flash point obtained compares favourably well with flash point of other vegetable oils: 247°C for linseed, 228°C for palm oil, 255°C for soybean oil and 270°C for peanut oil (Demirbas, 2008). The value obtained was also higher than that of other commercial lubricants (Table 2). A high flash point is desirable for lubricants because it provides good resistance to combustion and a low degree of evaporation at normal temperatures. For a lubricant, flash point in the range of 149°C to 265°C are required for the lightest and heaviest oils, respectively.

Pour point which is the lowest temperature at which the oil becomes solid is relatively high for this oil when compared with other commercial grade lubricants (Table 2). A low value of pour point is required for a lubricant to function well at low temperature. Cloud and pour point of 37 and 32°C, respectively, were observed for the refined Dika nut oil. These values are too high and, show that the oil has poor low temperature property. The low temperature property can be improved by introducing appropriate pour point depressant additives (Godfrey and Herguth, 1996).

The refined oil has a specific gravity of 0.928 at 15°C and this falls within the range 0.86 to 0.98 exhibited by mineral oils (Godfrey and Herguth, 1996). The value of specific gravity obtained for this oil shows that the oil is lighter than water and will float when spilled in water. It is therefore not suitable for use in underwater military operations (Marth, 2007).

For the refined Dika nut oil to serve its intended function as a lubricant, a high oxidative stability is required. Refined Dika nut oil has an oxidative stability of 250 hours which is relatively high compared to the values for other vegetable oils such as, soybean and linseed (Honary, 2004). Vegetable oils generally have poor oxidative stability, but could be improved by adding oxidation inhibitor additives to suppress the oxidation reaction, so as to prevent the formation of more acid.

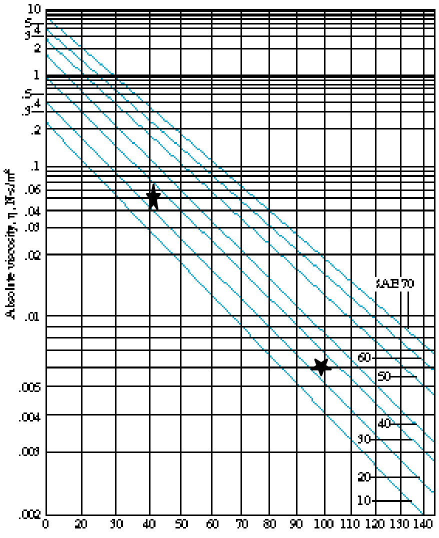

Figure 1: *SAE lubricating oil chart showing the position of refined Dika nut oil at 40 and 100°C; ★, Dika nut oil; SAE chart from Hamrock et al. (1998).*

4. CONCLUSION

The physical and chemical properties of refined Dika nut oil were evaluated to verify the suitability of the oil for use as lubricant. In view of the biodegradability of vegetable oils, the Dika nut oil with acid value of 0.3 mgKOH/g; iodine value of 0.518%; saponification value of 199.72mgKOH/g; flash point of 296°C and specific gravity of 0.928 showed a strong potential for use as environmentally friendly lubricant. The oil, however, requires the addition of appropriate viscosity index improver and pour point depressant to make it suitable for use at temperature below 32°C. On the basis of its viscosity, the oil was ranked between SAE 20 and 30 lubricating oil at 40°C and 100°C. Conclusively, Dika nut oil provides a source of future lubricant and economic benefits while reducing environmental impact.

Table 1: Properties of Dika nut oil

S/N	Properties	Values
1	Acid Value (mgKOH/g)	0.3
2	Saponification value (mgKOH/g)	199.72
3	Iodine value (%)	0.518
4	Kinematic Viscosity at 40 °C (cSt)	57.57
5	Kinematic Viscosity at 100 °C (cSt)	6.78
6	Viscosity Index	71
7	Flash point (°C)	296
8	Cloud point (°C)	37
9	Pour point (°C)	32
10	Specific gravity at 15 °C	0.928
11	Oxidative stability (hours)	250

Table 2: Properties of Dika nut oil and other types of lubricant

Properties	Oil Type			
	A	B	C	D
Kinematic Viscosity at 40°C	48.7	108.5	68.4	57.57
Kinematic Viscosity at 100°C	8.7	15.4	8.8	6.75
Viscosity Index	160	149	101	71
Flash point	220	220	236	296
Cloud point	-	-	-	37
Pour point	- 58	- 33	- 12	32
Specific gravity at 15°C	0.921	0.872	0.885	0.928

A is Biodegradable hydraulic oil SAE 10W (ISO VG 46); B is Engine oil SAE 10W-40; C is Way lubricant ISO 68; and D is the refined Dika nut oil. Properties of the commercial lubricants were taken from Abidakun (2009)

REFERENCES

Abidakun, O.A. Mechanical expression and lubricity of *Irvingia gabonensis* (Dika nut) oil, M.Sc. thesis, Department of Mechanical Engineering, Obafemi Awolowo University, Ile-Ife, Nigeria, 2009.

Adeeko, K.A. and Ajibola, O.O. Processing factors affecting yield and quality of mechanically expressed groundnut oil. Journal of Agricultural Engineering Research, 45: 31-43, 1990.

Akbar, E. Yaakob, Z. Kamarudin, S.K. Ismail, M. and Salimon, J. Characteristic and composition of *Jatropha Curcas* oil seed from Malaysia and its potential as biodiesel feedstock. European Journal of Scientific Research, 29(3): 396-403, 2009.

Akinoso, R. Igbeka, J. and Olayanju, T. Process optimization of oil expression from sesame seed (*Sesamum indicum Linn.*). Agricultural Engineering International: the CIGR Ejournal, Manuscript FP 06 011. Vol. VII, 2006.

Atangana, A.R. Ukafor, V. Anegbeh, P. Asaah, E. Tchoundjeu, Z. Fondoun, J.M. Ndoumbe, M and Leakey, R.R.B. Domestication of Irvingia gabonensis: The selection of multiple traits for potential cultivars from Cameroon and Nigeria. Agroforestry Systems, 55: 221-229, 2002.

Bongardt, F. Schmid, K. and West, R. Environment-friendly basic oil for formulating hydraulic fluids, US Pat. 5451334 United States Patents and Trademark Office, 1995.

Dara, S.S. A Textbook of Engineering Chemistry Tenth Revised Edition. S. Chand and Company ltd: New Delhi, 2007.

Demirbas, A. Relationships derived from physical properties of vegetable oil and biodiesel fuels. Fuel, 87: 1743–1748, 2008.

Faborode, M.O. and Favier, J.F. Identification and Significance of the Oil-point in Seed-oil Expression. Journal of Agricultural Engineering Research, 65: 335-345, 1996.

Fasina, O. O. Mechanical expression of oil from conophor nut (*Tetracarpidium cocophorum*), M.Sc. thesis, Department of Agricultural Engineering, Obafemi Awolowo University, Ile-Ife, Nigeria, 1988.

Godfrey, D. and Herguth, W.R. Physical and Chemical Properties of Industrial Mineral Oils affecting Lubrication. Lubrication Engineering, 52(2): 145-148, 1996.

Hamrock, B.J. Jacobson, B.O. and Schmid, S.R. Fundamentals of Machine Elements. WCB McGraw Hill, London, 1998.

Honary, L.A.T. Biodegradable/Biobased Lubricants and Greases. http://www.machinerylubrication.com/article_detail.asp?articleid=240, 2004. (Retrieved on 5th April, 2008).

Ibrahim, A. and Onwualu, A.P. Technologies for extraction of oil from oil-bearing agricultural products: A review, Journal of Agricultural Engineering and Technology, 13: 58-70, 2005.

Iseghohi, T. Vision 20-20-20: Reality or Rhetoric—Nigeria's GDP must hit $800bn to realize 202020 dream. http.//www.nigeriaeconomicnews.com, 2008. (Retrieved 28th April, 2008).

Leakey, R.R.B and. Tchoundjeu, Z. Diversification of tree crops: Domestication of companion crops for poverty reduction and environmental services. Cambridge University Press, 37: 279-29, 2001.

Leakey, R.R.B. Greenwell, P. Hall, M.N. Atangana, A.R. Usoro, C. Anegbeh, P.O. Fondoun, J.M. and Tchoundjeu, Z. Domestication of Irvingia gabonesis: Tree-to-tree variation in food-thickening properties and in fat and protein contents of Dika nut, Food Chemistry, 90(3): 365-378, 2004.

Marth, J.S. Renewable Lubricant Manual: Biobased Oils, Fluids and Greases. http.//www.renewablelubricants.com/RenewableLubricantsManual, 2007. (Retrieved on 12th May, 2008).

Nigeria Vision 2020, Concept Paper for Development of Vision 2020. http./.www.nv2020.org, 2008. (Retrieved on 10th June, 2009).

Ogunsina, B.S. Koya, O.A. and Adeosun, O.O. Deformation and fracture of Dika nut (*Irvingia gabonesis*) under uniaxial compressive load. International. Agrophysics, 22: 249-253, 2008.

Oseni, M.I. Ette, A.O., and Lortyer, H. The rheological behaviour of straight and blended natural oil lubricant. Ife Journal of Technology, 15: 63-71, 2006.

Petlyuk, A.M. and Adams, R.J. Oxidation stability and tribological behaviour of vegetable oil hydraulic Fluids. Tribology Transactions, 47(2): 182-187, 2004.

Willem, P. Kuipers, N.J.M. and Haan, A.B. Gas assisted mechanical expression of oil seeds: Influence of process parameters on oil yield. The Journal of Supercritical Fluids, doi: 10.10/jsuperflu2008. 01.010, 2008.

Ife Journal of Technology, Vol. 18 (2), 19-25, 2009

Full Paper

EVALUATION OF PHYSICO-CHEMICAL PROPERTIES AND PROXIMATE COMPOSITION OF PROBIOTICATED GINGER-BASED BEVERAGES

T.M. Ukeyima
Department of Food Science and Technology
University of Agriculture, Makurdi, Benue State

H.A. Adeniran
Department of Food Science and Technology, Obafemi Awolowo University, Ile-Ife, Osun State
hadeniran@oauife.edu.ng

S.H. Abiose
Department of Food Science and Technology, Obafemi Awolowo University, Ile-Ife, Osun State

ABSTRACT

The study evaluated the effect of *probiotication* on the physico-chemical characteristics and proximate composition of two ginger-based functional drinks. Probiotic ginger and ginger with garlic beverages were produced by inoculating the beverages with Lactic acid bacteria (LAB), *Lactobacillus plantarum* and *Lactobacillus bulgaricus* isolated from fermented sorghum grains and yoghurt, respectively. The beverages were stored at both ambient (27 ± 1 °C) and refrigeration (4 ± 1 °C) temperatures for a period of four weeks. Titratable acidity, pH, reducing sugars and proximate composition of the beverages were determined. Results showed that probiotic isolates reduced the pH of the beverages from 4.17 ± 0.40 to 3.04 ± 0.20 and increased the titratable acidity from 0.35 ± 0.10 to 0.84 ± 0.15. There was a reduction in total reducing sugars and carbohydrate content from 0.65 ± 0.22 mg/ml and 7.88 ± 0.03 % to 0.51 ± 0.15 mg/ml and 6.71 ± 0.10%, respectively. The crude protein and fat content increased from 2.33 ± 0.02 to 2.72 ± 0.01 % and 0.05 ± 0.01 % to 0.29 ± 0.02%, respectively throughout the period of storage. Health promoting drinks with minimal physico-chemical and proximate changes could be produced by inoculating ginger-based beverages with probiotic LAB.

Keywords: Physico-chemical, proximate, probiotic bacteria, ginger beverage.

1. INTRODUCTION

A food can be regarded as functional if it is satisfactorily demonstrated to affect beneficially one or more target functions in the body, beyond adequate nutritional effects, in a way that is relevant to either improved stage of health and well being and/or reduction of risk of disease. Functional food may be considered as a therapeutic aid available without prescription. With functional food, various functions of organisms can be modulated (Gibson and Williams, 2000; Tomasik and Tomasik, 2003)

Japan, the birthplace, of the concept of functional food has adopted Foods for Specified Health Use (FOSHU) since 1991 to describe functional foods. Foods identified as FOSHU are required to provide evidence that the final product, but not isolated individual component(s), is likely to exert a health or physiological effect when consumed as part of an ordinary diet. Moreover, FOSHU products should be in the form of ordinary foods (i.e. not pills or capsules) (Roberfroid, 2000)

Fermented beverages constitute an integral part of the diet in most tropical and sub-tropical countries. The biochemical changes in plant materials during fermentation into beverage products have been investigated (Abiose and Adedeji, 1994)

Ginger beverage is produced with ginger rhizome as the major constituent and other minor constituents such as garlic, aloe vera, fruit juice and sweetened with sucrose or honey while ginger with garlic beverage is produced using ginger, garlic and sweetened with honey.

Ginger (*Zingiber officinale*) along with some 1,400 species of plants is placed in the family Zingiberaceae. Ginger contains volatile oil (inc. borneol, citral), phenols, alkaloid, and mucilage (Foster, 2008)

For ages, it has been embraced by the Chinese in the treatment of elevated blood pressure, elevated body temperature, persistent coughs, all kinds of colds and flu, and other related problems of the respiratory system. Fresh and dried ginger is used as two distinct and different herbal remedies. Fresh ginger has been applied in the treatment of fevers, headaches, and to alleviate the pain and discomfort of aching muscles in the body. Dried ginger remedy is used for the treatment of internal colds, and for physical symptoms such as cold and clammy hands, a weakening of the pulse rate, and a pale or white complexion in patients. Ginger-based preparations are also used in the treatment of joint stiffness, in the topical alleviation of abdominal cramps, in the treatment of kidney stone attacks, to treat stiffness in the neck, to treat neuralgia in different parts of the body. In addition, ginger compresses are employed topically to treat toothache, bladder inflammation, prostatitis and extreme tension in the body. Disorders such as nausea, accumulated intestinal gas, motion sickness, colic can also be treated using herbal remedies made from the ginger.

Garlic (*Allium sativum*) is a member of the Amaryllis family (Amaryllidaceae), which also includes leeks, onions, and shallots. It is a perennial with an underground bulb and is composed of pungent bulblets commonly called cloves (Harris, 1997).

Garlic is made up of several important components. When garlic bulbs are crushed, alliin, an odourless sulphur-containing chemical derived from the amino acid cystein, is converted into another compound called allicin. Allicin appears to be at least one of the primary active compounds that gives garlic its characteristic odor and many of its healing benefits. Allicin confers infection – fighting action, and the ability to lower blood pressure and cholesterol on garlic. Its antimicrobial properties on *Salmonella*, *E. coli*, and some gram-positive bacteria have been documented (Quattara et al., 1997.

Honey is carbohydrate-rich syrup produced by bees, primarily from floral nectars. Besides a high content of a range of saccharides, there are also organic acids, amino acids, mineral matter, colours, aromatic substances and a trace amount of fats. Besides, honey contains very valuable but unstable compounds, such as enzymes, substances of hormonal character, some vitamins and a few minor compounds. Honey has been demonstrated in many studies to have antibacterial effect, on a range of enteropathogenic strains including *Salmonella typhi*, *Vibrio cholerae* and *Yersinia enterocolitica*. It has also been successfully applied in the treatment of abdominal wounds, ulcers, wounds, gangrene and a host of other illnesses (Obi et al., 1994).

The lactic acid bacteria, a group of probiotic microbes, have been found to play a fundamental role in the gut, which enables them to influence the colonization of the gut by other organisms, which are beneficial to the host (Havenaar and Veld, 1992.; Senjong et al, 2000). Other beneficial characteristics that influence their choice include their: easy reproducibility, ability to survive the environmental conditions of the location where they are active, their genetic stability without plasmid transfer, the absence of allergic, toxic, mutagenic or carcinogenic reactions neither its fermentation products nor its cell components being deleterious after consumption by the host, ability to remain viable during processing and, ability to adhere to and colonize the location where they are active (Havenaar, and Veld, 1992; Wolfgand, et al., 1999; Senjong, et al, 2000). For some time now, lactic acid bacteria and bifidobacteria are employed as probiotics in foods especially in fermented dairy products. The new trend is to incorporate probiotics in other foods and drinks as a result of quest of consumers for health promoting functional foods.

There is a rising global demand by consumers for these products due to their health promoting potentials. This work therefore, evaluates the physico-chemical changes associated with ginger-based beverages inoculated with probiotic lactic acid bacteria and stored at both ambient and refrigeration temperatures for a period of four weeks.

2. MATERIALS AND METHODS

2.1. Materials

Ginger Sorghum grains, ginger rhizomes and garlic were obtained from a local market in Ile-Ife, Osun State; pure honey was obtained from a reputable supplier on campus while yoghurt was prepared in the laboratory. The pathogenic organisms, *Escherichia coli* and *Staphylococcus aureus* used were obtained from the Department of Microbiology, Obafemi Awolowo University, Ile-Ife.

2.2. Bacterial Isolates For *probiotication*

Standard methods were employed in isolation and characterization of Lactobacilli spp. from steeped water of sorghum and maize grains, and yoghurt (Harrigan, 1998).

They were identified as *Lactobacillus plantarum* and *L. bulgaricus*

2.3. Preparation Of Probiotic Ginger And Ginger With Garlic Beverage

Ginger beverage was prepared using the modified method of (Osuntogun and Aboaba, 2004). This was done by peeling 400 g of wholesome fresh ginger rhizomes and wet milling with 500 ml of water. After wet milling, water (4.5 liters) was added to the smooth paste and subsequently strained through a clean white muslin cloth to obtain the ginger extract. The filtrate was left for 8 hours to sediment with a clear supernatant. The supernatant was sweetened by adding 1000 ml of pure honey. The sweetened ginger extract was kept in the refrigerator for 3 hours for the second sedimentation where the supernatant formed was decanted and dispensed into 500 ml screw cap glass bottles.

The ginger beverage was sterilized by autoclaving at 121°C for 15 minutes, allowed to cool to ambient temperature and finally inoculated separately with 10% probiotic isolates (*Lactobacillus plantarum* and *Lactobacillus bulgaricus*). Ginger with garlic beverage was prepared following the same procedure except that 50 g of garlic was added and milled thoroughly. Inoculated beverages were subsequently stored at ambient and refrigeration temperatures for a period of four weeks. On weekly basis, pH, titratable acidity, reducing sugar content as well as the proximate composition of the *probioticated* ginger, and ginger with garlic beverages were evaluated.

2.4. Titratable Acidity and pH Determination

Titratable acidity was determined according to (Harrigan, 1998) method while pH was measured using a Pye unicam Model 290 pH meter (AOAC, 2000).

2.5. Reducing Sugar Determination

This was determined using the dinitrosalicyclic acid (DNSA) method which involved boiling a known amount of sample with known amount of DNSA and determining its absorbance at 540nm in a spectrophotometer. Absorbances of samples were used as estimates of sugar concentrations when compared with a standard glucose calibration curve. The curve was obtained by plotting absorbances of glucose (of varying concentrations) boiled with DNSA reagent using a Pharmacia Biotech Novaspec 2 model spectrophotometer (Miller, 1959; Adeniran and Abiose, 2009).

2.6. Proximate Composition

Protein, fat, ash, moisture, crude fibre, carbohydrate and total solid content of the probioticated samples over the period of storage to assess the effect of probiotication on the samples (AOAC, 2000).

2.7. Statistical Analysis

The data obtained were subjected to analysis of variance and means of triplicate values were compared using Duncan's multiple range test (Steel et al., 1997).

3. RESULTS AND DISCUSSION

3.1. Titratable Acidity and pH of Probiotic Ginger and Ginger with Garlic beverages

The total titratable acidity values of ginger beverage inoculated with *Lactobacillus plantarum* is shown in Fig.1. At ambient temperature storage, the total titratable acidity increased from an initial value of 0.40 to 0.84 at the 4th week while at refrigeration temperature it increased from 0.40 to 0.59 at the 4th week of storage. There was an initial increase in total titratable acidity from 0.45 to 0.83 and 0.67 at ambient and refrigeration temperatures respectively in ginger with garlic beverage at the 4th week of storage.

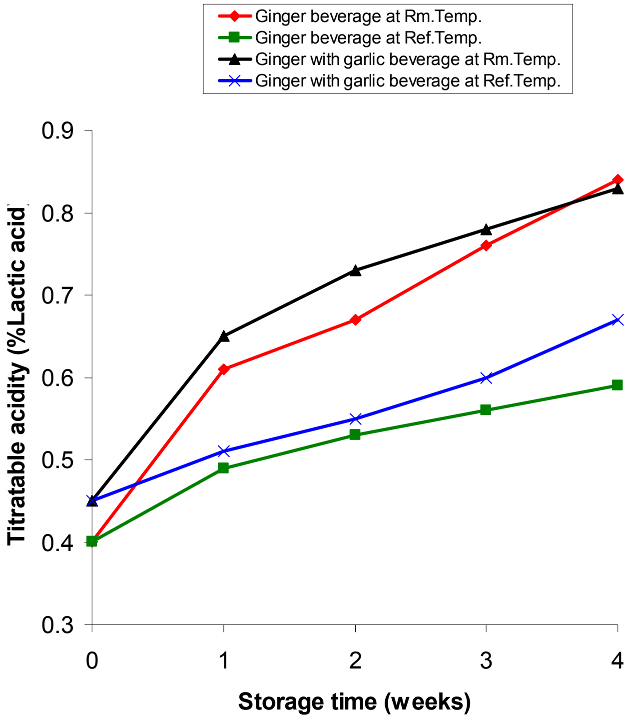

Fig.1: Percentage titratable acidity of ginger and ginger with garlic beverages inoculated with L. plantarum stored at ambient and refrigeration temperatures.

The changes in pH of the beverages inoculated with *Lactobacillus plantarum* is shown in Fig.2. At ambient temperature, the pH declined from an initial value of 3.92 to 3.04 after 4 weeks of storage while during refrigeration storage, the pH ranged between 3.92 and 3.51. A similar trend was observed in ginger with garlic beverage. Ginger is reported to contain 9.11 % wet weight starch (Oti and Mgbolu, 1987). Utilization of the sugars and/or the starch could have caused production of organic acids as end products of fermentation thus lowering the pH of the medium (Schillinger and Lucke, 1987). There was a significant difference ($p < 0.05$) in the change in pH between ginger and ginger with garlic beverages stored at ambient and refrigeration temperatures. The relatively stable pH values of samples stored at refrigeration temperature could be attributed to the effect of cold storage on the microbial cells and its metabolic activities (Yoon et al, 2004).

Ginger beverage that was inoculated with *Lactobacillus bulgaricus* exhibited a similar trend in the increase of titratable acidity and decline in pH values during the period of storage at both storage temperatures (Figs 3 and 4).

3.2. Total Reducing Sugar Content of Probiotic Ginger Beverage

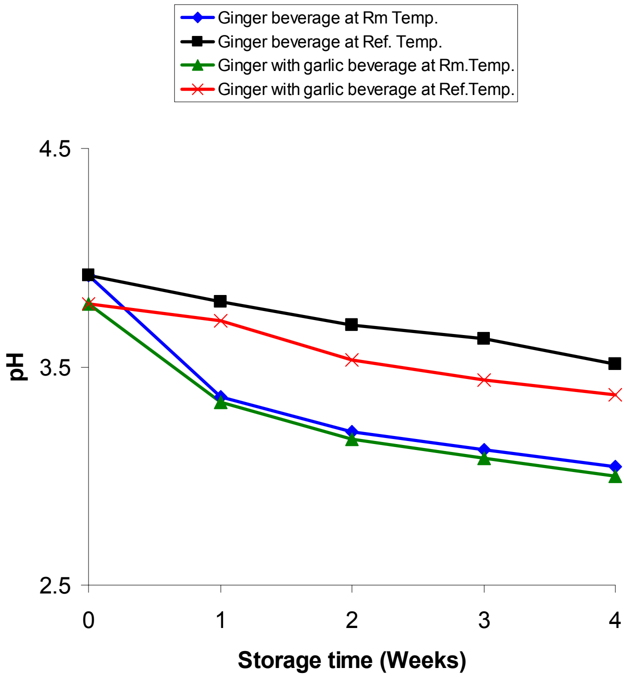

Fig. 2: pH values of ginger and ginger with garlic beverages inoculated with L. plantarum stored at ambient and refrigeration temperatures

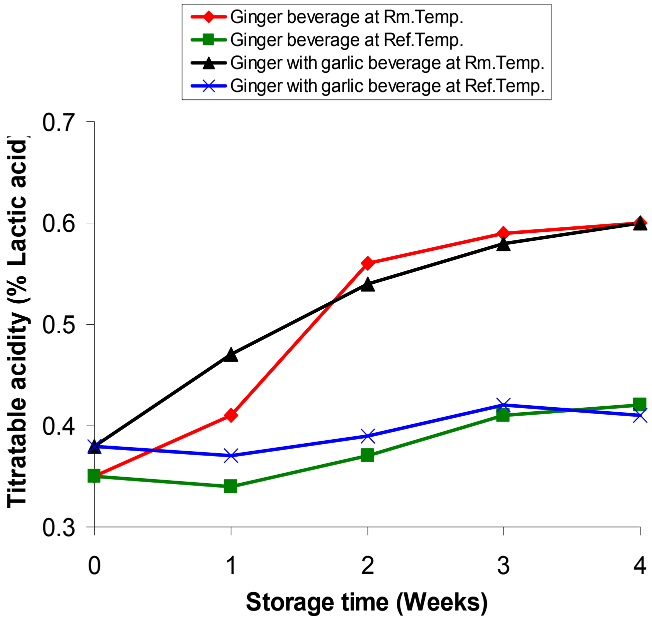

Fig. 3 Percentage titratable acidity of ginger and ginger with Garlic beverages inoculated with L. bulgaricus stored at ambient and refrigeration temperatures

The total reducing sugar content of ginger and ginger with garlic beverages inoculated with *Lactobacillus plantarum* and stored at ambient and refrigeration temperature is presented in Fig 5. The reducing sugar content of ginger samples increased from the initial value of 0.65 mg/ml to 0.70 mg/ml after the first week of storage at ambient temperature. During the remaining period of storage, the sugar content decreased consistently to 0.51 mg/ml at the 4th week of storage. At refrigeration temperature just as in

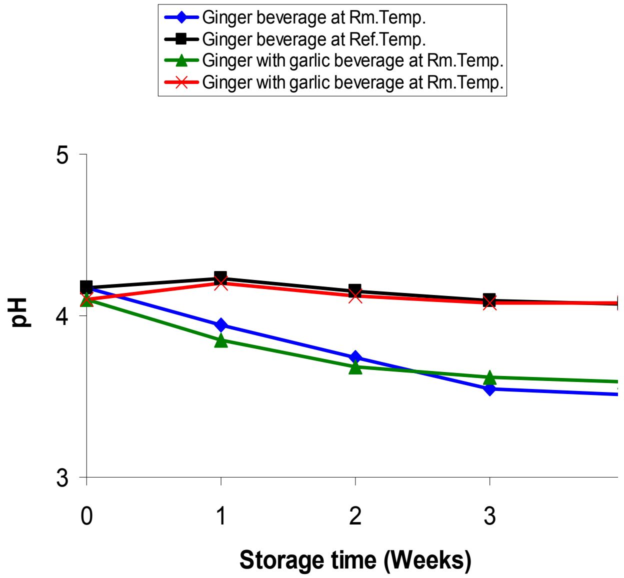

Fig. 4: pH values of ginger and ginger with garlic beverages inoculated with L. bulgaricus stored at ambient and refrigeration temperatures

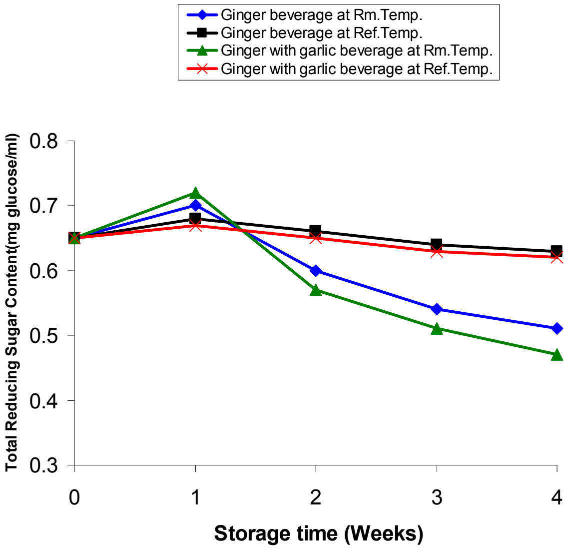

Fig. 5 Total reducing sugar content of ginger and ginger with garlic beverages inoculated with L. plantarum stored at ambient and refrigeration temperatures

ambient temperature storage, a gradual decrease in sugar content was observed in the two samples of ginger and ginger with garlic beverages. There was no significant difference ($p > 0.05$) in the decrease of reducing sugars in ginger and ginger with garlic beverages inoculated with *Lactobacillus plantarum* and stored at ambient and refrigeration temperatures. Samples *probioticated* with *Lactobacillus bulgaricus* displayed a similar trend, the initial sugar content at week zero increased slightly from 0.65 to 0.68 mg/ml at week one and gradually reduced to 0.62 mg/ml at the end of storage period. During refrigeration storage the sugar content was relatively stable throughout the storage period. A similar trend was observed in ginger with garlic beverage as presented in Fig.6.

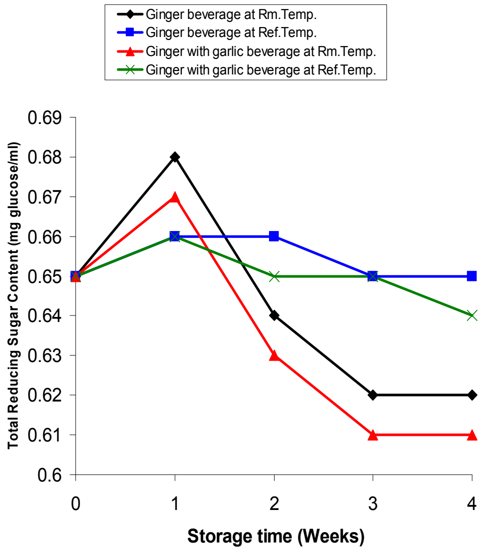

Fig. 6 Total reducing sugar content of ginger and ginger with garlic beverages inoculated with L. bulgaricus stored at ambient and refrigeration temperatures

Also ginger and ginger with garlic beverages containing *Lactobacillus bulgaricus* showed no significant difference ($p > 0.05$) in the decrease in reducing sugars at both ambient and refrigeration temperatures throughout the storage period.

The initial increase in reducing sugar content of all the probiotic beverages within the first week of storage could have been as a result of hydrolytic activities of the probiotic organisms which hydrolyzed the carbohydrate component of the beverages into fermentable sugars. It has been reported (Singleton, 1997) that certain hydrolytic bacteria liberate enzymes which hydrolyze a range of compounds as nutrients. The fermentable sugars are found to be good substrates for the growth of microorganisms (Brankori and Baras, 2001; Ray, 2004). After hydrolysis, the sugars were subsequently utilized by the increased population of LAB leading to its gradual decrease from 10.27 g/100g to 9.64 g/100g and 9.73 g/100g during ambient and refrigeration temperature respectively at the 4th week of storage.

3.3. Carbohydrate Content of Probiotic Ginger Beverage

The carbohydrate content of ginger beverage inoculated with *Lactobacillus plantarum* decreased consistently from the initial value of 7.88 % to 6.41 % and 6.71 % at the 4th week during ambient and refrigeration temperature storage respectively. The consistent decrease in carbohydrate content was also observed in ginger with garlic samples throughout the period of storage at both temperatures. In samples that were inoculated with *Lactobacillus bulgaricus*, a similar trend was noticed as there was a consistent reduction in the carbohydrate content throughout the period of storage as presented in Tables 1- 4.

The reduction of carbohydrate content in ginger and ginger with garlic beverages inoculated with *Lactobacillus plantarum* and *Lactobacillus bulgaricus* showed a significant difference ($p < 0.05$) when stored at ambient and refrigeration temperatures. The consistent reduction in carbohydrate content of all the probiotic samples could have been caused by the activities of the metabolizing organisms (Singleton, 1997; Brankori and Bars, 2001).

Table 1: Proximate analysis of ginger beverage inoculated with L. plantarum stored at ambient and refrigeration temperatures.

Time in weeks	Sample code	% Protein	% Fat	% Ash	% Moisture	% CHO	Total Solids g/100g
0	GLpiRm	2.33 ± 0.02	0.05 ± 0.01	0.06 ± 0.01	89.68 ± 0.01	7.88 ± 0.03	10.32 ± 0.01
	GLpiRe	2.33 ± 0.02	0.05 ± 0.01	0.06 ± 0.01	89.68 ± 0.01	7.88 ± 0.03	10.32 ± 0.01
1	GLp1Rm	2.63 ± 0.03	0.23 ± 0.03	0.24 ± 0.01	90.15 ± 0.01	6.75 ± 0.05	9.85 ± 0.08
	GLp1Re	2.28 ± 0.04	0.21 ± 0.02	0.21 ± 0.01	90.09 ± 0.17	7.21 ± 0.01	9.91 ± 0.10
2	GLp2Rm	2.64 ± 0.01	0.25 ± 0.01	0.23 ± 0.02	90.25 ± 0.27	6.63 ± 0.01	9.75 ± 0.11
	GLp2Re	2.33 ± 0.01	0.28 ± 0.02	0.20 ± 0.02	90.20± 0.13	6.99 ± 0.06	9.80 ± 0.13
3	GLp3Rm	2.67 ± 0.02	0.29 ± 0.01	0.27 ± 0.01	90.32 ± 0.16	6.45 ± 0.07	9.68 ± 0.07
	GLp3Re	2.48 ± 0.06	0.31 ± 0.01	0.24 ± 0.01	90.28 ± 0.12	6.69 ± 0.05	9.72 ± 0.06
4	GLp4Rm	2.72 ± 0.01	0.28 ± 0.03	0.22 ± 0.02	90.37 ± 0.22	6.41 ± 0.03	9.63 ± 0.02
	GLp4Re	2.49 ± 0.01	0.29 ± 0.02	0.18 ± 0.02	90.33 ± 0.10	6.71 ± 0.10	9.67 ± 0.05

GLp = Ginger beverage inoculated with *L. plantarum* i – 4 =Period (weeks) Rm = Room,
Re = Refrigeration Temperature. Values are means ± SE of replicate

Table 2: Proximate analysis of ginger beverage inoculated with L. bulgaricus stored at ambient and refrigeration temperatures.

Time in weeks	Sample code	% Protein	% Fat	% Ash	% Moisture	% CHO	Total Solids g/100g
0	GLbiRm	2.33 ± 0.07	0.05 ± 0.01	0.06 ± 0.01	89.73 ± 0.18	7.83 ± 0.04	10.27 ± 0.05
	GLbiRe	2.33 ± 0.07	0.05 ± 0.01	0.06 ± 0.01	89.73 ± 0.18	7.83 ± 0.04	10.37 ± 0.05
1	GLb1Rm	2.49 ± 0.04	0.15 ± 0.02	0.18 ± 0.03	90.03 ± 0.26	7.15 ± 0.08	9.97 ± 0.02
	GLb1Re	2.47 ± 0.02	0.12 ± 0.02	0.13 ± 0.01	90.12 ± 0.09	7.16 ± 0.07	9.88 ± 0.07
2	GLb2Rm	2.54 ± 0.01	0.20 ± 0.03	0.21 ± 0.01	90.30 ± 0.22	6.65 ± 0.06	9.70 ± 0.05
	GLb2Re	2.50 ± 0.02	0.18 ± 0.03	0.17 ± 0.02	90.14 ± 0.39	7.01 ± 0.05	9.86 ± 0.10
3	GLb3Rm	2.55 ± 0.40	0.21 ± 0.01	0.18 ± 0.01	90.35 ± 0.26	6.76 ± 0.01	9.70 ± 0.02
	GLb3Re	2.52 ± 0.02	0.18 ± 0.01	0.12 ± 0.01	90.26 ± 0.30	6.95 ± 0.05	9.74 ± 0.09
4	GLb4Rm	2.58 ± 0.01	0.21 ± 0.05	0.15 ± 0.02	90.36 ± 0.11	6.70 ± 0.10	9.64 ± 0.06
	GLb4Re	2.53 ± 0.01	0.18 ± 0.04	0.10 ± 0.01	90.27 ± 0.14	6.92 ± 0.09	9.73 ± 0.11

GLb = Ginger beverage inoculated with *L. plantarum* i – 4 =Period (weeks) Rm = Room,
Re = Refrigeration Temperature. Values are means ± SE of replicate.

Table 3: Proximate analysis of ginger with garlic beverage inoculated with L. plantarum stored at ambient and refrigeration temperatures.

Time in weeks	Sample code	% Protein	% Fat	% Ash	% Moisture	% CHO	Total Solids g/100g
0	GGLpiRm	2.34 ± 0.02	0.07 ± 0.02	0.06 ± 0.01	89.64 ± 0.05	7.89 ± 0.05	10.36 ± 0.05
	GGLpiRe	2.34 ± 0.02	0.07 ± 0.02	0.06 ± 0.01	89.64 ± 0.05	7.89 ± 0.05	10.36 ± 0.05
1	GGLp1Rm	2.77 ± 0.06	0.23 ± 0.03	0.27 ± 0.01	90.37 ± 0.11	6.49 ± 0.04	9.76 ± 0.08
	GGLp1Re	2.37 ± 0.05	0.21 ± 0.02	0.23 ± 0.02	90.30 ± 0.13	6.89 ± 0.08	9.70 ± 0.06
2	GGLp2Rm	2.84 ± 0.05	0.30 ± 0.01	0.22 ± 0.01	90.28 ± 0.41	6.36 ± 0.03	9.72 ± 0.12
	GGLp2Re	2.64 ± 0.05	0.28 ± 0.01	0.19 ± 0.02	90.34 ± 0.45	6.55 ± 0.08	9.66 ± 0.10
3	GGLp3Rm	2.86 ± 0.03	0.32 ± 0.01	0.29 ± 0.01	90.36 ± 0.15	6.17 ± 0.05	9.64 ± 0.05
	GGLp3Re	2.67 ± 0.03	0.34 ± 0.01	0.22 ± 0.02	90.38 ± 0.24	6.39 ± 0.10	9.62 ± 0.04
4	GGLp4Rm	2.93 ± 0.01	0.29 ± 0.02	0.28 ± 0.03	90.50 ± 0.10	6.00 ± 0.09	9.50 ± 0.10
	GGLp4Re	2.67 ± 0.01	0.32 ± 0.02	0.24 ± 0.02	90.43 ± 0.26	6.34 ± 0.01	9.57 ± 0.05

GLp = Ginger beverage inoculated with *L. plantarum* i – 4 =Period (weeks) Rm = Room, Re = Refrigeration Temperature. Values are means ± SE of replicate.

Table 4: Proximate analysis of ginger with garlic beverage inoculated with L. bulgaricus stored at ambient and refrigeration temperatures.

Time in weeks	Sample code	% Protein	% Fat	% Ash	% Moisture	% CHO	Total Solids g/100g
0	GGLbiRm	2.40 ± 0.02	0.06 ± 0.01	0.06 ± 0.01	89.85 ± 0.24	7.63 ± 0.05	10.15 ± 0.03
	GGLbiRe	2.40 ± 0.02	0.06 ± 0.01	0.06 ± 0.01	89.85 ± 0.24	7.63 ± 0.05	10.15 ± 0.03
1	GGLb1Rm	2.43 ± 0.03	0.19 ± 0.02	0.20 ± 0.05	90.04 ± 0.15	7.14 ± 0.07	9.96 ± 0.10
	GGLb1Re	2.44 ± 0.02	0.16 ± 0.02	0.15 ± 0.05	90.09 ± 0.15	7.16 ± 0.06	9.91 ± 0.02
2	GGLb2Rm	2.64 ± 0.01	0.21 ± 0.01	0.24 ± 0.01	90.22 ± 0.20	6.69 ± 0.03	9.78 ± 0.02
	GGLb2Re	2.51 ± 0.02	0.18 ± 0.02	0.22 ± 0.15	90.17 ± 0.01	6.93 ± 0.05	9.84 ± 0.01
3	GGLb3Rm	2.66 ± 0.02	0.23 ± 0.01	0.22 ± 0.01	90.30 ± 0.02	6.59 ± 0.06	9.70 ± 0.02
	GGLb3Re	2.42 ± 0.01	0.19 ± 0.01	0.18 ± 0.01	90.27 ± 0.02	6.94 ± 0.03	9.73 ± 0.02
4	GGLb4Rm	2.67 ± 0.01	0.21 ± 0.02	0.19 ± 0.02	90.31 ± 0.02	6.62 ± 0.03	9.69 ± 0.02
	GGLb4Re	2.48 ± 0.02	0.18 ± 0.02	0.16 ± 0.15	90.27 ± 0.01	6.91 ± 0.04	9.73 ± 0.01

GLb = Ginger beverage inoculated with *L. plantarum* i – 4 =Period (weeks) Rm = Room
Re = Refrigeration Temperature. Values are means ± SE of replicate.

3.4. Total Solid Content of Probiotic Ginger based-Beverages

The total solid content of ginger beverage inoculated with *Lactobacillus plantarum* reduced from an initial value of 10.32 g/100 g to 9.63 g/100 g and 9.67/100 g at the 4th week during ambient and refrigeration temperature storage respectively as presented in Table 1. A similar trend was observed in ginger with garlic beverage as the total solid decreased during the storage period as shown in Table 2. There was a significant difference ($p < 0.05$) in the reduction of total solid in both ginger and ginger with garlic beverages when stored at ambient and refrigeration temperatures. When *Lactobacillus bulgaricus* was inoculated into the samples the initial value of total solid reduced from 10.27 g/100g to 9.64 g/100g and 9.73 g/100g during ambient and refrigeration temperature respectively at the 4th week of storage. In *Lactobacillus bulgaricus* inoculated ginger with garlic beverage, a similar trend of reduction in total solids was observed at both ambient and refrigeration temperatures throughout the period of storage as presented in Tables 3 and 4. Also, there was a significant difference ($p < 0.05$) in the decrease of total solid between samples stored at ambient and refrigeration temperatures.

The reduction in total solids of the probiotic samples stored both at ambient and refrigeration temperature was probably due to utilization of nutrients by increasing microbial population.

3.5. Crude Protein Content Of Probiotic Ginger Beverages

The crude protein content of ginger beverage inoculated with Lactobacillus plantarum and stored at ambient and refrigeration temperatures is presented in Table 1. The protein content increased from the initial value of 2.33% to 2.72% and 2.49% at the 4th week during ambient and refrigeration temperature storage respectively. There was also an increase in the protein content of ginger with garlic beverage inoculated with Lactobacillus plantarum (Table 2). The increase in protein content between ambient and refrigeration temperature storage of ginger and ginger with garlic beverages inoculated with *L. plantarum* was significantly different ($p < 0.05$).

When *Lactobacillus bulgaricus* was inoculated into ginger beverage, the protein content increased from the initial value of 2.33 to 2.58% and 2.53% at the 4th week during ambient and refrigeration temperature storage respectively (Table 3). In ginger with garlic beverage inoculated with *Lactobacillus bulgaricus* (Table 4), the protein content similarly, increased over the period of storage at both ambient and refrigeration temperature. There was no significant difference in the crude protein content between ginger beverage stored at ambient and refrigeration temperature($p > 0.05$) but there was significant difference ($p < 0.05$) between ambient and refrigeration temperature storage of ginger with garlic beverage.

The non-reduction in the protein content of all samples may be due probably to protein synthesis and the antioxidant properties of ginger extracts as well as dead probiotic microbes which could have increased its protein content. (Kikuzaki et al, 1994; Belewu et al., 2005) observed that most of the isolated compounds from ginger exhibited very strong antioxidant effect on the metabolism of proteins by microorganisms in ginger extract.

3.6. Crude Fat Content of Probiotic Ginger Beverage

The crude fat content of ginger beverage inoculated with *Lactobacillus plantarum* and stored at ambient and refrigeration temperature is as shown in Table 1. The fat content increased from the initial value of 0.05% to 0.28% and 0.29% during ambient and refrigeration temperature respectively at the 4th week of storage. A similar trend was observed in all the samples as the crude fat content increased both at ambient and refrigeration temperature storage as presented in Tables 2, 3 and 4. There was no significant difference ($p > 0.05$) in the increase of fat content between ginger and ginger with garlic beverages inoculated with *Lactobacillus plantarum* and stored at ambient and refrigerated temperature. However, a significant difference ($p < 0.05$) exists between samples inoculated with *Lactobacillus bulgaricus* and stored at ambient and refrigeration temperature.

The increase in crude fat content over the period of storage in all samples could be due to the effect of antioxidant properties of ginger and garlic on lipid metabolism of probiotic isolates. Krishnakantha and Lokesh, 1993; Belewu et al., 2005 reported that ginger inhibits lipid oxidation and scavenges super-oxide anions.

4. CONCLUSION

This study has shown that two probiotic bacterial isolates (*L. plantarum and L. bulgaricus*) exhibited capability of surviving in ginger and ginger with garlic beverages for a period of four weeks as their metabolic activities led to changes in the physico-chemical parameters of the beverages. The consistent increase in the percentage titratable acidity with a corresponding decrease in pH values, reduction in fermentable sugar content as well as total solid content indicated the viability of the probiotic bacteria isolate in the beverages. These changes are considered desirable as lowered pH and higher titratable acidity play an important role in preservation of fermented drinks. No significant difference was observed between the two beverages that are inclusion of garlic in a set of the beverage did not produce any significant effect on the physic-chemical properties or proximate composition of the beverages ($p > 0.05$). More importantly, presence of probiotic LAB in drinks like ginger-based extracts combines the health promoting potentials of the microbe with that of ginger and/or garlic.

BIOGRAPHY OF AUTHORS

UKEYIMA Moses Terkula, the first author finished his M.Sc. in Department of Food Science and Technology, Obafemi Awolowo University, Ile-Ife in December 2008. He worked on a thesis entitled 'A study of the production of probiotic ginger beverage' from which this article was extracted .

ADENIRAN, H.A., the corresponding author holds a doctoral degree in Food Science and Technology and he teaches Food Microbiology courses in the Department of Food Science and Technology. He has published eight articles in local and International Journals on utilization of agricultural wastes in production of enzymes, blends of bittering agents as substitutes for hops in production of sorghum beer, production of probiotic roselle extract.

ABIOSE, S.H., is a Professor in the same Department. She has also published several articles in the area of Biotechnology and fermentation of foods, utilization of agricultural wastes in production of enzymes, production of probiotic roselle extract. She has supervised six Ph.D. and ten M.Sc candidates including the first and the second authors.

REFERENCES

Abiose S.H. and Adedeji, A.A. Biochemical Changes during Fermentation of Plantain. Nigerian Food Journal.12: 92-99, 1994.

Adeniran, H.A and Abiose, S.H. Production of Fungal ∃-amylase and Amyloglucosidase on some Nigerian Agricultural Residues. Food Bioprocess Technol. DOI 10.1007/s 11947-008-0141-3, 2009

Adesunkanmi, K. and Oyelami, O.A The pattern and outcome of burn injuries at Wesley Guild Hospital, Ilesha, Nigeria: a review of 156 cases. Journal of Tropical Medicine and Hygiene 97: 108-112, 1994

AOAC. Official Methods of Analysis of the Association of Official Analytical Chemists. William Horwitz (Ed). Association of Official Analytical Chemists. Pub. 17th Edition. Washington, DC. , 2000.

Belewu, M.A., Belewu, K.Y. and Nkwunonwo, C.C. Effect of biological and chemical preservatives on the shelf life of West African Soft Cheese. African Journal of Biotechnology. 4 (10): 1076-1079, 2005.

Brankori, S.D and Baras, J. Comparative Study on biochemical activity of the intestinal isolates of *Lactobacillus* species V3 and *Bifidobacterium* species A71 in Different Substrates. Journal of Serbian Chemical Society. 66 (9): 581-589, 2001

Foster, S. Ginger: Your Food is your Medicine. http;//www.stevenfoster.com/education/monograph/ginger/html. Retrieved on 03/06/2008

Gibson, G.R. and Williams, C.M. Defining functional foods. In: Gibson, G. R. and Williams C. M. (Eds.). *Functional Foods: Concept to Product.* Woodhead publishing Limited. Abington Hall, Cambridge CB1 England, 2000.

Havenaar, R. and Veld, J.H.J. Probiotics: A General View. In: Wood, B. J.B, (Ed.). The Lactic Acid Bacteria Vol.1 Elsevier Science, Pub. London., 1992.

Harris, L.J. Garlic. Safe methods to store preserve and enjoy. University of California. Division of Agriculture and Natural Resources. Publication 7231, 1997.

Harrigan, W.F.Laboratory Methods in Food Microbiology. Academic Press, San Diego, 1998.

Kikuzaki,H. Kawasaki,Y. and Nakatani, N. Structure of antioxidative compounds in ginger. ACS-symp-ser. Washington DC. American Chemical Society. 547: 237-243. 1994.

Krishnakantha, T.P. and Lokesh, B.R. Scavenging of superoxide anions by spice principle. Indian Journal of Biochemistry. 30(2): 133-134, 1993.

Miller, G.L. Use of Dinitrosalicyclic Acid Reagent for Determination of Reducing Sugar. *Analytical Chemistry*. 31: 426 – 428, 1959.

Obi, C.L., Ugoji, E.O., Edun, S.A., Lawal, S.F. and Anyiwo, C.E The antibacterial effect of honey on diarrhoea causing bacterial agents isolated in Lagos, Nigeria. African Journal of Medical Science. 23: 257-260, 1994.

Osuntogun, B. and Aboaba, O. Microbiological and Physico-Chemical Evaluation of some Non-alcoholic Beverages. Pakistan Journal of Nutrition 3(3): 182 – 188, 2004.

Oti, E. and Mgbolu, N.I.Research note: Chemical composition and organoleptic assessment of fresh and stored Nigerian ginger (*Zingiber officinale*). Nigerian Food Journal. 5: 76 – 79, 1987.

Quattara, B., Simard, R.E., Holley, R.A., Piette, G.J.P. and Begin, A. Antibacterial activity of selected fatty acids and essential oils against six meat spoilage organisms. International Journal of Food Microbiology. 37: 155-162, 1997.

Ray, B. Fundamental Food Microbiology. 3rd edition. CRC Press. LLC, 2000 N.W corporate Blvd. Boca Raton, Florida, 2004.

Roberfroid, B. Defining functional foods. In: Gibson, G. R. and Williams, C.M. (Eds). Functional foods: concept to product. Woodhead Publishing Limited. Abington Hall, Abington England, 2000.

Senjong, O., Randy, W. and Saehum, K. *Lactobacillus acidophilus* 30SC: Human Isolate for potential use as probiotic strains. http://www.foodcy2000.or.kr/visitor/session3/s3-top3-01.htm,2000. Retrieved on 12/09/07.

Singleton, P.Bacteria in Biology, Biotechnology and Medicine. 4th edition. John Wiley & Sons Ltd. N.Y USA., 1997.

Steel, R.G.D., Torrie, J.H. and Dickey, D. Principles and procedures of Statistics Third Edition, McGraw-Hill, New York, 1997.

Tomasik, P.J. and P. Tomasik, Probiotics and Prebiotics. American Association of Cereal Chemists, Inc. 80(2): 113-117, 2003

Wolfgand, K.Mattila – Sandholm, T. and von Wright, A. Detection and estimation in fermented and non-fermented dairy products: probiotic bacteria. In the Encyclopedia of Food Microbiology. 3: 1783-1789, 1999.

Yoon, K.Y., Woodams, E.E. and Hang, Y.D.
Probiotication of Tomato Juice by Lactic Acid Bacteria. The Journal of Microbiology. 42 (4): 315-318, 2004.

Schillinger, U. and F.K. Lucke, F.K. Identification of Lactic acid bacteria isolated from Meats and meat product. Food Microbiology. 4: 199 – 208, 1987.

Ife Journal of Technology, Vol. 18 (2), 26-30, 2009

Full Paper

CHARACTERISATION OF SUN-DRIED PALM FRUIT WASTE BIOMASS MATERIALS

Y.A. Salako
Department of Agricultural Engineering
Obafemi Awolowo University, Ile-Ife, Osun-State, Nigeria.

O.K. Owolarafe
Department of Agricultural Engineering, Obafemi Awolowo University, Ile-Ife, Osun-State, Nigeria
owolarafe@yahoo.com

A.N. Anozie
Department of Chemical Engineering, Obafemi Awolowo University, Ile-Ife, Osun-State, Nigeria.

ABSTRACT

Palm fruit waste biomass, namely: shell, palm fiber and the empty fruit bunch (EFB) were characterized in this study for proper selection as fuel. Fresh fruit bunches (FFB) were processed to obtain the required waste products. These waste products were sun-dried for 11 days. Fuel properties such as the moisture content, bulk density, ash content, volatile matter, fixed carbon content and the calorific value were determined at interval of 3 days. The results indicate that moisture content has a direct effect on other properties. The moisture content was found to exhibit direct variation with the bulk density and the volatile matter, as they decrease with a decrease in the moisture content. The calorific value, fixed carbon content and the ash content exhibit an indirect variation with the moisture content as they increased with decreasing moisture content. After 11 days of drying, the moisture contents of the shell, fiber and EFB decreased from 31.16-6.58, 49.46-3.32 and 57.37-7.71%, respectively; the bulk densities reduced from 0.31-0.28, 0.15-0.08 and 0.31-0.08 g/cm3, respectively; the ash contents increased from 6.55-12.67, 3.46-8.27 and 5.18-16.46%, respectively; the volatile matter decreased from 81.39-73.59, 87.17-77.15 and 84.60-62.80%, respectively; the fixed carbon contents increased from 12.065-13.747, 9.363-14.58 and 10.22-20.74%, respectively; the calorific values increased from 10.87-14.94, 7.57-16.45 and 5.57-13.99, respectively.

Keywords: palm fruit, waste biomass materials, moisture, drying-scheduling, fuel characteristics, energy

1. INTRODUCTION

Palm fruit biomass has the potential to generate energy that can favorably compare with other non-fossil fuel source of heat energy like coal [Chow et al., 2008]. The solid wastes from palm fruit milling operations are: shell, palm fiber and empty fruit bunch (EFB). In large- and medium-scale mills, these waste products are referred to as by-products, because they are plowed back into the milling operation to serve as fuel to generate steam and electricity required in the mill. Although palm fruit by-products can be used for other purposes, research has shown that it is better and more economical to use it to generate energy for the mill [Menon *et al.* 2003]. This practice will not only save the processor the tedious task of waste disposal but also enhance environmental friendliness. This will also reduce the cost of production thereby having a direct economic benefit on the processing operation. This scheme has been in operation in most large scale plants [Hassan *et al.*, 2003].

In most small-scale mills in Nigeria, there are environmental challenges due to ineffective utilization of biomass waste through inappropriate disposal of large amount of it which has constituted environmental hazards and causing serious problems in the cleaning of the environment. It therefore becomes imperative to develop an appropriate technology for the processing of palm fruit at small scale level, to utilize these wastes. This will not only facilitate the recycling of the waste but also ensure higher oil yield at a relatively lower cost.

The palm fruit biomass immediately after extraction contains very high moisture content, usually in the range of 31, 49 and 57% for shell, fiber and EFB, respectively, depending on the method of extraction. This high moisture content reduces their calorific value and consequently limits their potentials as fuel materials. A way to improve on the amount of heat release per kilogram of the fuel material (calorific value), is to dry the biomass. Drying of the biomass will reduce their bulkiness, and enhance better handling of the fuel materials. This drying can be achieved by direct sun-drying; in fact it is the cheapest means of reducing the moisture content of these biomass materials to a level suitable for combustion. This study undertakes the characterization of sun dried palm fruit biomass materials with a view to provide useful data for their utilization

2. MATERIALS AND METHOD

2.1. Waste Preparation

Fresh fruit bunches were obtained from a palm fruit plantation and quartered. The fruits were manually separated from the quartered bunches to obtain the empty fruit bunch. The fruits obtained were then sterilised for 90 minutes and digested for 10 minutes based on an earlier study of Owolarafe et al. [2008]. The digested mash was pressed with a hydraulic screw press to extract the crude oil. The cake was manually pulverised after which the fiber and nuts were separated. The

EFB, fibre and shell obtained were sun-dried for 11 days. The experiment took place between December and January (dry season) of the years 2008 and 2009, respectively. The average ambient temperature was in the range of 28 - 32 oC and the average relative humidity (obtained from psychometric chart using the wet and dry bulb temperatures) was in the range of 33- 40%.

2.2. Determination of The Properties Of The Biomass

Samples of the biomass were taken to determine some fuel performance parameters such as moisture content, ash content, volatile matter, fixed carbon and specific heating or calorific value at drying interval of 3 days.

2.2.1. Determination of moisture content

The moisture content in the fuel was determined using the standard method prescribed in ASTM D2016-25 [Debdoudi *et al*., 2005]. Each sample was heated in an oven for 1.5 h at 105°C. The moisture content was calculated as given by the equation:

$$\frac{W_i - W_f X100\%}{Wi} \quad \text{.................} (1)$$

Where:

W_i = initial weight of the material (before drying)

W_f = weight of the material after drying

2.2.2. Determination of Ash content

The ash content was determined by following the procedure of ASTM D-5142 as reported by Debdoudi *et al.* [2005]. About 2 g of the biomass samples were burnt in muffled furnace at 800°C for 5 h and allowed to cool down in a desiccator. The ash content was calculated using the equation below.

$$\%\text{ Ash content} = \left(\frac{\text{final weight* 100}}{\text{Initial weight}}\right) \quad \text{.........} (2)$$

2.2.3. Determination of volatile matter

The volatile matter was also determined according to ISO 562/1974 as reported by Debdoudi *et al.* [2005]. About 2 g of the samples of the fuel materials were burned in crucible covered with lid placed in a furnace at temperature of 950°C for 5 minutes and allowed to cool down in a desiccator [Lindley, 1989]. The volatile matter content was calculated using the equation below.

$$\%\text{ Volatile Matter} = \left(\frac{(\text{initial weight - final weight})\text{* 100}}{\text{Initial weight}}\right) \quad \text{.........} (3)$$

2.2.4. Determination of fixed carbon

The fixed carbon of the material was determined as reported by Debdoudi *et al.* [2005] using the relationship below:

FC = 100 - %Ash- %VM. .... (4)

The bulk density was determined by calculating the ratio of the mass to the volume occupied. A container of a known volume was weighed. The container was filled with each sample and reweighed. The difference between the initial weight of the container and the new weight gave the weight of the sample. The bulk density of the sample was calculated as:

$$\left(\frac{Msc - Mc}{Vc}\right) \quad \text{............} (5)$$

Where:

M_{sc} = weight of sample + container.

M_c = weight of container.

V_c = volume of container.

2.2.5. Determination of calorific value

Also the net calorific value was determined using the relationship below [Bello, 2008].

NCV= 18.7 (1-AC-MC) – (2.5 MC) 6

Where:

NCV = Net (lower) calorific value

AC = ash content, MC = moisture content

All experimental work was carried out in three replications. The data obtained were subjected to statistical analysis [SAS, 2002].

3. RESULTS AND DISCUSSION

3.1. Physical properties of the fresh palm fruit waste

Table 1 shows the properties of the wet wastes. The bulk densities of the shell, fibre and EFB at 0-day of drying were found to be 0.31, 0.15 and 0.31 gcm^{-3}, respectively, while the moisture contents were 31.16, 49.46 and 57.37%, respectively.

Table 1: Properties of wet palm fruit processing waste

	Moisture content (%)	Ash content (%)	Volatile Matter (%)	Fixed carbon (%)	Net calorific value MJkg^{-1}	Bulk density gcm^{-3}
Shell	31.16	6.55	81.39	12.06	10.87	0.31
Fibre	49.46	3.46	87.17	9.36	7.57	0.15
EFB	57.37	5.18	84.60	10.22	5.57	0.31

The ash contents at this moisture content were 6.55, 3.46 and 5.18%, respectively, while the volatile matter ware found to be 81.39, 87.17 and 84.60%, respectively. The fixed carbon contents at the 0-day of drying were 12.07, 9.36 and 10.22%, respectively, and the net calorific values were found to be 10.87, 7.57 and 5.57 MJkg-1, respectively. These values compare well with those obtained by Hussain et al. [2003] on the palm fruit wastes from some Malaysian mills.

3.2. Effect of Drying On Moisture Content of the Palm Wastes

Figure 1 shows the moisture migration pattern of the palm wastes within 0 – 11 days of drying. It was observed that the moisture contents of the shell and fibre dropped rapidly within 0 – 3 days of drying, while the moisture content of the EFB dropped rapidly between 3 – 6 days of drying. The average moisture content of the shell reduced from 31.16% at the 0 day of drying to 6.58% after 11 days of drying, while the average moisture content of the fibre dropped from 49.46-3.32% .The average moisture content of the EFB dropped from 57.37-7.71% after 11 days of drying. Statistical analysis of the effect of drying on moisture contents of the biomass materials indicated that the effect was significant at 99.88% [SAS, 2002]. The moisture content of biomass material is an important parameter that determines their combustibility. The lower the moisture content, the higher the potential of the biomass materials as fuel [Hurstboiler, 2009; Cassidy and Ashton, 2007].

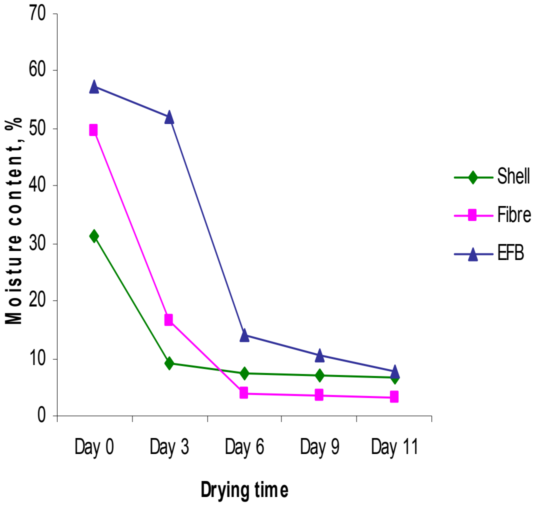

Fig 1: Moisture migration of the palm fruit waste biomass

3.3. Effect of Drying On Bulk Density of the Palm Wastes

Fig 2 shows the effect of drying time (days) on the bulk density of the biomass materials. The average bulk density of the shell reduced from 0.31gcm-3 at the 0 day of drying to 0.28gcm-3 after 11 days drying, while the average bulk density of the fibre dropped from 0.15-0.08 gcm-3. The average bulk density of the EFB dropped from 0.31-0.08 gcm-3 after 11 days of drying. Drying is a way of removing moisture from agricultural materials. The longer the drying time the lower the moisture content. Reduction in moisture content of agricultural products usually brings about reduction in weight particularly with materials with high moisture contents as these biomass materials. This automatically results in reduction in the bulk density especially when appreciable amount of volume doesn't occur. The bulk density therefore reduced as the moisture content reduced (brought about by increasing drying time) as shown in Figures 1 and 2. The effect of drying on bulk densities of the materials was observed to be significant at 99.99% [SAS, 2002]. The data presented here are very useful for the design of the furnace/boiler that will utilise the biomass as fuel materials. In addition low moisture content improves handling of the material and this affects transport cost [Hurstboiler, 2009].

3.4. Effect of Drying On Ash Content of the Palm Wastes

The effect of drying on the ash content of the palm fruit waste is shown in Figure 3. The average ash content of the shell increased from 6.55% at the 0 day of drying to 12.66% after 11 days of drying, while the average ash content of the fibre increased from 3.46-8.27%, the average ash content of the EFB increased from 5.18-16.46% after 11 days of drying. Since increasing drying time brings about reduction in moisture content, the ash contents of the materials increased with increased in drying time. Figures 1 and 3 showed that the ash contents of the fuel materials increased with decrease in moisture content. Drying was observed to significantly affect the ash content of the materials ($p<0.0001$). The result of the ash content of the wet fuel materials obtained compared favourably with the findings of Chow *et al.* [2008]. The ash content of pinewood has also been reported to have increased with reduction in moisture content [Szemmelveisz *et al.* 2009].

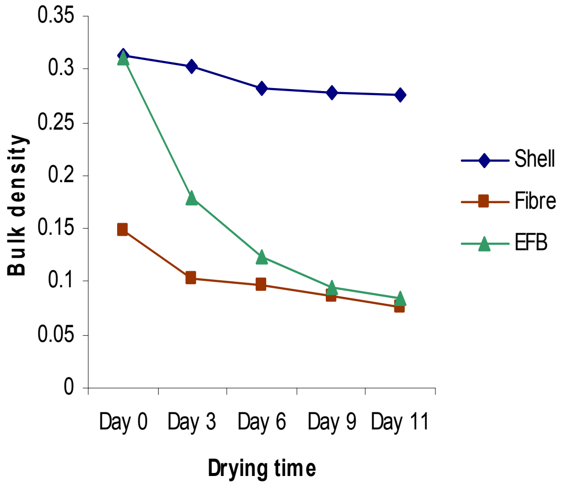

Figure 2: Effect of drying time on the Bulk density of the palm fruit waste biomass

3.5. Effect of Drying On the Volatile Matter of the Palm Wastes

The volatile matter of the fuel materials reduced with increasing days of drying as shown in Figure 4. This implies that volatile matter is directly proportional to the moisture content. The average volatile matter of the shell reduced from 81.39% at the 0 day of drying to 73.59% after 11 days of drying, while the average volatile matter of the fibre dropped from 87.17-77.15%, the average volatile matter of the EFB dropped from 84.60-62.80% after 11 days of drying. The effect of drying was observed to significantly ($p < 0.0001$) affect the volatile matter of the palm fruit wastes. This result is also found to be in agreement with the findings of Chow et al. [2008] and Szemmelveisz et al. [2009] on palm fruit wastes and pinewood, respectively.

3.6. Effect of Drying On the Fixed Carbon Content of The Palm Wastes

The average fixed carbon of the shell increased from 12.07% at the 0 day of drying to 13.75% after 11 days of drying, while the fixed carbon content of the fibre increased from 9.36-14.58%, the average fixed carbon content of the EFB increased from 10.22-20.74% after 11 days of drying as shown in Figure 5.

Statistical analysis of the effect of drying on the fixed carbon content of the materials indicated that drying significantly affected the property at 95%. The findings of Chow *et al.* [2008] and Szemmelveisz *et al.* [2009] on palm fruit wastes and pinewood, respectively, corroborate the current results on effect of drying time on the fixed carbon contents. In the current study an optimum fixed carbon content was however observed for a particular drying time.

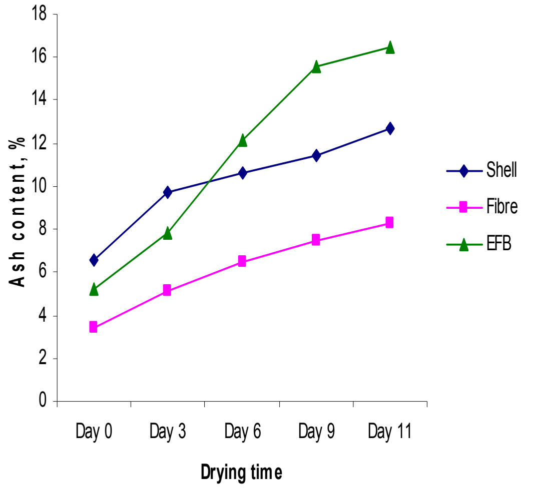

Fig 3: Effect of drying time on the Ash content of the palm fruit waste biomass

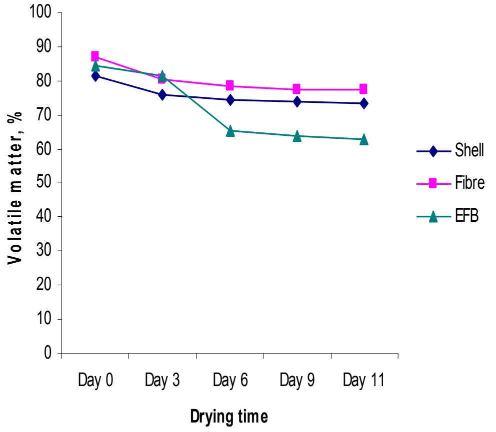

Figure 4: Effect of drying time on the Volatile matter of the palm fruit waste biomass

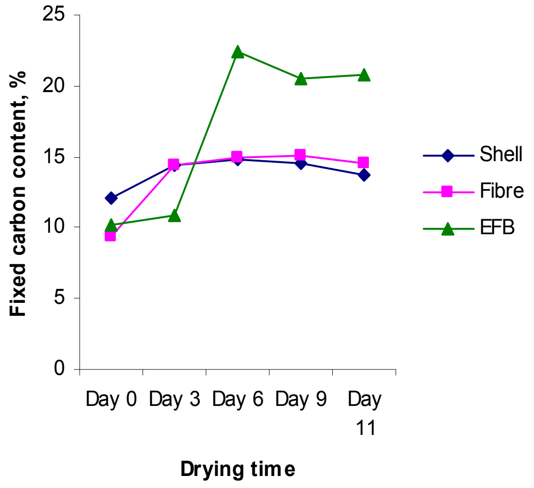

Figure 5: Effect of drying time on the fixed carbon content of the palm fruit waste biomass

3.7. Effect of Drying On the Calorific Value of the Palm Fruit Wastes

The net calorific value of shell at 0-day of drying was 10.87 MJkg-1 and increased to 14.94 MJkg-1 after 11 days of drying, while the net calorific value of fibre and EFB increased from 7.57 and 5.57 to 16.45 MJkg-1 and 13.99 MJkg-1, respectively (Figure 6). Drying significantly affected the calorific value at 99.99%. The increase in the calorific value is as a result of decrease in the moisture content of the fuel materials (Figure 1). This is in agreement with findings of Cassidy and Ashton [2007] on wood. Hussain et al. [2003] also reported that palm fruit wastes with high moisture content with some Malaysian mills has low calorific values Calorific value of the biomass materials is very important in the numerical simulations of thermal conversion system for the biomass materials [Changdong and Azevedo, 2005]. The calorific value of biomass material influences the choice of energy conversion system for the material.

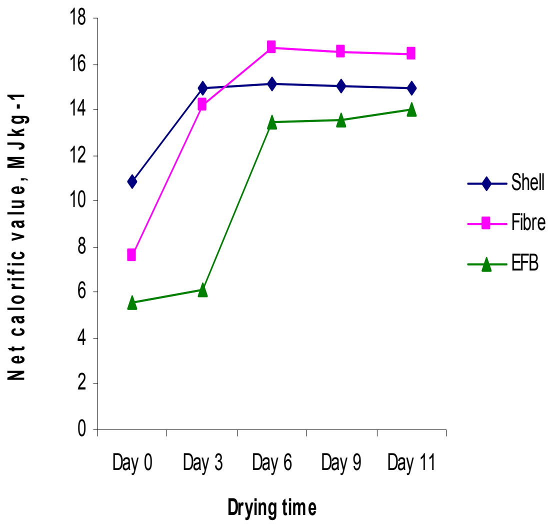

Figure 6: Effect of drying time on the Net calorific value of the palm fruit waste biomass

4. CONCLUSIONS

Ineffective utilization of biomass residues from the oil mill constitutes environmental hazard and pollution, and also emits strong irritating smell due to microbial decomposition activities at dump sites. This calls for an efficient utilisation of these readily available by-products as fuel for this industry by reducing the moisture content to improve its calorific value, which can be achieved by direct sun drying. This study has shown that the calorific value of shell, fibre and EFB after the 6th day of sun drying increases from 10.87-15.08 $MJkg^{-1}$, 7.57-16.45 $MJkg^{-1}$ and 5.57-13.99 $MJkg^{-1}$, respectively, during the dry season. This implies that a sun drying scheme can be planned for the utilisation of biomass residues as fuel in palm oil processing industry. This will prevent the processor from over relying on other conventional sources of energy and hence save considerably cost of energy. The data generated is also useful in the design of the furnace/boiler that will utilise the waste materials. These measures will go a long way in improving the oil extraction efficiency and economics of the small and medium scale processors in the Nigerian palm oil industry.

REFERENCES

Bello, O.O. Characterisation of palm fruit processing wastes into fuel. Unpublished B.Sc. Thesis of the Department of Agricultural Engineering, Obafemi Awolowo University Ile-Ife, Nigeria, 2008.

Cassidy, P and Ashton, S. How Wood Properties Influence Utilization. In: Hubbard, W.; L. Biles; C. Mayfield; S. Ashton (Eds.). 2007. Sustainable Forestry for Bioenergy and Bio-based Products: Trainers Curriculum Notebook. Athens, GA: Southern Forest Research Partnership, Inc. p 169-172, 2007.

Changdong S, Azevedo, J.L.T., Estimating the higher heating value of biomass fuels from basic analysis data. Biomass and Bioenergy, vol 28, pp 499-507, 2005.

Chow, M.C.; Mohd, B.W. and Chan, K.W. Availability and Potential of Biomass Resource from Malaysian Palm Oil Industry for Generating renewable Energy, Oil palm Bulletin 56; p. 23-28, 2008.

Debdoudi, A., El amarti, A., and Colacio, E. Production of fuel briquette from esparto partially pyrolyzed. Energy Conversion and Management 46 1877-1884, 2005.

Hurstboiler Biomass Fuels (http://www.hurstboiler.com). 2009.

Hussain, Z; Zamal, Z.A. and Abdullah, M.Z. Analysis of biomass-residue based cogeneration system in palm oil mills. Biomass and Bioenergy, 24, 117 – 124, 2003.

Lindley, J.A. and Vossoughy, M. Physical Properties of Biomass Briquette, ASAE. 1989.

Menon, N.R; Ab Rahman, Z., and Abu Bakar, N. . mpty Fruit Bunches Evaluation: Mulch in Plantation vs. Fuel for Electricity Generation. Malaysian Palm Oil Board, 2003.

Owolarafe, O.K., Taiwo E.A. and Oke, O.O. Effect of processing condition on yield and quality of hydraulically expressed crude palm oil. International Agro Physics, vol. 22, no 3, pp 349-352, 2008.

SAS. Guide for Personal Computers. Version Ed. SAS/STA, SAS Inst. Inc., 2002.

Szemmelveisz, K. Szűcs, I. B. Palotás, A.B and Juhász, B. Characterization of the Combustion Properties of Solid Biofuels. European Combustion Meeting (http://combustion.uni-miskolc.hu ,) 2009.

Ife Journal of Technology, Vol. 18 (2), 31-34, 2009

Full Paper

THE STUDY OF DIETHYLENE AMINE AND SODIUM CHROMATE AS CORROSION INHIBITORS FOR MILD STEEL IN CASSAVA FLUID

O.E. Olorunniwo
Department of Materials Science and Engineering, Obafemi Awolowo University, Ile-Ife, Nigeria

L.E. Umoru
Department of Materials Science and Engineering, Obafemi Awolowo University, Ile-Ife, Nigeria
lumoru@oauife.edu.ng

P.O Atanda
Department of Materials Science and Engineering, Obafemi Awolowo University, Ile-Ife, Nigeria

ABSTRACT

This report presents the investigation of sodium chromate and diethylene amine as inhibitors of corrosion of a mild steel in cassava fluid. The inhibition study was carried out using the weight loss immersion technique. The inhibitive potentials of the two inhibitors was evaluated based on a determination of the corrosion rates in the presence and absence of the inhibitors, determination of the pH of various cassava fluids and a calculation of the inhibition efficiencies of the two inhibitors at different levels of concentrations. The results of this study show that diethylene amine is a much better inhibitor of the corrosion of mild steel in cassava fluid than sodium chromate. The inhibition efficiencies by diethylene amine are higher than 85% for the 0.5, 1.0 and 1.5 M concentrations investigated. In the case of sodium chromate, inhibition efficiencies only become significant for 1.0 M and 1.5 M concentrations. Generally, the pH of all cassava fluid with and without inhibitors increased with duration of exposure and the corrosion rates of the mild steel decreased with increase in the pH of the cassava fluid.

Keywords: Corrosion, inhibitors, diethylene amine, sodium chromate, cassava, efficiency

1. INTRODUCTION

NST-44 mild steel is one of the Nigeria made steel that is often used as a constructional material because of its mechanical strength and ease of fabrication. The agro-allied industries in Nigeria make use of this steel for the production of machines such as grater, hammer mills, etc. Sadly, the life span of these machines has been reduced considerably because of the corrosive effect of cassava. The cyanide content of cassava has been identified by many investigators as the main species responsible for corrosion (Fontana and Greene, 1987; Alagbe *et al.*, 2005). Several studies have investigated the inhibition of metal corrosion by various types of organic and inorganic compounds (Trethewey and Chamberlain, 1995). Inhibition by these compounds is mainly as a result of adsorption of molecules or ions at the metal surface forming a protective layer. The extent of inhibition depends on the nature of the metal, the metal surface condition, the mode of adsorption, the chemical structure of the inhibitor and the type of corrosion media (Thomas, 1981; Maayta, 2002). Corrosion inhibition of iron and steel in various media has been the subject of numerous studies (Umoru *et al.*, 2005; Loto, 2003, Loto and Mohammed, 2000).

The inhibitive effect of chromate and nitrite on the corrosion of iron has been extensively studied since 1950 (Azambuja *et al.*, 2003). The inhibitive effect of molybdate and tungstate ions, which are weaker oxidizing agents than chromate anion, on the corrosion of iron have also been investigated (Pryor and Cohen, 1953). It is noted in these previous works that the inhibitive behaviour of the molybdate and tungstate ions greatly depend on the presence of dissolved oxygen. Among the various inorganic inhibitors so far studied, it is well known that chromate is one of the most effective even though little is known about its activities in cassava environments. The inhibitive effects of numerous organic inhibitors on the corrosion of iron and steel have also been carried out (Loto and Muhharnmad, 2000; Loto, 2003; Alagbe *et al.*, 2005; Umoru *et al.*, 2005; Rajappa and Venkatesha, 2003). A literature survey showed only limited systematic work done to the corrosion inhibition of NST-44 mild steel in various media. The purpose of the present research is to study the inhibitive effect of sodium chromate (inorganic compound) and diethylene amine (organic compound) on the corrosion of NST-44 mild steel in cassava fluid. There is yet to be any reported study on the effect of these additives as corrosion inhibitors for NST-44 mild steel in cassava medium.

2. MATERIALS AND METHODS

Corrosion coupons were cut from the steel obtained and machined appropriately to reduce the cold working effect of the sheared edges. Subsequently, each of the coupons was subjected to grinding on emery papers 240, 320, 400 and 600 grits. The oil and grease stains on the specimens were removed with petroleum spirit. Afterwards, the coupons were weighed on a FB 153 Mettler Toledo digital weighing balance and then kept in desiccators prior to exposure. Peeled cassava tubers were crushed and squeezed to extract the cassava fluid used for the experiment. As soon as the cassava fluid was ready, different media containing 0.5, 1.0 and 1.5M concentrations of sodium chromate and diethylene amine inhibitors were prepared. The seventh medium without any inhibitor was used as the control experiment. Finally, the corrosion coupons were exposed to the various media.

Specimens were later withdrawn periodically at intervals of 48 h and washed thoroughly under running tap. Thereafter, they were dried, reweighed and the corrosion rates calculated in millimeter per year (mmpy). The corrosion rates have been calculated in mmpy using the expression:

$$\text{mm}/\text{yr} = \frac{87.6W}{DAT}$$

where, W is the weight loss in mg, D is the density of the specimen in g cm^{-3}, A is the total exposed surface area of the specimen in cm^{2} and T is the exposed time in hours.

The NST-44 mild steel rods used for this work were obtained from Osogbo Steel Rolling Mill, Osogbo, Osun State, Nigeria. And the experimental work was carried out in the Materials Laboratory of the Department of Materials Science and Engineering, Obafemi Awolowo University, Ile-Ife, Nigeria. The mild steel rods' dimensions are 25 mm diameter and 10 mm thickness. The chemical composition of the steel is: - C- 0.33; Mn- 0.09. P-0.02. S- 0.02; Ni- 0.03; Cr- 0.45; Mo -0.02; Sn- 0.01 ; Fe (balance).

3. Results

Fig. 1 shows that the corrosion rates of the steel in cassava after inhibiting with 0.5 M sodium chromate did not vary much from those without inhibition. However, with 1.0 and 1.5 M inhibition the corrosion rates were significantly lowered. The results contained in Fig. 2 show that the corrosion rates of mild steel were much lower in the diethylene amine inhibited cassava fluid than in the uninhibited medium at 0.5, 1.0 and 1.5 M concentrations.

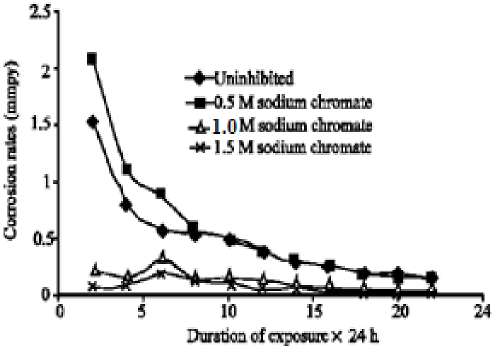

Figure 1: Effects of sodium chromate on the corrosion inhibition of a mild steel in cassava fluid

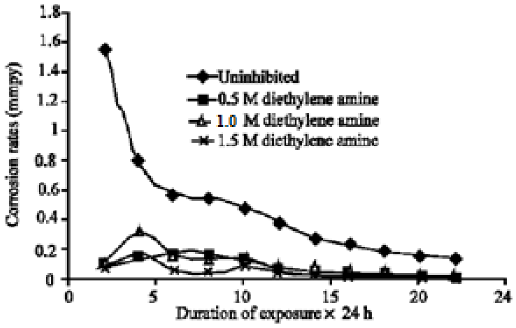

Figure 2: Effect of diethylene amine on the corrosion inhibition of a mild steel in cassava fluid

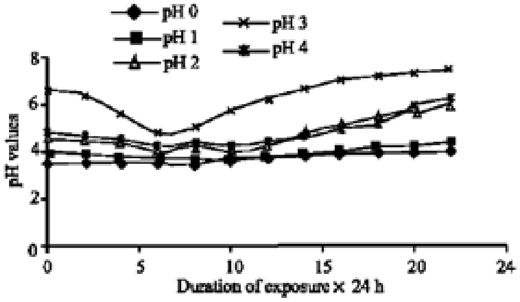

Figure 3: Variation of pH values of cassava fluid with or without sodium chromate

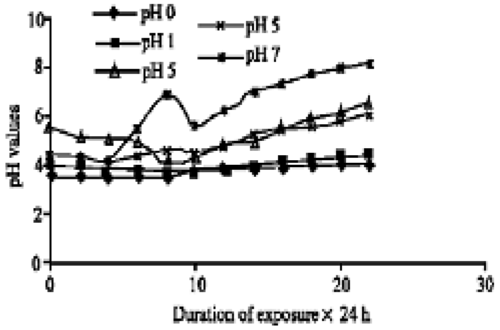

Figure 4: Variation of pH values of cassava fluid with or without diethylene amine

Figs. 3 and 4 show the effects of corrosion products and inhibitor presence on the pH of corrosion media. It is clear from these figures that the pH of the cassava (pH=0) without steel specimens and inhibitor changes linearly but at a low rate. The pH of the cassava medium (pH=1) with immersed steel specimens but without inhibitor was greater than (pH=0) though only lightly. From Fig. 3, the effects of sodium chromate on the pH (pH 2, pH 3 and pH 4) can be said to decrease slightly initially to a minimum after about 6 to 8 days of exposure and later increased almost linearly. The three curves respectively represent the influence of the three concentrations; 0.5 M, 1.0 M and 1.5 M of sodium chromate investigated.

The effect of diethylene amine on the pH is similar to those of sodium chromate (Figs 3 and 4) except that the pH curves, pH 5 and pH 6 representing 1.0 M and 1.5 M diethylene amine did not vary as much as the curve of pH 7 representing 1.5 M diethylene amine. From these Figs. 5 and 6 it can be said that the pH of the inhibited cassava media varies inversely with the corrosion rates of mild steel. Fig. 7 shows that sodium chromate only become significantly efficient at 1.0 M concentration and beyond. It exhibited little or no efficiency at 0.5 M concentration. Unlike the former, diethylene amine shows efficiency greater than 85% at concentration of 0.5 M. This efficiency according to Fig.8 is similar to those exhibited by 1.0 M sodium chromate inhibited cassava fluid. The increase in the inhibition efficiencies of the two inhibitors with increase in their concentrations is similar to an earlier research on inhibition of mild steel corrosion in seawater by *Theobroma cacao* and *Cola acuminata* leaves extracts (Umoru *et al.*, 2005).

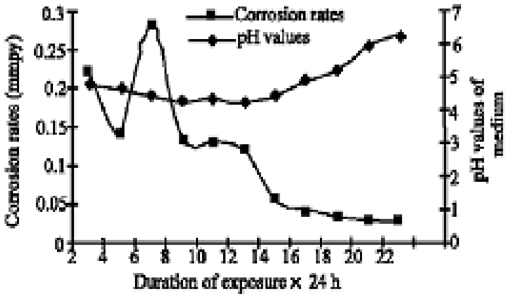

Figure 5: RElationship between corrosion ra tes and the pH values of cassava fluid inhibited with 1.0 M sodium

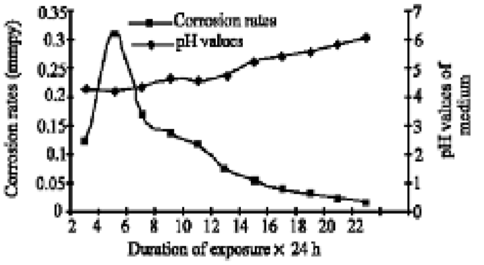

Figure 6: Relationship between corrosion rates and the pH values of cassava fluid inbitited with 1.0 M diethylene

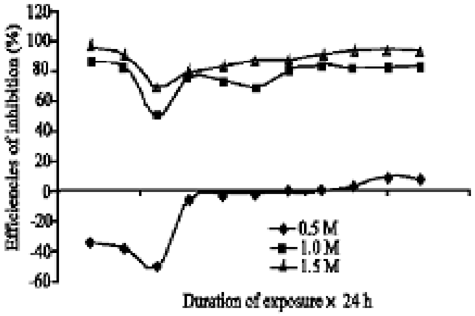

Figure 7: Variation of the inhibition efficiencies of sodium chromate with concentration and duration of exposure

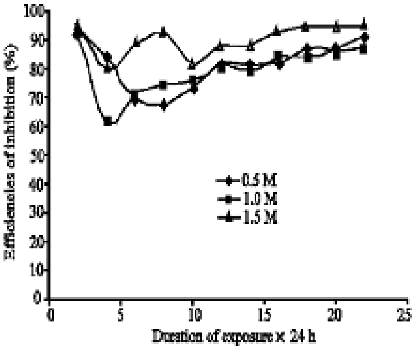

Figure 8: Variations of the inhibition efficiencies of diethylene amine with concentration and duration of exposure

4. DISCUSSION

One of the most aggressive ions in cassava fluid is the cyanide ion (CN-). Cassava contains cyanogens and cyanates both of which are easily reduced to form hydrogen cyanide acid, HCN and cyanate ion, CN respectively during fermentation according to Equations 1 and 2 (Fontana and Greene, 1987).

$$\frac{1}{2}C_2N_2 + H^+ + e^- = HCN \qquad (1)$$

$$OCN^- + 2H^+ + 2e^- = CN^- + H_2O \qquad (2)$$

The pH variation of cassava fluid with time of exposure without any sample immersed in it can be traced to Eq. 1 during which acidity of the juice is increased. That is the decrease in the pH values of the juice for the first few days (i.e., the first 192 h) could be associated with the release of the HCN above. When all the linamarin (C_2N_2) has been hydrolyzed, the release of HCN is stopped and the acidity of the juice reached its peak (Fig. 3 and 4). This result corroborates the findings III an investigation of the inhibitive potential of some amino acid derivatives in cassava fluid (Alagbe *et al.*, 2005). Beyond this point, the cassava fluid begins to experience an increase in pH probably because of increasing dilution of the fluid without corresponding production of HCN. With the immersion of a mild steel in the cassava fluid it is most probable that corrosion sets in with dissolution of iron at the anode (Eq. 3), dissociation of HCN (Eq. 4) and consumption of dissolved oxygen and the electrons produced at the anode according to Eq. 5

$$Fe = Fe^{2-} + 2e^- \qquad (3)$$

$$HCN = CN^- + H^+ \qquad (4)$$

$$O_2 + H_2O + 4e^- = 4\ OH^- \qquad (5)$$

The overall reaction initially is suspected to be that of equation (6) when $Fe(CN)_2$ is formed.

$$Fe^{2+} + 2CN^- + 2H = Fe(CN)_2 + H_2 \qquad (6)$$

However, as soon as all the cyanogens have been consumed and the production of HCN is halted, the overall reaction is expected to have changed to those of Eq. 7 and 8 leading to the release of ferrous hydroxide, $Fe(OH)_2$ or in the presence of surplus oxygen ferric hydroxide, $Fe(OH)_3$ as the corrosion products.

$$Fe^{2+} + 2(OH)^- = Fe(OH)_2 \qquad (7)$$

$$Fe^{2+} + 3(OH)^- = Fe(OH)_3 \qquad (8)$$

These products are probably responsible for the increase in the alkalinity of the cassava medium resulting in subsequent increase in pH (Fig. 3 and 4). The increased pH reduced the attacks of the mild steel by the cassava medium as shown in Fig. 5 and 6. This trend is supported by Pourbaix diagram for iron-water system where $Fe(OH)_2$ and $Fe(OH)_3$ are the products of corrosion in alkaline environment (Umoru *et al.*, 2003). The inhibition produced by sodium chromate in this work supports earlier reports of its potential in aqueous environment (Trethewey and Chamberlain, 1995).Sodium chromate according to the literature (Roberge,2000) is a passivating inhibitor that is capable of causing a large anodic shift of corrosion potential thereby forcing a metallic surface into the passivating range. It is an oxidizing anion that passivates steel in the absence of oxygen. This perhaps explains its active role as an inhibitor of steel in cassava at higher concentrations. It is important to point out the characteristic of anode inhibitors to accentuate corrosion when used in insufficient quantity because of unfavourable anode cathode area effect. From the results of this work, it is clear that sodium chromate exhibited to follow at 0.5 M this characteristic as it was unable to inhibit mild steel corrosion in cassava fluid (Fig. 7). "When it was however applied in excess of 1.0 M concentration, inhibition of mild steel corrosion in cassava slurry increased significantly.

Inhibition of metal corrosion by organic compounds is a result of adsorption of molecules or ions at the metal surface forming a protective layer. The extent of adsorption depends on the nature of the metal, the metal surface condition, the mode of adsorption, the chemical structure of the inhibitor and the type of corrosive media (Thomas, 1981). Heteroatoms such as oxygen, nitrogen, phosphorus, sulphur and the presence of aromatic rings or triple bonds in the structure of organic inhibitors enhance the adsorption process (Rajappa and Venkatesha, 2003 and Bentiss *et al.*, 2000). They do so by acting as chemisorptions centers. The protective properties of these compounds depend on the electron densities at the chemisorptions center. The effectiveness of the inhibitor increases with higher electron densities at the center (Rajappa and Venkatesha, 2003). Diethyleneamine, (C_2H_5) NH only contains nitrogen as a heteroatom. It is thus explainable that the inhibitive protection from diethylene amine is dependent on the electron density around nitrogen chemisorption centers. The NH group must have interacted with the steel surface to increase the corrosion resistance of NST-44 mild steel in the diethylene amine inhibited cassava fluid.

5. CONCLUSIONS

It may be concluded therefore that although mild steel in cassava fluid environment suffered corrosive attack the addition of diethylene amine and sodium chromate as inhibitors reduced the corrosion rates substantially. The inhibitive efficiencies of sodium chromate and diethylene amine increased with increase in concentrations of the inhibitors. The results of this study also showed that diethylene amine is a more active inhibitor of the corrosion of mild steel in cassava fluid than sodium chromate the reason being that its efficiencies of inhibition were greater than 85% for all the concentrations investigated unlike the case of sodium chromate at lower concentrations.

REFERENCES

Alagbe, M., Umoru L.E, Afonja A.A and Olorunniwo, O.E. Investigation of the effect of different amino acid derivatives on the inhibition of NST-44 mild steel corrosion in cassava fluid, *Bostwana J. Technol.*, 2005 (In review).

Azarnbuja, D.S., Martini E.A.A and Muller, L. Corrosion behaviour of iron and AISI 304 stainless steel in tungstate aqueous solutions containing chloride. *J. Braz. Chern. Soc.*, 14: 570-576, 2003.

Bentiss, F. Traisnel, and Lagrenee, M. Inhibitor effects of triazole derivatives on corrosion of mild steel in acidic media. *Br. Corrosion J.*, 35: 315-320, 2000.

Fontana, M.G. and Greene N.D. Corrosion Engineering, 3rd Edn., McGraw- Hill, New York, 1987.

Loto C.A. and A Mohammed, The effects of cashew juice extract on corrosion inhibition of mild steel in HCl. *Corrosion Prevention and Control*, 47: 50, 2000.

Loto, C.A., The effects of bitter leaf on the corrosion inhibition of mild steel in H_2S04 and HCL, Corrosion Prevention and Control, 50: 44-47, 2003.

Maayta, A.K., Organic corrosion inhibitors for aluminium in sodium hydroxide. *J. Corrosion Sci. Eng.*, 3: 25, 2002.

Pryor, M. J. and Cohen M, The inhibition of the corrosion of iron by some anodic inhibitors J. *Electrochem. Soc.*, 100: 204, 1953.

Rajappa, S.K. and. Venkatesha T., Inhibition studies of a few organic compounds and their condensation products on the corrosion of zinc in hydrochloric acid medium. *Turk. J. Chern.*, 27: 189-196, 2003.

Roberge, P.R., Handbook of Corrosion Engineering. McGraw-Hill, 2000.

Thomas, J.G.N., Some new fundamental aspects in corrosion inhibition. 5th European Sympos. On corrosion inhibitors, Ferrara, Italy (1980) University Ferrara, pp: 453, 1981.

Trethewey, K.R and Chamberlain, J. Corrosion for Science and Engineering, 2nd EOO., Harlow Essex, Addison Wesley, London. pp: 286-292, 1995.

Umoru, L.E, Imasogie B.I. and Olajumoke A.M, Corrosion characteristics ofNST-37-2 and NST-60-Mn steel reinforcement in concrete under different environmental conditions, *NSE Technical Transactions*, 38: 56-65, 2003.

Umoru, L.E, Fawehinrni I.A, and. Fasasi A.Y. Investigation of the inhibitive influence of *Theobroma cacao* and *Cola acuminata* leaves extracts on the corrosion of a mild steel in sea water, Proceedings of the 3rd Nigeria Materials Congress 2004, Engineering Materials Development Institute, Akure, Nigeria, 7-9 December, 2004, pp: 152-157, 2005.

Ife Journal of Technology, Vol. 18 (2), 35-41, 2009

Full Paper

EMISSION INVENTORY OF ANTHROPOGENIC ACTIVITIES AT SOUTHEASTERN LAGOS

L.A. Jimoda
Department of Chemical Engineering
Ladoke Akintola University of Technology, Ogbomoso, Nigeria.
lukumanjimoda@yahoo.com

J.A. Sonibare
Department of Chemical Engineering
Obafemi Awolowo University, Ile-Ife, Nigeria

F.A. Akeredolu
Department of Chemical Engineering
Obafemi Awolowo University, Ile-Ife, Nigeria.

ABSTRACT

Air inversion accompanying foggy dispersion and visibility reduction to less than 20meters has become a permanent feature of Okobaba midsection part of the Third Mainland Bridge in the Southeastern part of Lagos in the last 10 years. This paper estimates the criteria air pollutants from some dominant sources in the area using emission factor approach. Mass of sawdust combusted in the area, average house fuel consumption for cooking, fuel consumption by vehicles, power generations, industries and domestic activities are combined with the appropriate emission factors to quantify the air pollutants from these sources. Particulate matter is emitted most from sawdust combustion followed by oxides of nitrogen (NO_x), oxides of sulphur (SO_x) and carbon monoxide (CO), in the reducing order. Emission from traffic showed that CO is emitted most from gasoline bus while diesel bus emits the lowest CO with the value, 11.1562×10^{10} tons/year and 14.9788×10^8 tons/year respectively. NO_x has its highest value of 14.8735×10^6 tons/year, from truck/trailer. It is followed by gasoline bus, car, diesel bus in the reducing order while it is least emitted from motorcycle with the value $330{,}340 \times 10^3$tons/year. In the power generation and industries, CO_2 emission per year has the highest value while aldehyde emission is the lowest. Most CO and CO_2 emissions from household activities in the area come from wood emission. This emission inventory information is expected to guide researchers and policy makers to know the fate and effects of aerosol emission in the area for adequate air quality management.

Keywords: Air Pollutants, Emission Inventory, Emission Factor

1. INTRODUCTION

The ongoing plan of Lagos State Government to turn Lagos into mega city status in the last five years has led to increasing researches into natural and anthropogenic emissions of air pollutants in the state. Air quality laws in most industrial cities are based on minimum permissible concentration of pollutants (O'Neil, 1993). To plan and execute air pollution control programs designed to meet the requirement of these laws, there is a need for emission inventory for identification and quantification of pollutants from possible sources. Dara (2003) gave the composition of a clean, dry air to be major components (Nitrogen. Oxygen and Water vapour), minor components (Argon and Carbon dioxide) and trace components (Neon, Helium, Methane, Nitrous oxide, Hydrogen, Sulphur dioxide, Nitrogen dioxide, Ammonia, Carbon monoxide, Ozone and Iodine). The proportion of these components of the atmosphere more or less remain constant up to a height of about 16km from the earth surface, above this height, gravitational separation begins which becomes significant above 130km. At this height, the atmosphere is a dynamic system with gases and particulate matters entering, undergo chemical transformation and leaving.

Air pollutants in the atmosphere are either natural r anthropogenic (man made). Natural pollution includes volcanoes, tornados, sea spray, sand storm, harmattan dusts and erosion re-entrainment. Anthropogenic pollution comprises of pollutants from transportation, domestic heating, electric power generation, refuse burning and industrial fuel burning/process emission. The presence of natural anthropogenic pollutants in the atmosphere has been linked to the formation of haze and changes in the atmosphere's radiative balance as well as adverse effects on human health, crops and materials (Weber, 2003).

The emissions from refuse burning are composed of SO_2, hydrocarbon, CO, particulate matter, NO_x (Jimoda, 1996). However, trash and wood burning produces Aldehyde apart from H_xC_y, NO_x, CO, SO_2 and particulate matter while burning plastics and treated wood produces heavy metals and dioxin. HCl gas is emitted from burning chlorinated organic plastics while mercury and mercury compounds are emitted from burning newspapers. Plastics such as polyvinylchloride (PVC) emit chlorinated dioxins and furans which are carcinogenic (Dara, 2003). Summarily, air pollutants from most solid wastes including sawdust contain particulate matters, sulphur oxides, carbon monoxide, oxides of nitrogen, poly-nuclear hydrocarbons, volatile organic compounds, aldehydes, dioxins and ferrous, heavy metals such as Hg, HCl gas and H_2S. However, determination of emission from open burning of sawdust in Southeastern Lagos requires estimates of its generation rate. According to Nest (1991), about 20kg of solid wastes is generated per capital per annum in Nigeria on the average, but Achankeng (2003) reported 0.3kg of solid wastes per capital per day for the city of Lagos. Similarly, Kofoworola (2007) gave an approximate of 1.1kg per capital per day of solid wastes in Lagos while a field survey of solid waste generation for households in the urban area of central Nigeria gave solid waste generation as 0.54kg per capital per day (Sha'Ato et al, 2007). Smith et al (1993) estimated the global carbon monoxide emission to be about 1100Tg/year of which about 350Tg/year is from biomass burning. Khalil and Rasmussen (1990) reported CO globally estimates from combustion of fossil fuel to be about 500Tg/year and ten years later, Jain (2007) reported estimated global CO emissions to be between 320 and 390Tg for the year 2000.

Transportation in Southeastern Lagos, like other areas of Lagos is mostly by road, either by public transport or private-owned like other developing countries (Figueroa et al, 2006). There is potential for vehicular emissions to concentrate on over 300 public transport routes and terminals. Southeastern Lagos which houses the popular third mainland bridge is not left out in its concentrated traffic throughout the days. Though, emissions from an individual car are generally low, in numerous cities across the world, the personal automobile is the single polluter as emissions from numerous vehicles on the road add up (EPA, 1992). Car ownership in Lagos is about 4.3 cars per 1000 in 1999 (Odeleye, 2001), there is usually traffic congestion (Khezwana and Maunder, 1994). Road transport emissions are in form of combustion emissions, evaporative emissions and fugitive dust emissions from paved and unpaved roads. Road transport combustion emissions are SO_2, NO_X, CO, PM, VOC, CO_2, CH_4, Pb and N_2O. Benzene at times constitutes road transport emission and accounts for about 24% of United Kingdom emission (Ginlay, 1997).

Industrial sources by far represent the most diversified type of pollution emission. Industrial pollutions are continually changing, this necessitate changes in the types and amount of emissions. Samara et al (2003) obtained three receptor sites within the urban area of Thessaloniki in an industrialized region of Northern Greece. In his studies, chemical source profiles were constructed for particulate emissions (PM_{10} of PM_{20}) from several urban and industrial sources. Pacyna et al (2001) estimated the anthropogenic emissions of mercury from anthropogenic sources in Europe in 1995 to be about 342 tons which corresponds to a decrease of about 45% compared to this emission in 1990. Combustion of fuels particularly coal was traced to be the main source of about half of the total emissions of mercury in the area. The decrease in mercury emissions in Europe in the last one decade was concluded to be the reduction of mercury emissions from industrial sources

Power generation is one of the sources of air pollutants emitting suspended particulate matters, SO_2, NO_x, CO, SO_3, metallic organic compounds and lead (Jimoda, 1996). In Nigeria, electricity availability from the national grid is a major problem. Presently, Nigeria consumes about 5,000 MW of electricity daily, but it has an average production of only 2,500 MW (Sonibare and Jimoda, 2009). Hence, the additional 2,500 MW comes from private electricity generators which rely on both gasoline (PMS) and diesel (AGO) for operation (Sonibare and Jimoda, 2009). Between 1991 and 1992 alone, 7438 generating sets were imported into the country (Akarakiri, 1999) and about 97 percent of firms operating in the country presently own generators (Tyler, 2002).

The common forms of cooking energy in use in Nigeria are wood fuel, kerosene, liquefied petroleum gas (LPG) and electricity (Anozie et al, 2007). The southeastern Lagos people are not different in term of energy carrier for cooking in this wise. Scarcity of kerosene always necessitates consideration of wood fuel as alternative (Dionco-Adetayo, 2001; Tabuti et al, 2003) and it has a major share of the energy consumption in Nigeria with over 50.45% (Ikuponiyi, 2006). Jabber and Probert (2002) found out that un-vented combustion appliances like portable kerosene and liquefied petroleum gas (LPG), stoves employed in domestic heating emits high rate of CO. Also, Rogaume et al (2002), concluded that a reduction in NOx may be a benefit from a reduction in temperature and a reduction in oxygen concentration while Akeredolu 1989, estimated CO emission to be about 6.42 x 109 kg from wood fuel in 1981 in Nigeria. Raiyani et al (1993) reported that about 50 – 80% of the TSP emissions from biomass and coal burning cooking stoves are in respirable fraction of $\leq 2\mu m$ size.

2. MATERIALS AND METHODS

The description of the Okobaba area of Southeastern Lagos where about 327 sawmill industries and 34 burning points were identified was discussed here. Also, source categories in the area which include sawdust combustion transportation, power generation, industries and household activities together with emission factor approach for estimating the criteria air pollutant were discussed.

2.1. The Study Area/Sampling Site

Southeastern Lagos is within Lagos Mainland Local Government and it is characterized by towns and villages comprising of Yaba, Ebute-metta, Iddo-Otto, Akoka, Maroko, Ijero, Oko Baba, Abule-ijesha and Olaleye. Major sources of emission present in this location make it an area of special interest in the emission inventory study. The site of interest is located at the center of Oko Baba which is characterized by about 327 sawmills and 34 burning points of sawdust between Ebute-metta and Oyingbo on the edge of the Lagoon. This is quite visible on the third mainland bridge, a major link between the mainland and the island parts of the city which is surrounded by various species of freshwater and water fishes around state's island and Atlantic coaster water (Abegunde, 1986). Figure 1 shows the sampling sites in the Southeastern part of Lagos State.

2.2. Emission Inventory of the Study Area

An emission factor base approach for the source categories identified in Okobaba area of southeastern Lagos was used to quantify the criteria air pollutants in the area. The procedure for emission estimate is shown in the emission factor approach calculation equations below:

2.2.1.Emission Factor Approach Calculation Equations

Akeredolu (1996) defined emission factor as number value which show the amount of pollutants emitted compared to some given base. This may be the amount of materials produced, raw materials used, size of process equipment or plant capacity. An emission factor based approach for source category is often used to determine the contribution of combustion activities to criteria air pollutants (Sonibare and Jimoda, 2009).

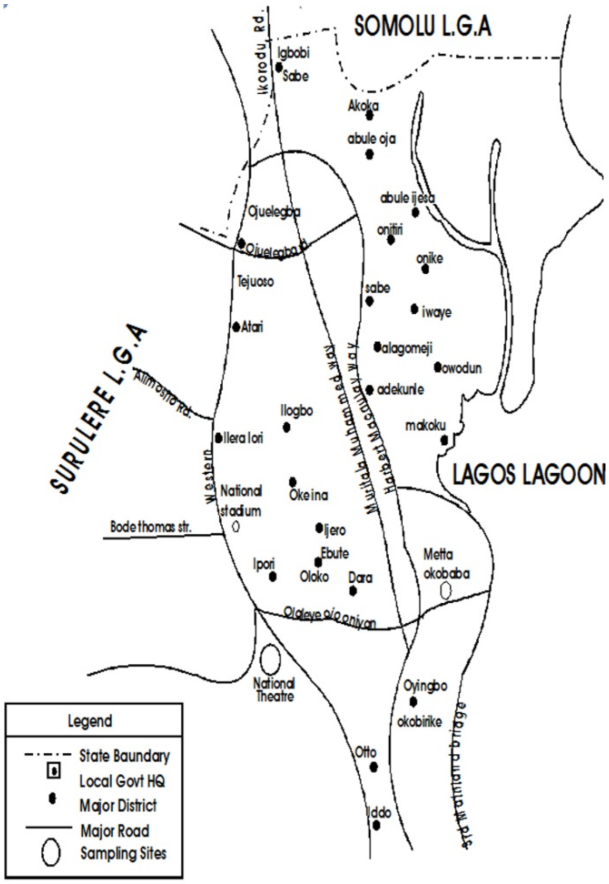

Fig 1: Map of Lagos Mainland Local Government Area showing sampling sites. Source: Abegunde (1986)

For sawdust combustion, criteria air pollutants which include NOx, SO_2, CO and particulate matters are estimated as:

$$\text{Criteria Air Pollutant Emitted/Year} = \frac{\text{Emission Factor (g) of Criteria Air Pollutant}}{\text{1Kg of Sawdust Combusted}} X \text{ Mass of Sawdust Combusted / Year } (Kg)$$

For transportation the criteria air pollutants emitted per year is estimated as:

$$\text{Criteria Air Pollutant Emitted/Year} = \frac{\text{Emission Factor (g) of Criteria Air Pollutant}}{\text{1Kg of Fuel Burnt}} X \text{ Yearly Fuel Consumption for each category of Traffic } (Kg)$$

For power generation:

$$\text{Criteria Air Pollutant Emitted/Year} = \frac{\text{Emission Factor (g) of Criteria Air Pollutant}}{\text{1Kg of Fuel Burnt}} X \text{ Yearly Fuel Consumption Level } (Kg)$$

The emission factors for gasoline fuel and diesel fuel are converted from ng/J to ng/kg using heating values of diesel and gasoline which are 44,900 J/g and 47,200 J/g respectively.

Similarly, for industries:

$$\text{Criteria Air Pollutant Emitted/Year} = \frac{\text{Emission Factor (g) of Criteria Air Pollutant}}{\text{1Kg of Fuel Burnt}} \text{ X Yearly Fuel Consumption Level for Industries (Kg)}$$

The emission factor approach calculation due to emissions from household activities is estimated as:

$$\text{Criteria Air Pollutant Emitted/Year} = \frac{\text{Emission Factor (g) of Criteria Air Pollutant}}{\text{1Kg of Household Fuel Burnt}} \text{ X Average Yearly Household Fuel Consumption from Cooking (Kg)}$$

2.2.2. Emission from Sawdust Combustion

Determination of emission from open burning of sawdust in the Southeastern Lagos requires sawdust generation rate. Volume of container used to dump sawdust at the burning points, total number of sawmills in operation, and average number of times the sawdust is being dumped per day was used to estimate mass of sawdust produced in the area. The daily rate was eventually obtained using 454kg/m3, the density of sawdust (Dosumu and Ajayi, 2002). The mass of sawdust produced from 327 sawmilling machines per week, per month and per annum was estimated using the number of days in a week, a month and a year respectively. This was estimated to be 57,174.3677kg per day, 400,220.5739kg per week, 1,715,231.031kg per month and 20,868,644.21kg per year. The calculated annual sawdust generation was combined with the emission factor for sawdust from AP-42 (EPA, 1995) to predict the criteria air pollutants generated from the combustion of sawdust in the area.

2.2.3. Emission from Transportation

In the emission prediction from transportation, fuel consumption and vehicle fleet are important parameters in emission factor approach. Traffics from the area are categorized as motor cycles, cars, buses and trucks/trailers. Traffic counts are used to know the numbers of each category of vehicles with counting done for weekdays and weekends from which annual traffic volume was estimated. The fuel consumption of different categories of vehicles is combined with the density of Diesel (AGO, $840kg/m^3$), and Petrol (PMS, $750kg/m^3$) to compute the mass of AGO/PMS consumed for transportation. These values were finally combined with the fuel based emission factors from European Countries (EU, 2006) and Asian nations (Yli-Tuomia et al, 2005) to predict the criteria air pollutants from traffic in the area.

2.2.4. Emissions from Power Generation

In the area, 327 sawmilling machines were identified using 42 electric power generators with each generator consuming an average of 50litres of AGO per day. Also, about 68 plane machines comprising of 37 diesel engines and 31 petrol engines are located in the area with each consuming about 25litres of AGO per day while the petrol engine consumes about 20litres per day. Therefore, for the sawmilling machines and plane machines, total fuel consumption per day is estimated to be 3,025litres AGO and 620litres of PMS.

Emission calculations from these electric power generators in the southeastern Lagos were done using fuel consumption level consumed in the area and the emission factor from electric power generations (using diesel and petrol) available in AP-42 (EPA, 1995).

2.2.5. Emissions from Industries

Industrial emissions depending on the raw-materials, products and by-products from the industries in the area are computed by identifying the emissions from the particular industries. The emission factors from such industries from AP-42 (EPA, 1995) were then used to estimate the emissions from the industries.

Four pure water manufacturing industries were identified in the area with an average consumption of 80litres of diesel per day. A tile manufacturing company is also located there. However, interaction with the Production Manager showed that the company is only polishing the imported materials. No significant pollutant was identified. However, the company has 2 diesel consuming standby generators with an average daily consumption of 60litres of diesel per day. Hence, the total daily consumption of diesel fuel was estimated to be 440litres for electric power generation. This consumption level was combined with emission factor from AP-42 (EPA, 1995) to estimate the emissions from industries in the area.

2.2.6. Emissions from Household Activities

The average house fuel consumption for cooking in Lagos for five years (Table 13) was combined with the relevant emission factor from AP-42 (EPA, 1995) to compute the potential emission of air pollutants from the combustion of wood fuel, LPG and kerosene for cooking. The population of Lagos Mainland relative to the population of the entire Lagos State (FGN, 2007) was used to get the average house fuel consumption for cooking in the area.

3. RESULTS AND DISCUSSION

The criteria air pollutants were calculated to be 36.1028 x 104kg, 0.4173 x 104kg, 2.7129 x 10^4kg and 0.2629 x 10^4kg for particulate matters, SO_X, NO_X and CO respectively. Particulate matters were identified as the main criteria air pollutant from sawdust combustion which is followed by NO_x, SO_x, and lastly CO. CO_2, Total Organic Carbon (TOC), POM and Aldehydes were not available in the AP-42 (EPA, 1995) and hence could not be estimated.

From Table 1, it can be seen that there are more cars on the road in the area estimated as 7,197,800 per annum while trucks/trailers were the lowest with the value 1,565,120 per annum. The annual estimates for buses and motor cycles were 5.004880 and 1,789,960 respectively. The annual estimates for traffic counts in weekend days are lower than their corresponding values for weekdays for all categories of vehicles. As shown in Table 3, the daily emission of CO was calculated to be 336214710.1g followed by car with the value 252195777.2g while diesel bus emits the lowest value of 4514167.309g. The daily emission of CO for truck/trailer and motorcycle were estimated to be 135778815.1g and 75474931.03g respectively.

As shown in Table 3, carbon monoxide (CO) was emitted mostly from gasoline bus with the value 122,718,360,000g per year followed by trucks/trailers which emit 49,559,267,000g per year while diesel bus emits the lowest value of CO of 1,647,671,068g per year. The CO emitted per year for motorcycles and cars were estimated to be 27,548,349,000g and 92,051,458,000g. NO_x had its highest daily emission of 448243834.3g from truck/trailer. This was followed by gasoline bus, car, diesel bus and motorcycle in the reducing order. Their values were 33213533.54g for gasoline bus, 24035525.77g for car, 8603175.956g for diesel bus and 995707.9976g for motorcycle respectively. Particulate matters were mainly from diesel bus and truck/trailer with values1811194.938g and 32101562.38g respectively.

From sawmilling and plane machines in southwestern Lagos, the emissions from gasoline and diesel consumed due to power generation are reported in Table 4. The results showed that for power generation due to gasoline, CO_2 was most emitted with daily emission of 1.4658715 x 106g while aldehyde has the lowest value of 6.3650523 x 102. Similarly, daily emission of CO2 of 8.10813 x 106g was the highest value for diesel-consumed power generation while aldehyde daily emission was the lowest with the value of 3.1946477 x 103g.

Industrial emissions from the area were taken as the emissions due to power generation from the identified industries in the area. Their daily emissions are 1.1793643 x 10^6g of CO_2, 3.1465205 x 10^4g of NO_X, 6.8041848 x 10^3g of CO, 2.2404023 x 10^3g of PM, 2.0910421 x 10^3g of SO_X and 4.6467603 x 10^2g of aldehyde in the reducing order. The tile-polishing and pure water industries in the area do not emit any significant pollutants in the area. The calculated emissions using emission factors as shown in Table – show that CO_2 is emitted most for all the household fuel types. However, CO_2 due to wood emission has the highest value of 2.25318 x 10^{10}g while CO_2 emission from LPG is the lowest. Particulate matter which is very important in the aerosol studies due to its health effect and visibility impairment was mainly from wood emission. SO_x from the wood emission also recorded the highest value of 2,650.8kg per year followed by 654kg per year from kerosene while SO_x emission from LPG was very low (3.50kg per year). NO_x emission was mostly from Kerosene with the value 61,104kg per year, followed by wood emission (17,230.2kg per year) and lastly, LPG emission of NO_x value 496kg per year. Over 95% of CO emitted came from wood emission, while CO_2 emissions were equally from wood emission. Total VOC, POM and Aldehydes emitted from wood emission were 151,095.6kg per year, 10.6kg per year and 15,904.8kg per year respectively. LPG emission and kerosene did not record any value for these since there were no values for these in the emission factor in AP-42 (EPA, 1995).

4. CONCLUSION

The criteria air pollutant from different sources is as summarized in the Table 8. The estimates represented above suggest that particulate matter emissions in the area are mostly from traffic, saw dust combustion and from household activities. SO_x is emitted mostly from power generation, saw dust combustion and household activities. Over 95% of NO_x and CO emitted in the area is from traffic while the remaining comes from other sources. Information such as CO_2, TOC, POM and Aldehydes for saw dust combustion, TOC, POM for power generation and industries, CO_2, TOC, POM and Aldehydes for traffic could not be obtained because they are not available in the emission factor data. The emission inventory information is important for policy makers studying the fate and effects of aerosol emissions in Southeastern Lagos. However, it is important to keep in mind that emission data are never complete or entirely accurate.

Table1: Traffic Counts of Vehicles at Third Mainland Bridge (Weekdays and Weekends)

Time	Motor cycles		Cars		Buses		Trucks/Trailers	
	Wd	We	Wd	We	Wd	We	Wd	We
Day 1	202	78	741	480	621	239	179	102
Day 2	217	84	823	531	519	331	181	113
Day 3	194	91	901	579	574	237	176	99
Mean Traffic Counts (1hour)	204	84	822	530	571	269	179	105
Annual Estimate	1,789,960 1,789,960	735,840 735,840	7,197,800 7,197,800	4,642,800 4,642,800	5,004,880 5,004,880	2,356,440 2,356,440	1,565,120 1,565,120	919,800 919,800

Wd = Weekdays; We = Weekends

Table 2: Fuel Consumptions for Various Categories of Traffic at Third Mainland Bridge

	Motorcycle (Kg)	Car (Kg)	Gasoline bus (Kg)	Diesel bus (Kg)	Truck/Trailer (Kg)
Per Day	132407.9784	1656480.067	1382169.519	387007.4654	14725487.33
Per Week	926855.8488	11595360.47	9675186.633	2709052.258	103078411.3
Per Month	3972239.352	49694402.02	41465085.57	11610223.96	441764619.8
Per Year	48328912.12	604615224.5	504491874.4	141257724.9	5374802875

Table 3: Daily Criteria Air Pollutants in Lagos Southwest

	CO (g)	NO_X (g)	PM (g)
Motorcycle	75474931.03	995707.9976	0
Car	252195777.2	24035525.77	0
Gasoline bus	336214710.1	33213533.54	0
Diesel bus	4514167.309	8603175.956	1811194.938
Truck/Trailer	135778815.1	448243834.3	32101562.38

Table 4: Daily Emissions from Power Generation.

	$NO_{X(g)}$	$CO_{(g)}$	$SO_{X(g)}$	$PM_{(g)}$	$CO_{2(g)}$	Aldehydes $_{(g)}$
PMS	1.5341971×10^4	5.9144505×10^5	7.9014443×10^2	9.6573208×10^2	1.4658715×10^6	6.3650523×10^2
AGO	2.1632329×10^5	4.677877×10^4	1.4375914×10^4	1.5402765×10^4	8.10813×10^6	3.1946477×10^3

Table 5: Criteria Air Pollutants from Industries using EF

	NO_X (g)	CO (g)	SO_X (g)	PM (g)	CO_2 (g)	Aldehyde(g)
Per Day	3.1465205×10^4	6.8041848×10^3	2.0910421×10^3	2.2404023×10^3	1.1793643×10^6	4.6467603×10^2
Per Week	2.20256435×10^5	4.76292936×10^4	1.46372947×10^4	1.56828161×10^4	8.2555501×10^6	3.25273221×10^3
Per Month	9.4395615×10^5	2.04125544×10^5	6.2731263×10^4	6.7212069×10^4	3.5380929×10^7	1.39402809×10^4
Per Year	1.14847998×10^7	2.4835274×10^6	7.63230366×10^5	8.17746839×10^5	4.3046797×10^8	1.6960675×10^5

Table 6: Household Fuel Consumptions for Cooking in Lagos (2000-2004)

Year	LPG (x 10^3litres)	Kerosene (x 10^3litres)	Wood Fuel (x 10^5tons)
2000	11,740	99,350	3.5
2001	10,027	80,426	3.6
2002	9,171	75,547	3.8
2003	5,007	86,987	3.9
2004	5,445	87,358	4.0

Source: NNPC (2005).

Table 7: Yearly Emission from Cooking Fuel Combustion.

Air Pollutants	Wood Emission(g)	LPG Emission (kg)	Kerosene (kg)
PM	229294200	14.5899	1460.02
SO_X	2650800	3.5015	654.112
NO_X	17230200	496.0592	61104.0021
CO	1673980200	58.3599	7472.2911
CO_2	2.25318×10^{10}	437699.25	41041124.31
TOC	-	17.50797	1524.721
Total VOC	151095600	-	-
POM	10603.2	-	-
Aldehydes	15904800	-	-

Table 8: Yearly Criteria Air Pollutants from Different Sources

Air Pollutants	Sawdust Combustion	Power Generation	Industries	Traffic	Household
PM $\times 10^4$kg	36.1028	0.5975	0.0818	1237.8156	23.0769
$SO_X \times 10^4$kg	0.4173	0.5536	0.0763	-	0.3308
$NO_X \times 10^4$kg	2.7129	8.4558	1.1458	18800.8489	7.8830
CO $\times 10^4$kg	0.2629	23.2952	0.2484	29352.5105	168.1511
$CO_2 \times 10^4$kg	-	349.4510	43.0468	-	6401.0624
TOC $\times 10^4$kg	-	-	-	-	15.2638
POM $\times 10^4$kg	-	-	-	-	0.0011
Aldehydes $\times 10^4$kg	-	0.0349	0.0169	-	1.5905

They need continuous upgrading and revision using the outcome of the latest research carried out within major international organizations and programmes.

ACKNOWLEDGEMENTS

Authors acknowledged the support of Mr. Alliyu of Regional Space Centre of Obafemi Awolowo University for providing Geographical Information System (GIS) equipment. Equally acknowledged is the assistance of Afolabi Teslim, Adeyemi Olufunmi, Tijani Monsur, and Ilyas Teslim, in the collection of traffic counts data from the field.

REFERENCES

Abegunde, A., Description and Characteristics of Physical Environment of Lagos State, *Unpublished B.Sc*; These Department of Geography, Lagos state university, 1986.

Achankeng, E., *Globalization, Urbanization, and Municipal Solid Waste Management in Africa* (African Studies Association of Australian and the Pacific), Conference Proceedings- Africa on a Global Stage, pp. 22, 2003

Akarakiri, J.B., Private Electric Power Generation as an Alternative in Nigeria, *Energy* 24(5), 445-447, 1999.

Akeredolu, F.A., *Environmental Engineering Notebook*, Department of Chemical Engineering, Obafemi Awolowo University, Ile-Ife, Nigeria (Unpublished), 1996.

Akeredolu, F.A., Atmospheric Problem in Nigeria, An Overview, *Atmospheric Environment* 23(4), 783 – 792, 1989.

Anozie, A.N., Bakare, A.R., Sonibare, J.A. and Oyebisi, T.O., *Evaluation of Cooking Energy Cost, Efficiency, Impact on Air Pollution*, 2007.

Dara, S.S., *A Textbook of Engineering Chemistry* (revised 10th edition), Chand S. and Company Ltd, Ram Nagar, New Delhi, 2006.

Dionco-Adetayo, E.A., Utilization of Wood Wastes in Nigeria: a feasibility overview, *Technovation* 21, 55-60, 2001.

Dosunmu, O.O. and Ajayi, A.B., *Problems and Management of Sawmill Waste in Lagos*, Proceedings of International Symposium on Environmental Pollution Control and Waste Management, 7-10 January 2002, Tunis, EPCOWM' 2002, 271-278, 2002.

EPA, *Compilation of Air Pollutant Emission Factors*, Vol. I, Stationary Point and Area Sources, fifth ed. (Research Triangle Park NC, USA, 1995), United States Environmental Protection Agency, Office of Air Quality Planning and Standards, 1995.

EPA, *Automobile Emissions,* An Overview U.S. Environmental Protection Agency, EPA 400-F-92-007, 1992.

EU, *Emission Inventory Guidebook*, Road Transport Activities, Laboratory of Applied Thermodynamics, Aristotle University Thessalonica, GR-54124, Thessalonica, Greece, 2006.

FGN, *Legal Notice on Publication of the Details of the Breakdown of the National and State,* 2006 Census, Federal Republic of Nigeria Official Gazette, Vol. 94, No 24, 1-26, 2007.

Figueroa, M.J., Daridson, O.R. and Mackenzie, G.A., *Matching Transport and Environment Agenda in Developing Countries,* World Energy Council, WEC, US, 2006.

Ginlay, A.J., "*The chemistry of atmospheric pollutant*", 1997, http//:www.Aetat.co.uk/airquil/ bulletins/welcome.html.

Ikuponiyi, F.S., Status of Renewable Energy in Nigeria, International Conference on Making Renewable Energy, *A*

Reality, Abuja/Port Harcourt/Calabar, Nigeria, pp. 48, November 21-27, 2006.

Jaber, J.O. and Probert, S.D., Purchased Energy Consumptions in Jordan's Commercial and Public-service Sector, *Applied Energy* 71, 31-43, 2002.

Jain, A.K., Global Estimation of CO Emissions using three sets of Satellite Data for Burned Area, *Atmospheric Environment*, In Press, 2007.

Jimoda, L.A., *Environmental Engineering Notebook*, Department of Chemical Engineering, Obafemi Awolowo University, Ile Ife, Nigeria (Unpublished), 1996.

Khalil, M.A.K. and Rasmussen, R.A., The Global Cycle of Carbon Monoxide: Trends and Mass Balance, *Chemosphere* 20, 227-242, 1990.

Khezwana, M. and Maunder, D.A.C., International Experiences of Deregulated Urban Public Transport Systems, *Indian Journal of Transport Management*, 457-464, July 1994.

Kofoworola, O.F., *Recovery and Recycling Practices in Municipal Solid Waste Management in Lagos, Nigeria*, Waste Management, In Press, 2007.

NEST, *Nigeria's Threatened Environment:* A National Profile. Nigeria Environment and study/Action Team, NEST, Ibadan, 1991.

NNPC, *Annual Statistical Bulletin*, January – December (2000–2004), Nigerian National Petroleum Corporation, Corporate Planning and Development Division (CPDD), Abuja, Nigeria, pp. 83, 2005.

Odeleye, J.A., *Towards Gender Sensitive Urban Transport Planning and Operations in Metropolitan Lagos, Nigeria*, Presented at the 4th IFUP Congress, Marrech, Morocco, pp. 19, October, 2001.

O'Neil, P.O., *Environmental Chemistry*, 2nd edition, Chapman and Hall, New York, 1993.

Pacyna, E.G., Pacyna, J.M. and Pirrone, N., European Emissions of Atmospheric Mercury from Anthropogenic Sources in 1995, *Atmospheric Environment* 35, 2987-2996, 2001.

Raiyani, C.V., Shan, S.H., Desai, N.M., Venkaiah, K., Patel, J.S., Parikh, D.J. and Kayshyap, S. K., Characterization and Problems of Indoor Pollution due to Cooking Store Smoke, *Atmospheric Environment* 27A11, 1643-1655, 1993.

Rogaume, T., Auzanneau, M., Jabouille, F., Goudeau, J.C. and Torero, J.L., The Effects of Different Airflows on the Formation of Pollutants during Waste Incineration, *Fuel*, 2277-2288, 2002.

Samara, C., Kouimtzis, T., Tsitouridou, R., Konias, G. and Simeonov, V., Chemical Mass Balance Source Apportionment of PM_{10} in an Industrialized Urban of Northern Greece, *Atmospheric Environment* 37, 41 – 54, 2003.

Sha' Ato, R., Aboho, S.Y., Oketunde, F.O., Eneji, I.S., Unazi, G. and Agwa, S., Survey of Solid Waste Generation and Composition in a Rapidly Growing Urban Area in Central Nigeria, *Waste Management* 27, 352-358, 2007.

Smith, K.R., Khalil, M.A.K., Rasmussen, R.A., Thorneloe, S.A., Manegdeg, F. and Apte, M., Greenhouse Gases from Biomass and Fossil Fuel Stoves in Developing Countries: A Manila Pilot Study, *Chemosphere* 26, 1-4, 479-505, 1993.

Sonibare, J.A. and Jimoda, L.A., Criteria Air Pollutants from Some Anthropogenic Combustion Processes in Lagos, Nigeria, *Energy Sources*, Part A, 31, 1-13, 2009.

Tabuti, R.R.S., Dhillion, S.S. and Lye, K.A., Firewood Use in Bulamoyi, Uganda Species Selection, Harvesting and Consumption Patterns, *Biomass and Bioenergy* 25, 581-596, 2003.

Tyler, G., *Public and Private Electricity Provision as a Barrier to Manufacturing Competitiveness*, Findings 221, World Bank, pp. 4, December 2002.

Weber, R., Short-term temporal variation in $PM_{2.5}$ Mass and chemical composition during the Atlanta Supersite Experiment, 1999; *Air and Waste Management Association* 53, 84-91, 2003.

Yli-Tuomia, Aarnioa, T., Pirjolab, C.L., Makela, T.D., Hillamod, R. and Jantunena, M., Emissions of Fine Particles, NO_X and CO from on-road vehicles in Finland, *Atmospheric Environment* 39, 6696-6706, 2005.

Ife Journal of Technology, Vol. 18 (2), 42-50, 2009

Full Paper

RELEVANCE OF EXERGY ANALYSIS IN THE ASSESSMENT OF THERMAL POWER PLANT PERFORMANCE

A.N. Anozie
Applied Thermodynamics and Process Design Research Laboratory
Department of Chemical Engineering
Obafemi Awolowo University, Ile-Ife, Nigeria

O.J. Odejobi
Applied Thermodynamics and Process Design Research Laboratory
Department of Chemical Engineering
Obafemi Awolowo University, Ile-Ife, Nigeria
oludareodejobi@yahoo.co.uk

O.P. Ayoola
Applied Thermodynamics and Process Design Research Laboratory
Department of Chemical Engineering
Obafemi Awolowo University, Ile-Ife, Nigeria

ABSTRACT:

Exergy analysis of a natural gas based thermal power plant at Egbin, Ikorodu, Lagos State, was done to: evaluate the exergy and energy efficiencies and irreversibilities of units, subsystems and overall system; identify the units with large thermodynamic irreversibilities and investigate the causes of irreversibilities in the units and how they can be minimized; study the effect of interaction of units on the performance of subsystems and overall system. Process simulation was done using HYSYS, commercial process simulator software, and exergy analysis was done using Microsoft Excel Spreadsheet. It was found that the condenser unit has the lowest exergetic efficiency and the highest energetic efficiency of 22.6% and 99.9%, respectively. The furnace/boiler unit was found to have the highest irreversibility of 1484.3 MW and the regenerative unit has the lowest irreversibility of 9.7 MW. The study of the units interaction revealed that the furnace/boiler unit made the highest contribution of about 67% to the overall process irreversibility while the least contribution of 9.7% came from the turbines/generator unit. It was found that the optimum natural gas mass flow rate which optimized the flue gas temperature and CO2 emission was 40,000 kg/h rather than the operating rate of 45,570 kg/h.

Keywords: Exergy, energy, thermal power plant, efficiency, irreversibility, units and subsystems.

1. INTRODUCTION

The rate of depletion of fossil fuel reserves and environmental impact of combustion of fossil fuel has necessitated the operation of power plants in the most efficient manner. Thermodynamic analysis, such as energy and exergy analysis, has increasingly attracted the interest to achieve this goal. Energy is always conserved in every device or process. Unlike energy, exergy is not always conserved but is destroyed. The major causes of thermodynamic imperfection of the thermal processes are not accounted for by energy or first law analysis. It is the exergy or second law analysis that accounts for the irreversibilities like the heat transfer through a finite temperature difference, chemical reactions, friction, mixing and unrestrained expansion (Cengel and Boles, 2004).

A number of studies on exergy analysis have been carried out by researchers (Bejan, 1988; Moran, 1982 and Mohamad and Bandpy, 2005) to evaluate the performance of thermal power plants at different operating conditions. Caton, 2000 examined analytically the exergy destruction during combustion processes in an internal combustion engine. The rates of exergy destruction in a spray combustion process for gas turbine application and in a fundamental laminar diffusion flame, respectively, were evaluated using computational fluid dynamic models (Datta, 2000). Sciubba and Su, 1986 had earlier done a second law analysis of the steam turbine power cycle to analyse the influence of reheat temperature and pressure on regenerative cycle performance. Nag and De (1997) also performed the second law analysis on gas and steam turbine combined cycles to study the effects of different operating parameters on the cycle performance. The comparison of coal-fired and nuclear steam power plants using energy and exergy analyses to identify areas with potential for performance improvement had also been investigated (Rosen, 2001). Dincer and Al-Muslim (2001) carried out analysis of a Rankine cycle reheat steam power plant to study the energy and exergy efficiencies at different operating conditions with varying boiler temperature, boiler pressure, mass fraction ratio and work output from the cycle. The generalized exergy balance and cost balance equations had been utilized to study the effects of the annualized cost of a component on the production cost in 1000 KW gas-turbine cogeneration system (Kwon, *et al.*, 2001). Rosen and Dincer (2003) had performed a thermoeconomic analysis of power plants and applied it on a coal fired electricity generating station. Alasfour and Alajmi (2000) investigated the exergetic destructions of a steam generation system. Three irreversible processes investigated were combustion, heat transfer and streams mixing processes and the results showed that at stoichiometric condition, the exergy was destroyed mainly by two irreversibilities, associated with heat transfer and combustion processes, and to a much lesser extent by streams mixing process.

The literature on exergy analysis reveals a lack of clear information on the exergy balance in practical natural gas based thermal power plants. And up till now there has not been any work done on the thermodynamic analysis of Egbin thermal power plant, one of the present major sources of electricity to the national grid, located in Ikorodu, Lagos State, Nigeria. The objectives of this study are to: evaluate the energy and exergy efficiencies and irreversibilities of units, subsystems and overall system; identify the areas with large thermodynamic irreversibilities and investigate the causes of irreversibilities in the units and how they can be minimized; study the effect of units interaction on the performance of subsystems and overall system.

2. PLANT DESCRIPTION

Egbin thermal power plant comprises of six independent 220 MW boiler-turbine sets. The sets are dual firing using either natural gas and/or high pour fuel oil (HPFO). Figure 1 shows the flow diagram of a complete set. Each set has three turbines, namely: high pressure turbine (T_1), intermediate pressure turbine (T_2) and low pressure turbine (T_3). The turbines are mounted on a single shaft and a generator is coupled directly with them. Single stage reheating is employed between T_1 and T_2. The super heated steam from the boiler (E_b) drives T_1, and the exhaust from T_1 goes through the reheater (E_r) and then enters T_2. Both the boiler (E_b) and reheater (E_r) are in the furnace (E_1). The exhaust from T_2 goes directly to T_3. The T_3 exhaust gets condensed in the condenser (E_3). The condensed steam in the condenser is pumped by the condensate extraction pump (CEP) into the steam air ejector (E_4) which removes air trapped in the process steam. The water is further pumped through the gland condenser (E_5), drain cooler (E_6) into the low pressure feed water heaters E_7, E_8 and E_9. The low pressure heaters (LPHs) utilize the extraction steam bled from different stages of T_3 to heat the process water. The drains from the LPHs are cascaded backward as a way of waste heat recovery to further heat up the process water. The drip from the drain cooler is fed back into the condenser. The water from E_9 enters the deaerator (E_{10}) which also removes air trapped in the process water. The pegging steam for deaerator comes from T_2 exhaust. The feed water from the deaerator is pumped into the furnace and high pressure heaters (HPHs), E_{11} and E_{12}, through the boiler feed pump (BFP). The extraction steam for the HPHs is coming from T_2 and the exhaust from T_1 cascaded backward into the reheater. Superheated steam from the boiler enters directly into T_1 where it provides shaft work that drives the turbine blade. Exhaust steam from T_1 goes back into the reheater before it passes on to T_2. The exhaust from T_2 enters directly into T_3 to provide shaft work that drives the generator to generate electricity. The exhaust steam from T_3 is condensed in the condenser using lagoon water as coolant.

3. THEORY

The specific exergy of a stream of material consists of the physical exergy and the chemical exergy terms.

$$E_j = E_j^{ph} + E_j^{ch} \quad \text{....................} \ (1)$$

The specific physical exergy (excluding kinetic and potential energy) was evaluated from the following equation:

$$E_j^{ph} = \left(h_j - h_o\right) - T_o\left(s_j - s_o\right) = \Delta h - T_o \Delta s \quad \text{....................................} \ (2)$$

The standard molar chemical exergy, e^{-CH} of substances considered in this study are given in Table 1 (Moran, 1999).

The molar chemical exergy of a gas mixture is given as (Moran, 1999):

$$e^{-CH} = \sum_{i=1}^{j} y_i \, e_i^{-CH} + \bar{R} T_o \sum_{i=1}^{j} y_i \ln y_i \quad \text{..........} \ (3)$$

Table 1: Standard Molar Chemical Exergy, e^{-CH} *(kJ/kmol) of Various Substances at 298K and* p_o.

Substance	Formula	Exergy(kJ/kmol)
Methane	$CH_4(g)$	831,650
Oxygen	$O_2(g)$	3,950
Carbon(IV) Oxide	$CO_2(g)$	19,870
Water	$H_2O(g)$	9,500
Nitrogen	$N_2(g)$	720

The exergy rate of a stream *j* was obtained from its specific value as:

$$\dot{E}x_j = \dot{m}_j E_j \quad \text{.................................} \ (4)$$

The energy rate of a stream *j* was obtained from its specific value as:

$$\dot{E}_j = \dot{m}_j \left(h_j - h_o\right) \quad \text{...........................} \ (5)$$

In the analysis of a plant unit where there is no power production the exergetic efficiency and the energetic efficiency are given by equations (6) and (7), respectively, as:

$$\psi = \frac{\sum \dot{E}x_{out}}{\sum \dot{E}x_{in}} \quad \text{...................................} \ (6)$$

$$\eta = \frac{\sum \dot{E}_{out}}{\sum \dot{E}_{in}} \quad \text{.....................................} \ (7)$$

The exergy efficiency in a unit or subsystem with power generation was evaluated as (Sengupta, *et al.*, 2007):

$$\psi = \frac{P_{net}}{\sum \dot{E}x_{in} - \sum \dot{E}x_{out}} \quad \text{..................} \ (8)$$

and the energy efficiency was estimated as:

$$\eta = \frac{P_{net}}{\sum \dot{E}_{in} - \sum \dot{E}_{out}} \quad \text{........................} \ (9)$$

$$\eta = \frac{Power\,produced}{Heat\,Supplied\,From\,Fuel} \quad \text{.............} \ (10)$$

The irreversibility, also called exergy destruction or exergy loss is calculated by setting up the exergy balance and taking the difference between all incoming or outgoing exergy flows. It has the formula given as (Cornelissen, 1997):

$$I = \sum_{in} \dot{E}x_i - \sum_{out} \dot{E}x_j \quad \text{........................} \ (11)$$

4. METHODOLOGY

In this work, process data were extracted from the process flow diagram prepared by the plant designers. The extracted data were used as input to the HYSYS (2003) process simulator to provide a heat and mass balnce for the plant. The mass balance was based on mass flow rates. The heat balance was based on temperature, pressure, heat loads and the mass flow rates. HYSYS (2003) was used to validate the data in the existing process flow diagram to ensure that a reliable balance was obtained at different points shown in Figure 1. In this simulation, the following assumptions were made: the natural gas burnt in the combustor was assumed to be 100% methane; the compressed air used in the combustor was standard air; unaccounted heat loss from the system due to radiation and convection was neglected; fuel was assumed to enter the combustor at room temperature; fuel undergoes complete combustion, hence the flue gas composition included oxygen, nitrogen, water vapour and carbon (IV) oxide only.

EXCEL spreadsheet was used for exergy and energy analysis. The exergetic and energetic efficiencies of the four major units that make up the complete plant, namely: the turbine and generator unit, the condenser unit, the regenerative unit and the furnace and boiler unit, were evaluated. The thermal power plant units were grouped into subsystems and overall system, as clearly marked out in Figure 1, for the purpose of studying the effect of interaction of the units on the energetic and exergetic efficiencies of the plant.

4.1. Analysis Of The Plant Units

4.1.1 The turbines/ generator unit

Only physical exergy was considered for the streams that cross the boundary of this unit. The exergy rate entering the boundary is:

$$\dot{Ex}_{in} = \dot{Ex}_1 + \dot{Ex}_{12} \text{ .... } (12)$$

The exergy rate leaving the unit is:

$$\begin{aligned}\dot{Ex}_{out} &= \dot{Ex}_5 + \dot{Ex}_6 + \dot{Ex}_7 + \dot{Ex}_{13} \\ &+ \dot{Ex}_{14} + \dot{Ex}_{15} + \dot{Ex}_{19} + \dot{Ex}_{20} \quad \text{...... } (13) \\ &+ \dot{Ex}_{21} + \dot{Ex}_{24}\end{aligned}$$

The exergetic and energetic efficiencies of the turbines /generator unit were evaluated using equations (8) and (9), where P_{net} is the generator power output.

4.1.2. The condenser unit

Like the turbines/generator, only the physical exergy was considered for the condenser unit. The streams entering the condenser were regarded as the cold streams, while the hot stream was the one leaving. The exergy rate entering the condenser is:

$$\dot{Ex}_{hot} = \dot{Ex}_{27} - \dot{Ex}_{27i} \text{ .... } (14)$$

and the exergy rate leaving the condenser is:

$$\dot{Ex}_{cold} = \dot{Ex}_{29} - \dot{Ex}_{28} \text{ .... } (15)$$

The energetic and exergetic efficiencies of the condenser were evaluated using equations (6) and (7), respectively.

4.1.3 The regenerative unit

The regenerative unit comprises the air ejector, gland condenser, deaerator, low pressure and high pressure heaters. Only the physical exergy was considered for the regenerative unit. The exergy rate of the inlet streams and power entering the regenerative unit is:

$$\begin{aligned}\dot{Ex}_{in} &= \dot{Ex}_9 + \dot{Ex}_{10} + \dot{Ex}_{15} + \dot{Ex}_{16} + \dot{Ex}_{19} \quad \text{.... } (16) \\ &+ \dot{Ex}_{20} + \dot{Ex}_{23} + \dot{Ex}_{26} + \dot{Ex}_{30} + P^{CEP} + P^{BFW}\end{aligned}$$

and the exergy rate leaving the regenerative unit is:

$$\dot{Ex}_{out} = \dot{Ex}_{33} + \dot{Ex}_{34} + \dot{Ex}_{39} + \dot{Ex}_{46} + \dot{Ex}_{51} \text{ ..... } (17)$$

The energetic and exergetic efficiencies of the regenerative unit were evaluated using equations (6) and (7), respectively.

4.1.4. The furnace/boiler unit

Both the physical and chemical exergy associated with fuel input, air for combustion of fuel and flue gas, as well as the heat exergy released from combustion of fuel in the furnace were accounted for in this unit.

4.2. Analysis Of Subsystems And Overall System

4.2.1 Reference unit for subsystem analysis or Subsystem I

The reference unit for subsystem analysis is the turbines/generator unit which is also denoted as Subsystem 1. The physical exergy for streams entering and leaving the subsystem I are given by equations (12) and (13) and the efficiencies were evaluated by equations (8) and (9).

4.2.2. Subsystem II

Subsystem II comprises the turbines/generator and condenser units. The exergy rate entering and leaving the subsystem are:

$$\dot{Ex}_{in} = \dot{Ex}_1 + \dot{Ex}_{12} + \dot{Ex}_{25} + \dot{Ex}_{28} + \dot{Ex}_{39} \text{ .. } (18)$$

and

$$\begin{aligned}\dot{Ex}_{out} &= \dot{Ex}_5 + \dot{Ex}_6 + \dot{Ex}_7 + \dot{Ex}_{13} \\ &+ \dot{Ex}_{14} + \dot{Ex}_{15} + \dot{Ex}_{19} + \dot{Ex}_{20} \quad \text{............ } (19) \\ &+ \dot{Ex}_{21} + \dot{Ex}_{29} + \dot{Ex}_{30}\end{aligned}$$

The net power output from the subsystem is:

$$P_{net} = G - P^{CCW} \text{ .... } (20)$$

where P^{ccw} is the power consumed by the condenser cooling water pump which was unknown and assumed to be zero in this analysis. The energy and exergy efficiencies of subsystem II were calculated using equations (8) and (9).

4.2.3. Subsystem III

Subsystem III comprises the turbines/generator, condenser and the regenerative units. The exergy rates entering and leaving the subsystem are:

$$\dot{Ex}_{in} = \dot{Ex}_1 + \dot{Ex}_{12} + \dot{Ex}_{28} \text{ .... } (21)$$

and

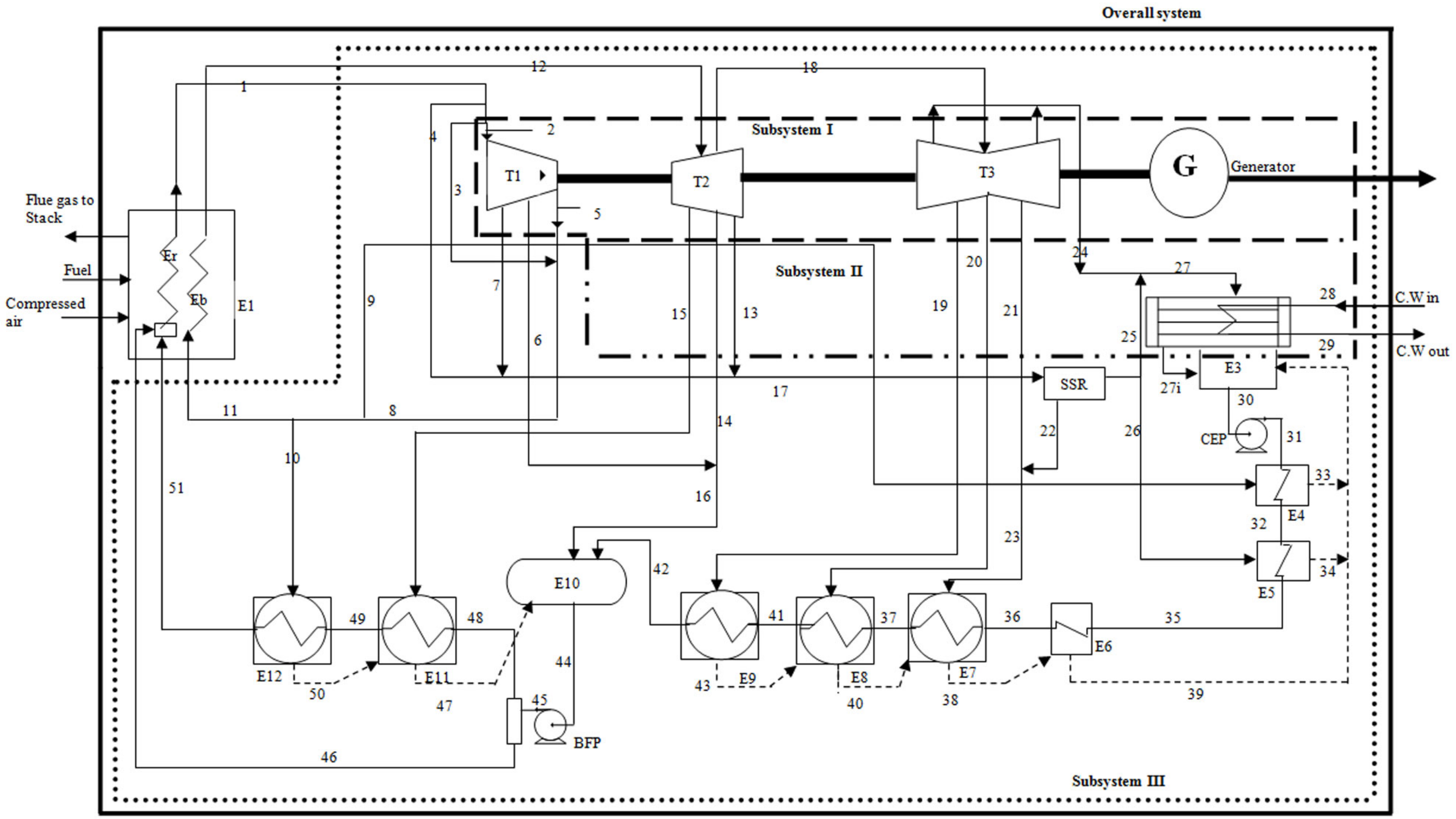

Figure 1. Process flow diagram of the plant showing the subsystems and overall system. Subsystem I: ; Subsystem II: ;Subsystem III ; Overall system ;

$$\dot{E}x_{out} = \dot{E}x_{11} + \dot{E}x_{29} + \dot{E}x_{46} + \dot{E}x_{51} \text{ .... } (22)$$

The boiler feed water pump (BFP) and the condensate extraction pump (CEP) power input were accounted for in the net power output from this subsytem and the net power output from the subsystem is:

$$P_{net} = G - P^{CEP} - P^{BFP} \text{ .... } (23)$$

The values of P^{CEP} and P^{BFP} were 543.04kJ/h and 40173.21kJ/h, respectively. The energy and exergy efficiencies of subsystem III were calculated using equations (8) and (9).

4.2.4. Overall System

The overall system comprises the entire cycle with the turbines/generator, condenser, regenerative and furnace/boiler units. In the analysis of overall system, the exergy due to reaction, that is, the chemical exergy due to combustion of fuel was taken into consideration in addition to the physical exergy due to the streams of material entering and leaving the overall system. In the overall system analysis it was assumed that the total auxiliary power consumption (P_{aux}) in the plant was 5% of the generated power.

The stoichiometric equation representing the complete combustion of methane in oxygen is

$$CH_4 + 2O_2 \longrightarrow CO_2 + 2H_2O \text{ ... } (24)$$

The specific exergy of reaction can be written as (Som, *et al*., 2005):

$$\bar{e}_{in}^{fuel} = (((\bar{h}_{CO_2} + 2\bar{h}_{H_2O}) - (2\bar{h}_{O_2} + \bar{h}_{CH_4})) - T_o((\bar{s}_{CO_2} + 2\bar{s}_{H_2O}) - (2\bar{s}_{O_2} + \bar{s}_{CH_4}))) \quad (25)$$

The molar enthalpies and entropies for the components taking part in the reaction are given in Table 2 (Perry and Green, 1997; Smith and Van Ness, 2004).

Considering the exergy input with fuel, air and circulating water, the total exergy flow rate entering the overall system is

$$\dot{E}x_{in} = \dot{E}x_{fuel} + \dot{E}x_{fuel}^{ch} + \dot{E}x_{air} + \dot{E}x_{air}^{ch} + \dot{E}x_{28} + \dot{E}x_{\mathcal{Q}} \text{ .... } (26)$$

Table 2: Molar enthalpy and molar entropy values

Species	Molar enthalpy ($\bar{h}$)	Molar entropy ($\bar{s}$)
CH4	$-74520 kJ/kmol$	$186.16 kJ/kmol^oC$
O2	0	$205.03 kJ/kmol^oC$
CO2	$-393509 kJ/kmol$	$213.69 kJ/kmol^oC$
H2O	$-241818 kJ/kmol$	$188.72 kJ/kmol^oC$

where $\dot{E}x_{\mathcal{Q}}$ is the exergy rate of reaction.

The exergy flow rate leaving the overall system is:

$$\dot{E}x_{out} = \dot{E}x_{flue\,gas\,to\,stack} + \dot{E}x_{29} + \dot{E}x_{flue\,gas}^{ch} \text{ .... } (27)$$

where $\dot{E}x^{ch}$ is the chemical exergy rate associated with the stream of material in question. The energy and exergy efficiencies of the overall system were calculated using equations (8) and (9).

5. RESULTS AND DISCUSSION

5.1. Physical and Thermodynamic Properties Of Streams

The parameters of the process streams and their calculated exergetic and energetic values at full load of 220 MW are presented in Table 3.

5.2. Components Exergy and Energy Efficiencies

The exergetic and energetic efficiencies of the four units in the plant are presented in Figure 2.

From Figure 2, it was observed that the regenerative unit has the highest exergetic efficiency of 93.6% and its energetic efficiency was 94.8%. The high exergetic efficiency in the regenerative unit could be due to low exergy loss resulting from heat recovery from turbines bleeds. The cascaded heat was used within the system thereby reducing energy losses to the environment. The consequence is high energy efficiency recorded in the regenerative unit. The condenser unit has the highest energy efficiency of 99.9%. The high energy efficiency in the condenser unit could be due to high performance of the water recirculating system in place. The lowest exergetic efficiency of 22.6% in the system occured in the condenser unit. The low exergetic efficiency in this unit could be due to high exergy destruction resulting from heat ejection from the process through the condenser. Condensation of steam coming out of low pressure turbine at about 106oC to about 42oC also invovled high exergy destruction. The furnace/boiler unit has exergetic efficiency and energetic efficiencies of 41.3% and 64.3%, respectively. The low energetic efficiency in the

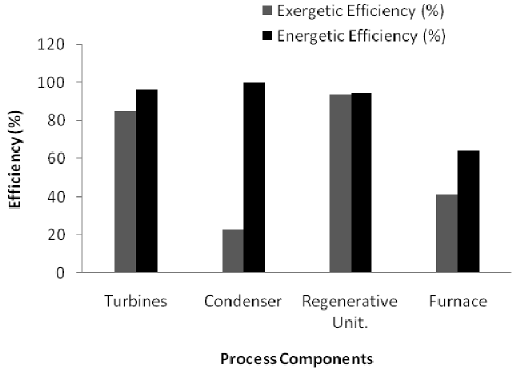

Figure 2: Exergetic and Energetic Efficiencies of the Plant Units

Table 3: Parameters of the streams and their exergetic and energetic values

Stream	Flow (kg/h)	T°C	PkPa	ΔH (kJ/kg)	ΔS (kJ/kg-K)	E (kJ/kg)	ex (kJ/kg)	Total Ex(kJ/kg)	$\dot{E}_{Xj}$ (kJ/h)	$\dot{E}_{j}$ (kJ/h)
1	647504	538	12500	3540	6.281	1667.6339	527.77778	2195.4117	1421537843	2292164160
2	645869	538	12500	3440	6.281	1567.6339	527.77778	2095.4117	1353361445	2221789360
5	629325	500.4	9779	3120	6.307	1239.8833	527.77778	1767.6611	1112433308	1963494000
6	3675	336.8	2689	3110	6.468	1181.8892	527.77778	1709.667	6283026.14	11429250
7	1762	336.8	2689	3110	6.468	1181.8892	527.77778	1709.667	3012433.21	5479820
8	634762	337.1	2689	3120	6.469	1191.5911	527.77778	1719.3689	1091390028	1980457440
9	540	337.1	2689	3023	6.469	1094.2264	527.77778	1622.0041	875882.238	1632223.044
10	50308	337.1	2689	3023	6.469	1094.2264	527.77778	1622.0041	81599784.5	152062735
11	579724	337.1	2689	3023	6.469	1094.2264	527.77778	1622.0041	940314730	1752294207
12	579724	538	3076	3453	7.029	1357.2904	527.77778	1885.0681	1092819245	2001575527
13	1081	328.3	495.1	3043	7.269	875.74637	527.77778	1403.5241	1517209.6	3289088.723
14	22593	326.6	495.1	3043	7.259	878.72737	527.77778	1406.5051	31777170.7	68742258.57
15	29942	434.6	1371	3253	7.129	1127.4804	527.77778	1655.2581	49561739.3	97390405.14
16	26268	326.6	495.1	3043	7.259	878.72737	527.77778	1406.5051	36946077.1	79923943.17
17	560900	328.3	495.1	3043	7.269	875.74637	527.77778	1403.5241	787236692	1706614121
18	537215	328.3	495.1	3043	7.269	875.74637	527.77778	1403.5241	753994223	1634549305
19	22332	252.8	227.1	2980	7.369	783.3011	527.77778	1311.0789	29279013.5	66549360
20	20953	175.4	86.45	2831	7.499	595.5481	527.77778	1123.3259	23537047.1	59317943
21	34739	100.7	27.29	2690	7.689	397.9091	527.77778	925.68688	32157436.4	93447910
22	1241	339.3	495.1	3063	7.309	883.82237	527.77778	1411.6001	1751795.78	3800730.365
23	35980	109	27.29	2623	7.729	318.62037	527.77778	846.39814	30453405.2	94362416.88
24	459191	105.7	1.353	2398	7.679	108.8901	527.77778	636.66788	292352159	1101140018
25	1040	339.3	495.1	3158	7.309	942.6421	527.77778	1470.4199	1529236.67	3284320
26	950	339.3	495.1	3063	7.309	883.82237	527.77778	1411.6001	1341020.14	2909503.503
27	460231	106.2	29.64	2613	7.679	323.52537	527.77778	851.30314	391796097	1202415741
27i	460231	42.1	29.64	74	0.241	1.873244	527.77778	529.65102	243761819.4	33926086.49
28	32590000	30	4.241	22	0.072	0.0796649	527.77778	527.85744	1.7203E+10	702081967.9
29	32590000	38.32	6.661	57	0.189	1.1055023	527.77778	528.88328	1.7236E+10	1872178250
30	541000	42	8.252	76	0.239	4.7314694	527.77778	532.50925	288087503	41103756.82
31	541000	42	9	76	0.239	4.7314694	527.77778	532.50925	288087503	41103756.82
32	541000	42.62	9	76	0.248	2.0485694	527.77778	529.82635	286636054	41103756.82
33	540	99.1	2689	323	0.96	36.459266	527.77778	564.23704	304688.004	174223.0438
34	950	99.1	495.1	323	0.962	35.863066	527.77778	563.64084	535458.802	306503.503
36	541000	69.18	30	363	1.089	38.004366	527.77778	565.78214	306088140	196185679.1
39	79265	99.07	98.14	683	1.943	103.42697	527.77778	631.20474	50032444	54109084.38
46	20000	163	709.5	613	1.674	113.61587	527.77778	641.39364	12827872.9	12252705.33
47	627504	163	709.5	613	1.674	113.61587	527.77778	641.39364	402477077	384431080.1
51	627504	200.4	3151	793	2.06	178.54927	527.77778	706.32704	443223045	497381800.1
52	647504	165.6	709.5	780	2.07	163.22857	527.77778	691.00635	447429375	505108674.4
Compressed Air	572760	30	865	3.0256	-0.607	183.9723	4.4939885	188.46629	107945951.4	1732942.656
Flue gas to Stack	618324	333.1	241	780	-0.261	857.8041	1154.8598	2012.6639	1244478393	482292720
Fuel	45570	27	243	3	-0.45	137.145	51978.125	52115.27	2374892854	136710

furnace/boiler unit when compared with other process components could be an indication of high heat loss from the combustion reaction of fuel with air in the furnace/boiler unit. The low exeregetic efficiency could equally be as a result of high exergy destruction in the combution reaction in the furnace. The turbines/ generator unit has exergetic efficiency of 85% and energetic efficiency of 96.3%. Unlike in the furnace/boiler unit, which served the function of the heat engine where process heat is being raised thereby subjected to high exergy and energy losses. The available work in the turbine/generator was useful for power generation. High energetic efficiency in the turbine/generator indicated low heat loss since there was no reaction taking place in the turbine/generator, only conversion of heat to power was involved. This was an indication that heat loss as a result of combustion of fuel could significantly effect process unit efficiency.

5.3. Components Irreversibilities

The irreversibilities associated with each of the four components in the plant are shown in Figures 3. It was observed that the furnace/boiler unit has the highest irreversibility (1484.3 MW) followed by the turbines/generator unit (259 MW). The irreversibility of the condenser unit was 31.8 MW, and that of the regenerative unit was 9.7 MW, which was the lowest.

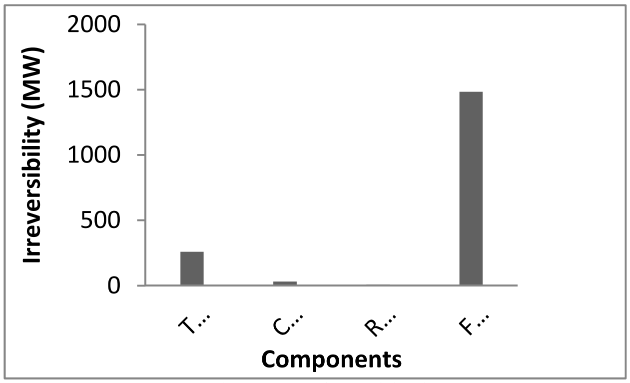

Figure 3: The irreversibilities of the plant units

The high irreversibilty in the furnace/boiler unit was an indication of significant exergy loss due to high entropy generation at conditions at which the unit operates to raise process steam. The furnace/boiler unit operates at high temperature and pressure, the available work at these conditions was used to produce heat to raise process steam. The combustion reaction in the unit was also highly exothemic hence, exergy destuction in these units was so high as reflected in the high irreversibility exhibited. The condenser and the regenerative units operate at low tempeartures and pressures, hence their entropy generations are low as reflected in their irrversibilities.

Examination of Figures 2 and 3 showed that condenser unit has low exergy efficiency and relatively low thermodynamic irreversibility. Also, the regenerative unit has high exergy efficiency and relatively low irreversibility. These situations arise because exergy efficiency values are quantitative measurements derived as the ratio of two numbers with the constraint that the ratio is not greater than 1, whereas irreversibilities are quantitative measurements derived as the difference between two numbers. In fact, four possible combinations of exergy efficiencies and irreversibilities can exist as shown below:

High exergy efficiency- Large irreversibility
High exergy efficiency- Small irreversibility
Low exergy efficiency- Large irreversibility
Low exergy efficiency- Small irreversibility

Thus, it is possible for the ratio of two large numbers to be high and the difference to be large as well, and the ratio of two small numbers to be high and the difference to be small.

Exergy analysis generates ideas about how improvements can be made in process components. Specifically, the furnace/boiler component was investigated further in order to find ways of improving its performance. It must be pointed out that the magnitude of losses in a unit does not always imply the greatest potential for improvement. To recover the losses in the furnace reactor, a reversible reactor which would be capable of extracting work directly from the reaction itself, similar to a fuel cell type of device, would be required. In practice, such a reactor cannot be built and the best that can be done is to extract heat from the reaction. It becomes justifiable to base the assessment of performance of reactors on the maximum practical target which is achieveable with current technology. It therefore becomes necessary to divide the total irreversibilities in reactors into inherent/unavoidable and non-inherent/avoidable irreversibilities (Debbigh, 1956). Linnhoff (1979) formulated a simple equation for evaluating the non-inherent/avoidable irreversibilities in chemical reactors as:

$$\dot{I}_{non-inherent} = \dot{I}_{actual} - \dot{I}_{best\ practice} \text{ ....(29)}$$

and further defined the most efficient operating conditions for identifying the "best practical" reactor, given the constraints of current technology. For an exothermic reaction, it was recommended that the strategy should be to use the reaction to boost as much heat as possible to as high a level as possible. The required operating conditions to achieve this strategy are: preheat to, or as close as possible to, reaction temperature; recover as much heat as possible directly from the reaction; run the reaction at, or as close to, the maximum feasible tempearture throughout; and optimize the mass flow rate. These conditions were applied to the furnace reactor. The temperature of the flue gas from the furnace is a function of the gas mass flow rate and this variation was derived by simulation and is shown in Figure 4. From Figure 4 it was observed that the optimum gas mass flowrate, at the point of inflexion, is 40,000kg/h giving an optimum flue gas temperature of 104.6oC. It was found from Figure 4 that operating the plant below the gas flow rate of 38,000kg/h is not realistic and that feasible operation lies between gas flow rate of 38,000 kg/h and 45,570 kg/h. It was found from simulation that operation

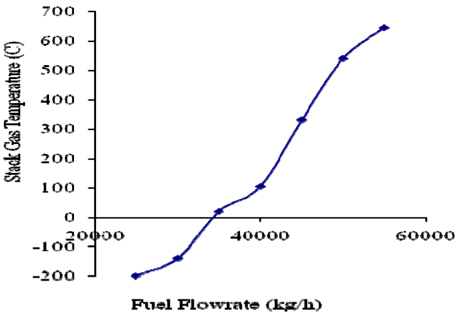

Figure 4: Variation of flue gas temperature with gas mass flow rate.

within this range of gas flow rate did not have any significant effect on the exergy efficiency of the thermal power plant. The variation of CO_2 emission with gas mass flow rate is shown in Figure 5.

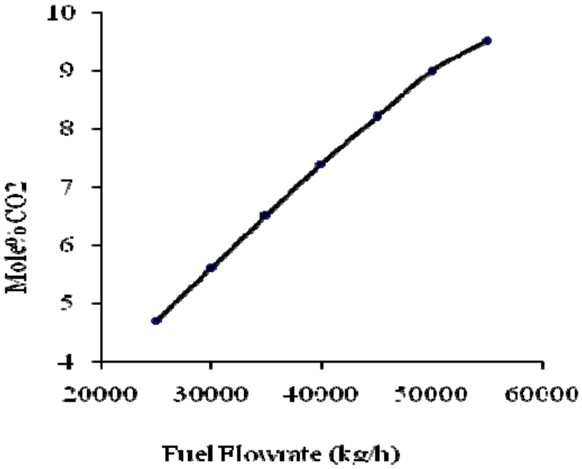

Figure 5: Variation of CO_2 emission with gas flow rate.

It was found that increasing the gas mass flow rate increased the CO_2 emission. Therefore, it is better to operate the plant at optimum gas flow rate of 40,000kg/h than at 45,570kg/h prevailing in the plant. The only improvement that can be made in the furnace/boiler unit to further enhance heat recovery from the flue gas is to use the flue gas to preheat the inlet air and gas streams to the furnace.

Boilers generally are known to have large thermodynamics heat loss due to combustion of fuel. The question now is: are there alternative technologies for energy recovery from the furnace heat which can be used in place of the bolier? Can work or power be recovered from the furnace hot gas? Gas turbines can not be used for work recovery in the present situation because the furnace gas is at low pressure. Also the use of heat engines to recover power from the furnace gas is not practicable in this case because of the high temperature of the gas. Therefore, heat recovery will remain, for the moment, the practical approach to energy recovery from the furnace hot gas, and the boiler is the practical technology to be used in the present situation. From all indications it is unlikely that much improvement can be made in the design and operating specifications of the furnace/boiler unit. This showed that high thermodynamic heat loss in units do not always imply the greatest potential for improvement and that high heat loss may be due to limitations of current technology.

5.4. Subsystems and Overall System Performances

The results of subsystems and overall system analyses are shown in Figures 6 and 7.

In subsystem I, which is also the reference turbines/generator unit for system analysis, the exergy and energy efficiencies were 85% and 96.3%, respectively, and the irreversibility was 259 MW, as previously determined.

In subsystem II, the exergy efficiency dropped slightly to 83% and energy efficiency also increased slightly to 99.8%. The subsystem irrversibility also increased to 312 MW. The increase in subsystem irreversibility indicated that inclusion of condenser in the process could result in increase in the exergy loss as a result of heat expulsion from the system through the condenser unit.

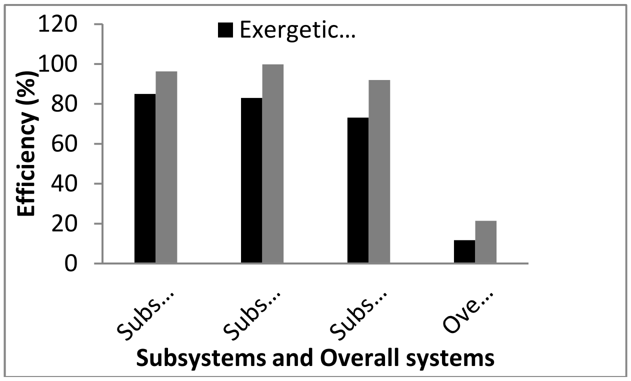

Figure 6: Exergetic and Energetic Efficiencies of Subsystems and Overall system

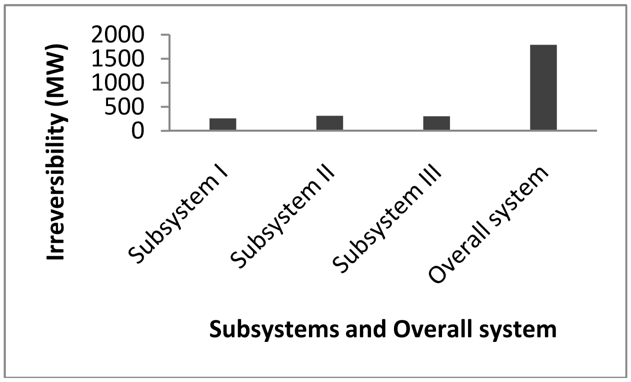

Figure 7: The irreversibility associated with subsystems interaction

In subsystem III, the exergy and energy efficiencies dropped to 73.1% and 92%, respectively. The subsystem irrversibility reduced to 301 MW. The reduction in subsystem irreversibility indicated that inclusion of regenerative unit in the process could result in reduction in the exergy loss as heat is being recovered from the turbine thereby reducing heat ejection into the environment and consequently reducing exergy destruction in the process. The regenerative unit had the lowest unit irreversibility and made significant contribution to redction in irreversibility due to system interaction.

In the overall system, the exergy and energy efficiencies were further lowered to 11.7% and 21.4%, respectively, by the introduction of the furnace/boiler unit. Also, the overall irreversibility was further increased to 1790 MW. The high energetic efficiency of the overall process over the exergetic efficiency was due to high exergy destruction originated from combustion of fuel with the air in the furnace/boiler unit. The study of the system interaction effects helped to identify the furnace/boiler unit as making the most significant contribution to increasing overall process irreversibility. The unit made 67.2% contribution to the overall process irrversibility of 2662 MW. The turbines/generator unit made the least contribution of 9.7%. The condenser and the regenerative units contibuted 11.7% and 11.3%, respectively, to the overall process irreveresibility. The highest contribution came from the furnace/boiler unit because of the entropy generation at high temperature and pressure at which the process steam was supplied from the furnace/boiler unit.

6. CONCLUSIONS

In this work, energy and exergy analyses were performed on 220 MW Egbin thermal power plant to study units, subsystems and overall system performances using HYSYS (2003) process simulator and Microsoft Excel Spreadsheet. It was found that the regenerative unit has the highest exergy efficiency; the furnace/boiler unit has the lowest energy efficiency; and the condenser unit has the highest energy efficiency. It was also discovered that process units interaction infleuenced the overall thermodynamic irreversibility of the process. The causes of thermodynamic irreversibilities in the units were identified. The study revealed that the optimum fuel flow rate of 40,000kg/h will reduce the flue gas temperature and CO_2 emission to the atmosphere. The overall system exergetic and energetic efficiencies were 11.7% and 21.4%, respectively. The subsystems and overall system study revealed that the furnace/boiler unit made the greatest contribution to the system irreversibility and the consequence was drop in both exergetic and energetic efficiencies of the overall system.

ACKNOWLEDGEMENT

The authors gratefully acknowledge the assistance received from the Management of Egbin Thermal Power Plant, Ikorodu.

REFERENCES

Alasfour, F.N. and Alajmi, H.F. Exergetic destructions in steam generation system: Azzour plant "Int. Jour of Exergy, 4 (3): 271-285, 2000.

Bejan, A. Advanced Engineering Thermodynamics, Wiley, New York, 1988.

Caton, J.A. On the destruction of availability (exergy) due to combustion processes - with specific application to internal-combustion engines" Energy, 25(11): 1097-1117, 2000.

Cengel, Y.A. and Boles, M.A. Thermodynamics, McGraw-Hill, 2004.

Cornelissen, R.L. Thermodynamics and Sustainable Development: The Use of Exergy Analysis and the Reduction of Irreversibility, PhD Thesis, University of Twente, Netherlands, 1997.

Datta, A. Entropy Generation in a Confined Laminar Diffusion Flame, Comb. Sci. Tech., 159, 39- 56, 2000.

Debbigh, K.G. The Second Law Efficiency of Chemical Processes, Chem. Eng. Sc., 16(1), 1956

Dincer, I. and Al-Muslim, H. Thermodynamics analysis of reheat cycle steam power plants, Int. J. Energy Res. 25, 727-739, 2001.

HYSYS, Version 3.2 (Build 5029), Aspen Technology Inc., Licensed to TEAM LND, Calgary, Alberta, Canada, 2003.

Kwon, Y. Kwak, H. and S. Oh, S. Exergoeconomic analysis of gas turbine cogeneration system, Exergy an Int. Journal, 1, 31-40, 2001.

Linhoff, B. Thermodynamics Analysis in the Design of Process Networks, Ph.D. Thesis, University of Leeds, UK, 1979.

Mohamad, J.E. and Bandpy, M.G.Exergetic analysis of gas turbine plants. Int. J. Exergy, 2(1): 263- 279, 2005.

Moran, J. Availability analysis: A Guide to Efficient Energy Use. Englewood Cliffs, NJ: prentice–hall, 1982.

Moran, M.J. Engineering Thermodynamics, Mechanical Engineering Handbook, Boca Raton CRC Press LLC, 1999.

Nag, P.K. and De, S. Design and operation of a heat recovery steam generator with minimum irreversibility, Applied Thermal Engineering, 17 (4): 385-391, 1997.

Perry, R.H. and Green, D.W. Perry's Chemical Engineer's Handbook, 7th Ed. McGraw-Hill, 1997.

Rosen, M.A. Energy and exergy based comparison of coal fired and nuclear steam power plants, Exergy an Int. Journal, 1 (3): 125-127, 2001.

Rosen, M.A. and Dincer, I. Exergy-cost-energy-mass analysis of thermal systems and processes, Energy Convers. Management,44(10): 1633–1651, 2003.

Sciubba, E. and Su, T.M. Second law analysis of the steam turbine power cycle: a parameter study In: Gaggioli, R. A., ed., Computer-Aided Engineering of Energy Systems", Proc. ASME Winter Annual Meeting, Anaheim, Cal., Exergy, Power engineering, Dec. 7-12, Second law analysis and modeling, 151-165, 1986.

Sengupta, S. Datta, A. and Duttagupta, S. Exergy analysis of a coal-based 210MW thermal power plant, Int. J. Energy Res., 31(1), 14-28, 2007.

Smith, J.M. Van Ness, H.C. Introduction to Chemical Engineering Thermodynamics, McGraw-Hill, 2004.

Som, S.K. Mondal, S.S. Dash, S.K. Energy and exergy balance in the process of pulverized coal combustion in a tubular Combustor. Journal of Heat Transfer, Transactions of the ASME 127, 1322-1333, 2005.

Ife Journal of Technology, Vol. 18 (2), 51-54, 2009

Full Paper

CHARACTERIZATION OF SOME NIGERIAN CLAYS FOR REFRACTORY UTILIZATION

K.F.K Oyedeko
Department of Chemical and Polymer Engineering
Lagos State University, Epe, Lagos State
kfkoyedeko@yahoo.com

E.A. Olugbade
Department of Chemical and Polymer Engineering
Lagos State University, Epe, Lagos State

ABSTRACT

Clay deposits from four locations in Auchi, Enugu, Lagos and Uyo were characterized for ceramic applications. The major characteristics investigated were their chemical compositions, bulk density, apparent porosity, cold crushing strength, water absorption and linear shrinkage. Chemical analysis was conducted using Atomic Absorption Spectrometry method, while water absorption and water shrinkage were evaluated by sample heating and weighing methods. Results obtained showed that the samples belong to the fire clay class. Alkali oxide content was low, at an average percent of 0.045 for Enugu, 0.060 for Lagos, 0.025 for Uyo and 0.050 for Auchi, imparting high refractoriness on the clays and making them suitable for ceramics, specifically refractory materials. Moreover, the average 54% of SiO2 and 42% of Al2O3 in Auchi and Uyo clays make them more suitable for the refractory purposes.

Keywords: clay, refractory, bulk density, porosity, absorption

1. INTRODUCTION

Clays are versatile industrial raw materials needed for the manufacture of domestic and industrial products such as pottery and ceramic wares, bricks, electrical insulators, paper, paint, ink, drugs, soaps, toothpaste, roofing and floor tiles. They also find applications in the manufacture of cement, plastics, fertilizers and insecticides. The use of clay products for construction and building purposes has greatly aided many developed and developing nations to execute housing policies. Clay products such as ceramic wares, burnt bricks, roofing and floor tiles are cheaper and more durable building materials than cement, especially under tropical conditions (Nnuka et al, 2001). They can, therefore be utilized to reduce overdependence on cement particularly in Nigeria.

According to Nnuka et al, (1992), the wide application of clay in homes and industries is based on its intrinsic properties such as high chemical stability, high aesthetic value, wear resistance, high strength at elevated temperatures, thermal shock resistance and others. The basic constituents of clay are the alumino-silicates and other mineral oxides such as hematite, magnesium oxide, calcium oxide, sodium oxide, potassium oxide and soluble sulphide salts. The characteristic properties of clay which determine the areas of application are influenced by the chemical structure of the dominant constituent minerals, with important properties including plasticity, color, dry strength, drying and firing shrinkages. The percentage of the mineral oxides in the clay ultimately determines its areas of application, while the quantity of the alkali metal oxides such as Na_2O, K_2O, CaO, indicates their suitability for making ceramic products.

Clay is the product of weathering of exposed rock. The agents of weathering are water (especially with solid matter in suspension), wind (with sand grains in suspension) and glaciers. The formation of clay from parent rock is primarily a chemical processes by which fine particles are separated from coarser grains. One of the commonest processes of clay formation is the chemical decomposition of feldspar. Granite contains alkali feldspar, quartz, plagioclase feldspar and some biotite with hornblende (Clews, 1969). The alkali feldspar, orthoclase, typical of the group with formula $KAlSi_3O_8$, is slowly attacked by water containing carbon oxide in solution, which leaches away the potash and some of the silica, leaving the aluminum silicate, kaolinite and in the course of time the feldspar in granite is transformed by percolating waters to clay, as shown in Eq. (1)

$$\begin{array}{c} 2KAlSi_3O_8 + 2H_2O + CO_2 \\ \Big\downarrow \\ Al_2O_3.2SiO_2.2H_2O + 4SiO_2\ K_2CO_3 \end{array} \tag{1}$$

1.1 Composition of clay

A pure clay mineral may be highly refractory but it may be very weak when burned owing to the absence of suitable impurities which would, if present, form a verifiable bond to unite the clay particles into a mass of great strength. The proportion of impurities allowable in clay depends on the purpose for which it is to be used. Clay to be used as a refractory material must be as free as possible from fluxes (e.g. silica, calcite, magnesite) as these would reduce its resistance to heat. The principal chemical components of clays may be classified as; silica, alumina, alkali-bearing minerals, iron compounds, calcium compounds, titanium compounds, manganese, complex alumino silicates often containing other elements, carbonaceous matter, moisture and colloidal water (i.e. water of constitution and of crystallization), exchangeable bases.

The particle size of clay is an important characteristic, since it influences other properties like plasticity and dry strength for instance, small particle size (< 0.1 microns) contributes to high drying shrinkage and great strength (Norton, 1956). Clay particles are small, hexagonal plate-like crystals, about 0.1 to 2 microns. This size lies in the colloidal range (0.001-1) microns and therefore clay has colloidal properties. The drying of clay is usually accompanied by shrinkage, which depends on the physical texture of the clay as well as the mineralogical compositions. As the film of water between the clay particles is drawn off by evaporation, the particles draw closer, thus making up the space previously occupied by water. The cumulative effect of the drawing close of each particle to its neighbour is the shrinkage of the entire mass.

Profound changes occur in clay during firing. A piece of fired clay differs both chemically and physically from raw clay. The first change is the completion of drying. At a kiln temperature range of 100°C to 150°C, all uncombined water (pore water and water of plasticity) in the clay evaporates and the clay dries completely. This final drying is carried out slowly to prevent bursting of the clay due to steam formation. The next change is dehydration of clay, which occurs between 350°C and 600°C. The chemically combined water, which is part of the molecular structure of clay, is driven off thus the clay loses its plasticity, becomes resistant to the slaking action of water, is porous and still quite fragile. As firing temperature increases, absorption decreases. The absorption value of clay is very important because it indicates how well the body has been fired, whether it is a vitreous or earthenware body, and something about its strength and water-tightness.

Between 350°C and 900°C, oxidation of organic compounds and inorganic sulphates present in the clay occurs. Complete oxidation of the carbon content yields carbon dioxide: in the case of insufficient oxygen in the kiln, partial oxidation occurs, yielding carbon monoxide.

Another change is quartz inversion. All clays have significant quartz content. Crystalline quartz has different forms, depending on temperature. When temperature increases, the quartz crystals arrange themselves into a slightly different order, accompanied by slight change in volume which is reversible. On cooling, the quartz changes and resumes its original crystalline form and size.

Finally, the clay is vitrified. The vitrification range starts about 900°C and extends up to the highest temperature clay can withstand without melting. Vitrification is the hardening, tightening and partial gasification of clay. It gives fired clay its characteristic hard, durable, dense and rock-like properties. Flux is usually added to reduce maturing temperature and hasten vitrification. Above red-hot heat, the fluxes start to soften and a glass is formed which acts like cement to make a strong body. Vitrification is accompanied by shrinkage in the clay which is caused by; a decrease in volume due to the expulsion of water, CO2 or SO2 and the drawing together of the crystals by the capillary forces of the glass and the consequent expulsion of air from the pores.

Clays are of different types. Kaolin clay has its chemical composition approaches the formula of the mineral kaolinite. It is highly refractive clay with melting point of about 1800°C. Ball clays are blue or black but usually turn white when fired. They are fine; they have higher iron content, plasticity and strength and are more fusible. 'Fire clay' refers to refractoriness or resistance to heat and clay which vary widely in other properties may be called fire clay if they are refractory. Stoneware clays are plastic clays which mature or become vitreous between 1200°C to 1300°C. Their fired colour ranges from a very light gray. Earthenware clays contain iron and other mineral impurities in sufficient quantities to cause the clay to become tight and hard, fired at between 950°C to 1100°C. Bentonite clay major constituent is the mineral, montmorillonite. Although its chemical composition is like that of clay, the physical nature is different in that it contains more colloidal matter.

A clay body is a mixture of various clays combined with other ingredients where necessary, to give a working basis for the type of ceramic required. Important qualities of clay include texture, plasticity, and colour, durability when unfired, during and after firing. Clay that is too plastic may be added to another that is non-plastic. Ground glass is added to provide lower maturing point while grog (clay which has been previously fired and ground to fine size) is added for texture. By this, a clay body is produced with the desired workable qualities. Examples of clay bodies include porcelain, whose main clay content is kaolin. Typical porcelain contains 40% feldspar, 9% silica, 40% kaolin and 11% ball clay. It is blue – white and transparent when fired at high temperature.

Literature (Aderibigbe, 1989; Ajunwa, 1990; Abdulahi, 2003; Badejoko, 2006) clearly shows that clay abounds in Nigeria in large quantities and at various locations. However, the bulk of clay consumed in Nigeria is imported from the USA, United Kingdom and Japan (Iwuanyanwu, 1990). The cost implication of the importation of refractories (clays that can withstand very high tempratures) alone as at 1990 was put at \$3,000 to \$3,400 per ton (Nnuka and Adekwu, 1997). The estimate at current inflation rates can only be imagined. It is therefore imperative that alternative source of this important raw material be sought locally and hence this study is to characterize some Nigerian clays for ceramic application so that industrialists can utilize them instead of importing clay with similar characteristics. This characterization is limited to clay samples from four locations in Nigeria: Auchi in Edo State, Enugu in Enugu State, Ejigbo in Lagos State and Ikot Ekwere in Uyo, Akwa – Ibom State, some of its major deposits in Nigeria.

2. MATERIALS AND METHODS

The clay samples were collected from different deposits in Auchi (Edo State), Enugu (Enugu State), Ejigbo (Lagos State) and Ikot Ekwere in Uyo, (Akwa-Ibom state). Collected samples were air-dried, weighed and sieved through a 100-mesh sieve. Test pieces for various experiments were rolled and pressed, dried and fired at a temperature before the determination of different parameters. Half gram (0.5 g) of each of the samples was weighed, ground to pass through 100-mesh sieve, and transferred into a crucible. About 1.4g of flux (1.2g Na_2CO_3 + 0.2g boric acid) was added to the samples, mixed well and heated at 1200°C for 25 minutes. This was then removed, while about 1g of K_2CO_3 was added to melt the surface, the mixture was heated again at 1200°C for about 5 minutes. The crucible was removed from the furnace and cooled in distilled water. It was then placed in a 250ml beaker and 60ml of 0.1M HCl added to form a solution which was left warm, agitated at intervals to facilitate complete dissolution. The solution was diluted to appropriate volume.

2.1 Linear Shrinkage

Test pieces were rolled in rods of 10cm. and marked along a line to maintain the same position after heat treatment. The samples were air-dried for 24 hours and oven-dried for another 24 hour, then fired at 800°C, 900°C and 1100°C, cooled to room temperature after each kiln temperature and measured. The fired linear shrinkage was calculated from equation 1. (Ekwere, 2005; Odo et al, 2003):

$$\text{Fired shrinkage} = \frac{\text{DL-FL}}{\text{DL}} \times 100\% \ldots\ldots\ldots\ldots\ldots\ldots \quad (1)$$

Where DL = dried length, FL = fired length.

2.2 Bulk Density

Clay samples were pressed into discs, air-dried for 24 hours, oven-dried and allowed to cool. Each specimen was weighed, and then suspended in a measuring cylinder containing water and the volume measured. The bulk density was calculated from equation 2 (Ekwere, 2005; Odo et al, 2003):

$$\text{Bulk density} = \frac{\text{Md}}{\text{V}} \ldots\ldots\ldots\ldots\ldots\ldots\ldots\ldots \quad (2)$$

When Md= dried mass and V = Volume.

2.3 Water Absorption.

To determine the water absorption capacity, the test pieces were dried for 24hours and fired to 800°C, 900°C and 1100°C at intervals. These were cooled and transferred into a 250ml beaker, filled with water. The specimens were allowed to soak in boiled water for 3 h and then left standing for 24hours. The soaked weight was recorded. The water absorption was calculated using equation 3 (Olubgade, 1999; Ekwere, 2005; Odo et al, 2003):

$$\text{Water absorption} = \frac{S-D}{D} \times 100\% \ldots\ldots\ldots \quad (3)$$

Where S = Soaked weight and D = Dry weight.

2.4 Apparent Porosity.

Test pieces were oven -dried for 24hours and fired at 800°C, 900°C and 1100°C respectively, cooled and transferred into a 250ml beaker. These were completely covered with water and boiled for 30mins. The soaked weight was recorded. The specimens were then cooled and weighed suspended in water using a beaker placed on a balance. The apparent porosity was calculated using equation 4 (Ekwere, 2005; Odo et al, 2003).

$$\text{Apparent porosity} = \frac{\text{W-D}}{\text{W-S}} \times 100\% \ldots\ldots\ldots\ldots\ldots \quad (4)$$

Where W = Soaked weight, D = Dry weight, S = Suspended weight.

2.5 Cold Crushing Strength

Test pieces of clay samples were prepared into discs on a flat surface. The test pieces were fired in a kiln at 800°C, 900°C and 1100°C respectively and then cooled to room temperature. Each specimen was placed on a compressive strength tester and load was applied axially by turning the hand wheel at a uniform rate till failure occurred. Cold crushing strength (CCS) was then calculated using equation (5) (Ekwere, 2005).

$$\text{CCS} = \frac{\text{Maximum load (KN)}}{\text{Cross-Sectional area}}\ (\text{m}^2) \quad \ldots\ldots\ldots\ldots\ldots (5)$$

3. RESULTS AND DISCUSSION

The chemical composition, physical characteristics and firing characteristics of the samples obtained during the study are presented in Tables 1, 2 and 3 respectively. The principal oxides present in all the samples were silicon oxide and aluminum oxide, thus characterizing them as the fire clay class. The low amount of alkali compounds makes them highly refractory and the presence of iron oxide and organic matter i.e. carboneaous matter explains the colour variations in the raw and fired states (Tables 1 and 3).

The cold crushing strength is the load bearing capacity of fire clays. The presence of fluxes enhances bond formation at elevated temperatures. The strength behaviour of investigated clays was found to increase with rise in firing temperature for Auchi and Enugu clays.(Table 2). But the strength of the Lagos clay increased up to 900°C then reduced at 1100°C. The strength of the Uyo clay reduced at 900°C and rose at 1100°C (Table 2). Several factors can be responsible for the behaviour of Lagos and Uyo clays. These include the chemical composition of the clay, the physical properties, mode of preparation of the materials, mode of manufacturing of the article, conditions of drying, conditions of burning and the temperatures at which the material is used or at which the strength is determined. The lime in the clay components would have combined to form some considerably low-temperature melting compounds, which increased the strength of the test pieces on cooling.

The water absorption and porosity at 900 °C shows a decline for that of 800 °C and that of 1100 °C for all samples (Table 3). This might be due to the fact that vitrification starts at about 900 °C to the highest temperature clay can withstand without melting and gives it characteristic hard, durable, dense and rock like properties. Verification is accompanied by shrinkage in the clay as temperature increased from 800 °C to 1100 °C.This is caused by a decreased in volume due to expulsion of water, CO_2 or SO_2. The lesser the drying shrinkage, the stronger the clay and the less apt it is to crack.

Grimshaw (1971) and Chester (1973) show that the linear shrinkage, bulk density and the porosity of all the samples make them suitable for porous fire clay bricks. Auchi and Enugu clays may be suitable for building bricks; Auchi and Uyo clays may be

Table 1. Chemical composition of the clay samples

Clay Source	SiO_2	Al_2O_3	Fe_2O_3	TiO_2	CaO	MgO	K_2O	Na_2O	LOI
Auchi	54.62	42.15	2.07	1.52	0.16	0.10	0.06	0.04	13.27
Enugu	46.72	37.38	0.68	1.30	0.12	0.09	0.07	0.02	13.72
Lagos	56.26	29.12	1.62	1.36	0.15	0.09	0.04	0.08	10.70
Uyo	53.42	44.03	1.47	0.38	0.12	0.10	0.04	0.01	12.42

Table 2, Physical characteristics of samples

	Bulk density (g/cm^3)			Cold crushing strength (KN/m^2)		
Source	800°C	900°C	1100°C	800°C	900°C	1100°C
Auchi	2.11	1.91	1.71	9,793	30,829	39,683
Eungu	1.84	2.00	1.98	25,128	39,785	50,273
Lagos	1.62	1.84	1.88	11,500	23,869	20,408
Uyo	1.78	1.92	2.58	20,555	16,011	19,412

Table 3. Firing characteristics of samples

	Linear shrinkage (%)			Water absorption (&)			Porosity (%)			Colour change			
Source	800°C	900°C	1100°C	800°C	900°C	1100°C	800°C	900°C	1100°C	25°C	800°C	900°C	1100°C
Auchi	5.18	3.67	4.20	16.50	10.92	13.5	20.00	15.24	18.74	Light brown	Reddish brown	Light brown	Light brown
Enugu	0.53	4.10	3.20	18.9	12.48	15.5	25.26	18.44	21.48	Red brown	Light red brown	Light brown	Light brown
Lagos	7.77	6.00	4.75	32.0	27.76	29.9	32.73	38.67	44.00	Off white	Off white	Yellow or white	Off white
Uyo	1.67	10.90	8.69	24.63	9.62	12.6	30.89	13.71	17.32	Dark brown	Pale brown	Light brick red	Buff

suitable for tiles while Enugu and Lagos clays may be suitable for fire clay brick. Enugu clay can be used for earthenware bodies. Due to their refractoriness they can be utilized as refractory materials for lining the walls of hot furnaces and other refractory applications.

5. CONCLUSION

The importance of sourcing for industrial raw materials locally has often been stressed by stake holders in the industrial sector, not only as a means of reducing dependency on imports and conserving foreign exchange but also as a way of reducing production cost and the consequent price of commodity. The physical and chemical properties of the clay samples from Auchi, Enugu, Lagos and Uyo, make them suitable for use as refractory materials. Refractories are needed to line the walls of a furnace, used in heat generation in many chemical processes. These refractories can come in form of bricks or tiles. Thus, Auchi, Enugu, and Lagos clay, are suitable for making fire clay bricks, while Uyo clay, as well as Auchi clay are suitable for making tiles. The clay samples are in commercial quantity (Badejoko 2006), so the problem of insufficient supply is adequately taken care of. It is hoped that industrialists will effectively exploit this cheap, abundant and versatile raw material for the nation's refractory needs and discontinue the practice of importing them.

REFERENCES

Aderibigbe, D.A. (1989). Mineral resources in Nigeria and the potential for the manufacture of ceramic products. The Nigerian Engineer. Vol.24, no.4. pp 61-69.

Ajunwa, J.C. and Oniklinam, E.P. (1990). Developing a domestic refractory industry. American ceramics society bulletin. Vol 69, no. 4, pp 656-657

Badejoko, T.A. (2006). Opportunities in Nigeria Solid Minerals Participation. Proceedings of the 36th AGM, NSChE, Ibadan, Nigeria. Pp 110-132

Chester, J.H. (1973). Refractories: production and properties. The iron and steel Institute, London. Pp 263-296

Clews, F.H. (1969). Heavy clay technology. Second edition. Academic press Inc. (London). Ltd .pp1-16, 200-207

Dinsdale, A. (1986) Pottery Science: materials, processes and products. Ellis Horwood limited. Pp 205-220

Ekwere .I.I. (2005). Characterization of some Nigeria clays for ceramic Application. B.Sc. thesis. Department of Chemical and Polymer Engineering, Faculty of Engineering, Lagos State University, Epe Nigeria.

Grinshaw, R.W. (1971). The chemistry and physics of clay. 4th edition. Ernest Benn limited. Pp 29-30, 271- 297, 807

Iwuaanyanwu, E.C. (1990). Local sourcing of materials for the 1990s. proc. Of 1990 Annual conference of NSE. pp 12-30.

Moore, F. (1965). 2. Rheology of ceramic systems. Maclaren and sons limited, London, England. Pp 51-67

Nnuka, E.E, Elechikwu and Ogo, D.U.I. (1992). Sustainable refractory sourcing of our industries. Conference proc. Of NMS annual conference. Pp 18-20
Nnuka E.E. and Enejore (2001). Nigerian Journal of Engineering Management. Vol 2, no.3. Besade publishing press. pp 9-13

Norton, F.H. (1956). Ceramics for the artist potter. Addison Wesley publishing company lnc. pp 128-136, 208-218.

Odo J.U and Nwajagu C.O. (2003). Possible Application of Eha-Alumona Clay Deposit in the Production of Refractories and Ceramics Ware. pp 109-111.

Perry R.H. and Green. D.W. (1999) Chemical Engineer Handbooks. (7th Ed) Mc Graw Hill Co.Inc. New York. pp. 28-63.

Rhodes, D. (1973). Clay and glazes for the pottery. 2nd edition, pitman publishing, Ptyled Melbourne. pp 13-18.

Ife Journal of Technology, Vol. 18 (2), 55-62, 2009

Full Paper

REPOSITIONING TERTIARY INSTITUTIONS WITHIN THE NIGERIAN INNOVATION SYSTEM FOR THE ACHIEVEMENT OF THE VISION 20:2020 MILLENNIUM DEVELOPMENT GOALS

M.O. Ilori
Technology Planning and Development Unit (TPDU
Obafemi Awolowo University, Ile-Ife

I.O. Abereijo
Centre for Industrial Research & Development (CIRD
Obafemi Awolowo University, Ile-Ife

S.A. Adegbite
Centre for Industrial Research & Development (CIRD)
Obafemi Awolowo University, Ile-Ife

A.A. Adeniyi
Technology Planning and Development Unit (TPDU)
Obafemi Awolowo University, Ile-Ife

ABSTRACT

The main focus of this paper is to understand the relevance of the tertiary institutions in the achievement of the Millennium Development Goals (MDGs) in Nigeria with the view of suggesting how they can be better positioned to assist the government in achieving the goals. The paper argues that while the Nigerian version of MDGs Documents is a welcome development, however it execution has its own challenges which require augmenting human capital and raising its quality. Therefore, the effective operation of the National Innovation System is an important factor for success in achieving MDGs, as it is the experience of some countries in the world. Therefore, the paper concludes that universities require restructuring so as to take responsibility for an active role in the more complex field of economic development, covering a portfolio of applied and basic research, consulting and community services, specialised training, distance learning and tech-based venture formation.

Keywords: Millennium Development Goal; National Innovation System; Tertiary Institutions; Repositioning.

1. INTRODUCTION

The fallout of the United Nations global conferences of the 1990s was the Millennium Declaration of 2000 which made a strong commitment to the right to development, to peace and security, to gender equality, to the eradication of the many dimensions of poverty and sustainable human development. The Millennium Development Goals (MDGs) that derive from this Declaration provide an agenda for global action. This agenda and the outcomes of the World Social Summit, the World Summit on Sustainable Development, the Doha Development Agenda, and the Monterrey Consensus are mutually supportive processes and essential building blocks of a worldwide partnership for sustainable development.

The Millennium Development Goals (MDGs) analytically anchored in the human development paradigm, representing a set of time-bound quantitative targets to reduce human poverty in its basic dimensions. They also represent a global commitment, a shared responsibility for both the developed and the developing world and provide a platform for addressing all challenges, especially human development challenges around the globe.

The MDGs have eight goals with the 21 targets (see http://www.un.org.millennium/declaration/ares552e.htm).

These are:

1. Eradicate extreme poverty and hunger
    - Halve, between 1990 and 2015, the proportion of people whose income is less than one dollar a day.
    - Achieve full and productive employment and decent work for all, including women and young people.
    - Halve, between 1990 and 2015, the proportion of people who suffer from hunger.
2. Achieve universal primary education
    - Ensure that, by 2015, children everywhere, boys and girls alike, will be able to complete a full course of primary schooling.
3. Promote gender equality and empower women
    - Eliminate gender disparity in primary and secondary education preferably by 2005, and at all levels by 2015.
4. Reduce child mortality
    - Reduce by two-thirds, between 1990 and 2015, the under-five mortality rate.
5. Improve maternal health
    - Reduce by three quarters, between 1990 and 2015, the maternal mortality ratio.
    - Achieve, by 2015, universal access to reproductive health.

6. Combat HIV/AIDS, malaria, and other diseases
    - Have halted by 2015 and begun to reverse the spread of HIV/AIDS.
    - Achieve, by 2010, universal access to treatment for HIV/AIDS for all those who need it.
    - Have halted by 2015 and begun to reverse the incidence of malaria and other major diseases.
7. Ensure environmental sustainability
    - Integrate the principles of sustainable development into country policies and programmes; reverse loss of environmental resources.
    - Reduce biodiversity loss, achieving, by 2010, a significant reduction in the rate of loss.
    - Halve, by 2015, the proportion of people without sustainable access to safe drinking water and basic sanitation.
    - By 2020, to have achieved a significant improvement in the lives of at least 100 million slum-dwellers.
8. Develop a global partnership for development
    - Develop further an open trading and financial system that is rule-based, predictable and non-discriminatory. Includes a commitment to good governance, development and poverty reduction, nationally and internationally.
    - Address the special needs of the least developed countries. This includes tariff and quota free access for their exports; enhanced programme of debt relief for heavily indebted poor countries; and cancellation of official bilateral debt; and more generous official development assistance for countries committed to poverty reduction.
    - Address the special needs of landlocked and small island developing states.
    - Deal comprehensively with the debt problems of developing countries through national and international measures in order to make debt sustainable in the long term.
    - In cooperation with pharmaceutical companies, provide access to affordable essential drugs in developing countries.
    - In cooperation with the private sector, make available the benefits of new technologies, especially information and communications technologies.

Since the commencement of this programme recent evidence suggests that progress in Africa in meeting the MDGs by the target date is picking up although a lot remains to be done (UNESC/ECA, 2008). Also, significant progress has been reported for indicators such as universal primary education and gender equality. Ghana, for example, is reported to be on track to meet the target of halving poverty by 2015. And there has been significant reduction in the prevalence of HIV. However, the continent's average annual growth rate of approximately 5.8 per cent still remains significantly lower than the 7 per cent annual growth rate required to reduce poverty by half by 2015. This growth is increasingly coming under threat from new developments.

However, if this surge is to evolve into a virtuous spiral that stimulates higher and sustained growth rates in a substantial number of African countries, a significant increase in investment in physical and human capital is needed over an extended period (The World Bank, 2008). This is because, as it is noted in this World Bank's report, there is an urgent need for countries in African to acquire the capabilities that will spawn new industries that create more productive jobs, multiple linkages, and more diversified exports. These capabilities derive from investment in physical assets, such as infrastructure and productive facilities, and in institutions and human capital. However, the salience of human capital is increased by the necessity of moving up the technological ladder in order to diversify into higher-value, knowledge- and research-intensive activities with good longer-term demand prospects (The World Bank, 2008).

Consequent on the above, it is the concern of this paper to further understand the relevance of the tertiary institutions in the achievement of the MDGs in Nigeria and therefore suggest how they can be better positioned to assist the government in achieving the Nigerian version of MDGs. In response to this initiative, the Nigerian governments, during Obasanjo's regime, at the three levels of government, have made efforts in the process of transformation of its political, economic and social systems. These efforts include the launching of "Economic Empowerment and Development Strategy" a document known as 'National Economic Empowerment and Development Strategy' (NEEDS) at the national level; 'State Economic Empowerment and Development Strategy' (SEEDS) at states level; and 'Local Economic Empowerment and Development Strategy' (LEEDS) at local governments level. These documents provides a framework for a nationally coordinated programme of action by the federal, state, and local governments; and focuses on four key strategies of re-orienting values, reducing poverty, creating wealth, and generating employment (Nigerian National Planning Commission, 2004). The Yar'adua's seven-point agenda is also a new response to the MDG initiatives.

However, while the revival of economic growth in Nigeria, as evidenced from the Nigerian version of MDGs Documents, is a welcome development yet it is important to be sustained over the future. This effort is indeed a necessity but with its own challenges. It is a necessity because this is the only way that poverty can be steadily reduced and progress made towards achieving the MDGs. It is a challenge because Nigeria is still lagging behind in meeting the pre-conditions for stable growth and is faced with tightening constraints on growth arising from inadequate infrastructures, instability in energy supply, inadequate food supply, and stiff entry barriers to the global markets for the manufacturing sector. All efforts at achieving the various targets set in the MDGs, and equally maintaining the momentum require harnessing more knowledge and capital as well as measures that will substantially enhance economic competitiveness and nurture expansion of new tradable activities. Investing heavily in physical infrastructure and productive capacity is important, however, maximising productivity and achieving competitiveness depends upon success in augmenting human capital and raising its quality. Therefore, the key to economic success in the present globalised world lies increasingly in how effectively a country can assimilate the available knowledge and build comparative advantage in selected areas with good growth prospects. It also depends on how it can enlarge the comparative advantage by pushing the frontiers of technology through innovation. While capital is a necessary and indeed the arbiter of economic success, survival in the world today is the capacity to mobilise knowledge and to use it to the full (The World Bank, 2008). In other word, economic success of a country depends on how effective it operates its National Innovation System (NIS).

2. THE NATIONAL INNOVATION SYSTEM

The National Innovation System (NIS) has been defined in different ways by various authors depending on the theoretical approach adopted. It as "the network of institutions in the public and private sectors whose activities and interactions initiate, import, modify and diffuse new technologies." (Freeman, 1987) This definition emphasises the interaction between the production system and the process of innovation.

The NIS is also described as being constituted by elements and relationships, located within or rooted inside the border of a nation state, which interact in the production, diffusion and use of new and economically useful knowledge. Often the interactions of the elements of the system are mutually reinforced in promoting learning to bring forth technical advances that nurture economic and social progress of a nation (Kwanjai, 2000), or may combine into constellations preventing learning processes (Lundvall, 1992). According to another author, such a system consists of the following distinct and interacting sub-systems (Lalkaka, 1999):

(i) Science and Technology (S&T) policy and policy instruments;
(ii) Technical human resources development;
(iii) Scientific research and its commercialisation;
(iv) Technology transactions in the international markets;
(v) Technical support and business development services;
(vi) Financing S&T; and
(vii) International cooperation.

Bound by the concept of innovation and the notion of a nation, the national innovation system, therefore, provides a framework for evaluating the totality of a nation's attempt at generating and applying knowledge for meeting the needs of her society.

3. ELEMENTS OF NATIONAL INNOVATION SYSTEMS

Using the generic model, three major elements of a national innovation system are identified as follows (Kwanjai, 2000):

(i) Educational institutions;
(ii) S&T and Research and Development (R&D) institutions; and
(iii) Firms and industries.

Higher educational institutions, particularly universities, perform the traditional functions of teaching and talent filtering by which new generations of scientists, technologists, and engineers are trained. They also have a social and statutory responsibility to participate in the generation of new knowledge through research and development activities which can be channeled and diffused by new ventures. In other words, tertiary institutions play important roles in four ways (Saint, 2004). First, through tertiary education, qualified and adaptable labour forces are trained, new knowledge accessed and/or generated; and even global knowledge is adapted for local use. Through this effort, poverty could be alleviated through direct contributions to economic growth. Secondly, tertiary education can also reduce poverty through redistribution and empowerment, by building of social capital and expanding opportunities for employability, income, and social mobility. Third, tertiary institutions also strengthen the entire education sector, by training and re-training of teachers and other professionals within the nation. Lastly, the outputs of the researches from tertiary institutions and technology adaptation can enhance food supply and rural incomes. Likewise, professionals, like doctors, nurses, teachers and administrators and so on, are trained to oversee and implement MDG activities. In addition, they foster relevant capacities in research, applied technology and community services that are essential for improving welfare levels for poor families, particularly vulnerable women and children, in those countries targeted by the MDGs.

Therefore, tertiary institutions, being key institutions of civil society, requires unique positioning, since their roles include assisting in developing the skills and creating the knowledge needed to provide effective services to the community and to make sound policy decisions at the government level (Figure 1). Also, they create the knowledge needed to better understand development challenges and identify locally relevant solutions.

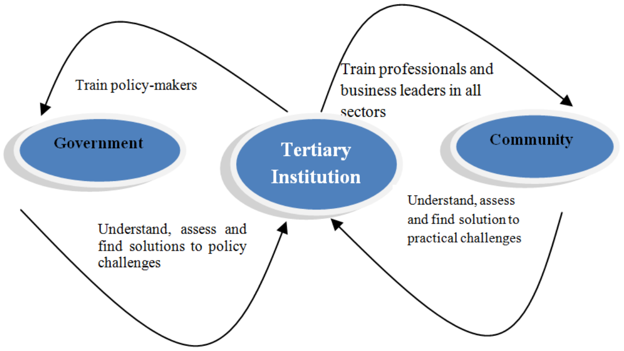

Figure 1: Interactions between Tertiary Institutions, Government and the Community (Association of Universities and Colleges of Canada, 2004)

For example, a good number of technology-based spin-offs in some regions in Europe and USA have emerged directly from academic research activities of universities. The pursuance of these functions has led to the emergence of new fields of science, processes and major new generic technologies of wide industrial and social significance (OECD, 1998).

The modern university also plays a more active role in consulting community services, specialised training and distance learning (Lalkaka, 1999). These are in response to the capacity building requirements of the global economic shift from resource endowments and factor costs to information- and experience-based knowledge. Public research and development institutes, another element of the NIS, are expected to undertake different lines of research that are of commercial applicability. These institutes vary in their mandates and sizes but derive their funding mainly from government sources. A current model of innovation systems, however, include at least some other types of actors (Figure 2), namely the financial system, technology brokers, industry and professional associations, the legal base, non-governmental organisations, press, public opinion, and international co-operation structures (Plonski, 2000; Oyelaran-Oyeyinka, 2002; Oyelaran-Oyeyinka and Barclay, 2003).

The innovative performance of an economy depends on how the individual institutions and actors (e.g. firms, research institutes, universities) perform in isolation and how they interact with other as elements of a collective system of knowledge creation and use, and on their interplay with social institutions (OECD, 1998). Without adequate development of these actors and institutions in the domestic and regional settings the innovation system remains underdeveloped and anaemic (Jinma, Disenso, and Bince, 2005).

4. PARTNERSHIP WITHIN THE NATIONAL INNOVATION SYSTEM

The need and the continuous search for knowledge within the national innovation system result in the development of partnership between the system's major actors. These partnerships cut across the public and private sectors. They are often facilitated and stimulated by the government and are defined by a joint contribution of financial research, human and infrastructural resources either directly or in kind. The partnerships within the national innovation system according to the types and characteristics of the actors are as follows (Cervantes, 1990):

(i) Universities-Industry Partnership
(ii) Government-Industry Partnership.
(iii) Research Institutes-Industry Partnership; and
(iv) Any combination of (i), (ii) and (iii).

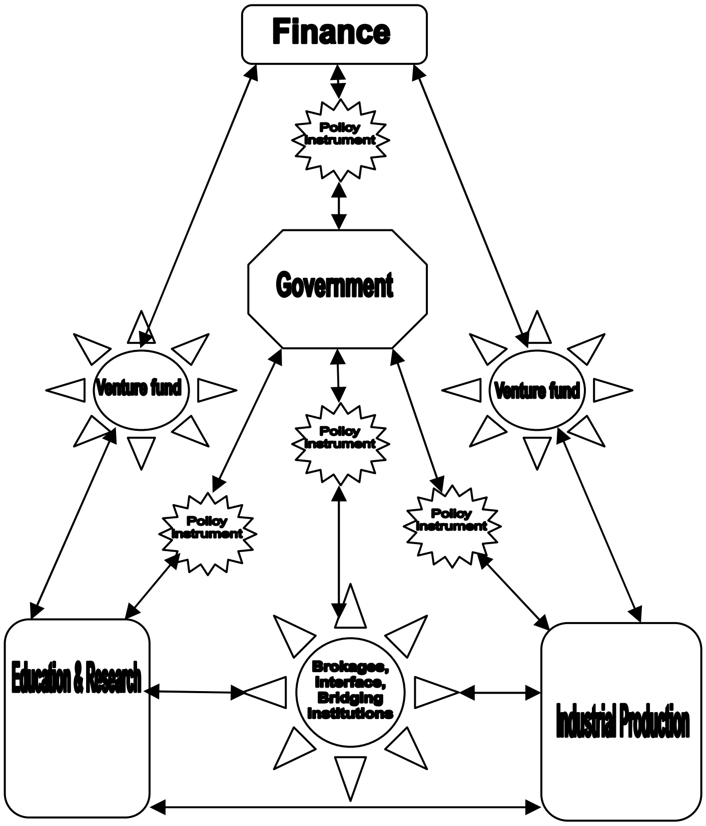

Figure 2: Typical Structure of Innovation among the Elements of the National Innovation System (Ilori, 2006) Adapted from (Tiftin, 1997).

It is noted that industry partnerships with research institutes are more common than those with universities in developed countries and have served as vehicles for meeting specific industry needs (Cervantes, 1990). Most of them started as collaborations with large firms, but the increasing prominence of small and medium-sized enterprises (SMEs) in their national economies has shifted focus to linkages involving groups of small firms and research provider. The University – Industry partnerships are spurred largely by the need for universities to look for additional sources of funds and industry's need to access a broader science for coping with the challenges of competition. Governments' inability to sustain previous growth rates in expenditure on university research has made these institutions more adventurous in seeking stronger linkages with industry (Senkers and Senker, 1997). This is reinforced by firms' willingness to take advantage of institutional innovations which are favourable to the introduction and diffusion of new technologies.

Three inter-related forces are dramatically changing the economic landscape today, which are technological innovation, entrepreneurship, and competitive global markets (Lalkaka, 2002). While the technological innovation is the process that drives a concept towards a marketable product or service, the entrepreneur is the agent of change who identifies an innovation to match a market opportunity and mobilises the human and financial resources to deliver the product or service at competitive costs and quality, in order to meet (or create) customer needs. Moreover, competitiveness is the ability to survive rivalries among the competitors through the use of wise decisions on factor endowments within an environment. The National Innovation System (NIS) integrates the roles and efforts of all the key players in the innovation system towards nation-wide economic development. The framework of globalisation within which the interactions among institutional players in the innovation system are taking place can create gap among nations because there is rapid movements of ideas, lifestyles and tastes, trade, business and finance. Hence, the solution lies in quickening the pace of technological innovation, with the impetus for change coming from all sections of society under competent political leadership Lalkaka, 2002).

Moreover, human capital also affects growth through multiple channels. This comes about by increasing allocative efficiency and the efficiency of asset management, utilisation, and maintenance; through entrepreneurship; and innovation, which raises productivity, unlocks new investment opportunities, and enhances export competitiveness. Therefore, by raising the level of education and its quality, countries in sub-Saharan African (SSA) may be able to stimulate innovation, promote the diversification of products and services, and maximise returns from capital assets through more efficient allocation and management. Hence, when tertiary institutions are equipped to impart quality education and conduct relevant applied research, they are more likely to cultivate multiple linkages with industry and to stimulate knowledge-based development through a variety of proven channels (The World Bank, 2008).

University-industry interaction is also seen as the most efficient form through which university inventions can get into practice. This is because university and industry can join and overlap research efforts to develop innovations and solve complex problems (Pavitt, 1998). In particular, this collective effort for knowledge development creates space for user-developer relations between the partners, which facilitates experimenting and testing products and concepts under development as well as further problem-solving based on fundamental research (Lee and Gaertner, 1994; Foray and Steinmueller, 2003). Moreover, it allows firms to become aware of new knowledge developments and to create new technological learning options on future technologies (Caloghirou, Ionnides and Vonortas, 2003). Therefore, as technological inter-disciplinarity and complexity, as well as competitive pressures to shorten product life increased, university-industry interaction has become acknowledged as crucial for the competitiveness of firms (Hagedoom, 2000; Pavitt, 1998; Calo ghirou, Ionnides and Vonortas, 2003).

The following are some examples of efforts of university Partnerships in Cooperation and Development (Association of Universities and Colleges of Canada, 2004):

(i) The partnership between the Memorial University of Newfoundland's Marine Institute and the Bunda College of Agriculture at the University of Malawi has been central to finding a new locally available protein source to replace the drastically depleted fish stocks in the country's main lake.
(ii) The partnership between the University of Western Ontario and the University of Costa Rica led to the piloting of the first survey of violence against women in Costa Rica,

providing a snapshot of the prevalence and costs of violence that will guide anti-violence policy and the delivery of gender-sensitive services.

(iii) The partnership between St. Francis Xavier University and the National Institute of Education in Bhutan is assisting Bhutan's national education reform by building the country's capacity to train all primary school administrators and headmasters in leading and running schools efficiently across the country. This was premised on the fact that leadership can make a difference in the quality of education in schools.

(iv) In South Africa, the University of Natal and the Kwazulu-Natal department of health partnered with McMaster University to research and design a primary health care training program with an important component on pregnancy, labour, post-natal care and prenatal transmission of HIV/AIDS. So far, the program has been delivered to 82 public health care nurses, 57 traditional birth attendants, 20 sangomas (traditional healers) and 565 female community leaders working throughout the province of Kwazulu-Natal.

(v) The partnership between the École de technologie supérieure and the Harbin University of Science and Technology in China led to technology transfer in hydroelectric-dam robotics and fostered new trade and cooperation initiatives between the two countries' universities and private sector enterprises.

5. REPOSITIONING OF TERTIARY INSTITUTIONS

The universities are therefore no longer teaching alone, but are restructured to take responsibility for an active role in the more complex field of economic development, covering a portfolio of applied and basic research, consulting and community services, specialised training, distance learning and tech-based venture formation (Lalkaka, 2002). That is, moving towards becoming an **entrepreneurial university**. Another important change in the function of the universities in the world today is the education curricula, where new courses are being introduced on the **management of knowledge**. This provides knowledge on key issues at the interfaces of science, engineering, business and civil society. The students are being exposed to **entrepreneurship development**, which seeks to transform the nascent entrepreneur into a successful enterprise-owner. For example, the Monterey Institute of Technology in Mexico runs technology incubators and a virtual university in Mexico with a consortium of 13 universities outside, addressing 9,000 degree and 35,000 non-degree student annually in Latin America. Also, the research universities have become seedbeds for innovation, with the University of California system earning $ 61 million in royalties and its 528 patents in 1997, while Stanford and M.I.T. each created 15 start-up companies (Lalkaka, 2002).

It is evident from the foregoing that knowledge resources have undoubtedly become the driver of modern economy. The only thing that endows a competitive edge on an organisation or a nation is what it knows, how it uses what it knows and how fast it can know something new (Prusak, 1996).

China's enviable and rapid economic emergence is contingent on selective investment in S&T human capital development hinged on radical educational reforms. The government adopted a plan of public subsidies that favours enrollment of the best minds in S&T Faculties that produce high externalities and contribute to greater innovation and ultimately economic growth. It is assumed that investing in very smart students in certain fields of study, such as research science or teaching, will spur the much needed technological change. Public spending per student increased from 13,000 Yuan (1,903 US Dollars) to 20,000 Yuan (2,929 US Dollars) between 1999 and 2002, while the public expenditure on education rose by 23 percent between 2005 and 2006, leading to an increase in the percentage of Gross Domestic Product (GDP) spent on education from 2.81 percent in 2005 to 3.01 percent in 2006 with the target of 4 percent by 2010.

Another significant feature of China's education reform is the increasing linkage among the elements of the NIS. China recognised the role of education, both formal and informal, in bringing about technological change and innovation and thus continued to increase their percentage of GDP spent on R&D. The lessons to be learnt from China experience are that economic growth is dependent on qualitative human capital and rational selective investment in education which generated unimaginable rate of economic growth as apparent in China's doubling of per capital GDP within 10 years. This landmark record took United States of America (USA) 40 years of selfless reforms (Martin, 2006).

6. CURRENT SITUATION IN TERTIARY INSTITUTIONS IN NIGERIA

Despite strong enrollment growth, most African tertiary institutions are not generating enough graduates, and many of them lack the skills needed to support national economic development in the 21st century (The World Bank, 2008). One important constraint on accelerating economic growth, as noted by this World Bank report, is in the choices made by policymaking bodies and capacity-building institutions responsible for higher-level human resource development. Specifically, in Nigeria the numbers of tertiary institutions include 101 approved Polytechnics and Monotechnics (49 federal-owned, 40 state-owned, and 12 private-owned) and 94 approved universities (27 federal-owned, 33 state-owned, and 34 private-owned) (NBTE, 2009; NUC, 2009). Likewise, over the past two decades tertiary student enrollments have increased far more quickly than tertiary budgets. In fact, enrollments more than tripled between 1991 and 2005, but the tertiary public financing was very poor. It is reported that public funding of education averaged 4.28 per cent of total government expenditure for a ten-year period (1990 – 2000) (Okebukola, 2002). Up till 1999, funding on education was well below 76 per cent of Gross Domestic Product (GDP) recommended by United Nations Educational, Scientific and Cultural Organisation (UNESCO). Even then, over 70 per cent of the allocation was expended on salaries and other personnel emolument. The UNESCO standard has never been met by any African country (Ilori, 2006).

Similarly, the total amount expended annually on research in the universities is approximately an average of 0.11 per cent of the Gross Domestic Product (GDP), which is made up of 98.81percent from government funding, 0 percent from industry and 4.46 percent from foreign agencies (Tables 1 and 2). The funds available to educate a student in the university continue to decrease drastically, thereby affecting educational quality and relevance (Donwa, 2006). The same situation is applicable in the Polytechnic where, according to another study it is revealed a mismatch between enrollment and available teachers, with huge staff shortfall over the years (Adeyemi, and Uko-Aviomoh, 2004). For example, between 1993/94 and 1999/2000 sessions the overall teacher to student ratio increased from 1:25 to 1:31. These trends are, in no doubt, making it increasingly difficult to provide the relevant knowledge and core skills needed for the country to boost competitiveness and sustain growth.

Another problem is the employers' complaint that majority of tertiary graduates are weak in problem solving, business understanding, computer use, teamwork, and communication skills. This is adduced to mismatches between the education provided and the capabilities required in the job market. Moreover, a combination of inadequate salaries, heavy teaching workloads resulting from declining staff-student ratios, deficient personnel management, and lack of research opportunities makes staff retention and recruitment increasingly difficult (Adeyemi, and Uko-Aviomoh, 2004). The linkage between the university and industry within the Nigerian Innovation System is very weak, due to some reasons, which include among others, cultural differences.

7. REPOSITIONING NIGERIAN TERTIARY INSTITUTIONS TO CONTRIBUTE TO THE ACHIEVEMENT OF MDGS

Considering these problems, it may be difficult for the tertiary institutions to play their role in the achievement of the Nigerian version of MDGs, the vision 2020:20 and the seven point agenda of Mr. President. Therefore, the following good practices are suggested to speed the journey toward a more effective and responsive tertiary education system in the country.

Table 1: Research Funding in Nigerian Universities

Year	Per cent Source of Funding			
	% GDP	Government	Industry	Foreign Agency
1990	0.01	100.0	-	-
1991	0.01	100.0	-	-
1992	0.02	100.0	-	-
1993	0.02	100.0	-	-
1994	0.02	100.0	-	-
1995	0.01	100.0	-	-
1996	0.01	100.0	-	-
1997	0.01	100.0	-	-
1998	0.01	100.0	-	-
1999	0.02	100.0	-	-
2000	0.30	100.0	-	-
2001	0.30	94.50	-	5.50
2002	0.30	87.84	-	12.16
2003	0.30	99.91	-	0.09
2004	0.30	99.93	-	0.07
Average	0.11	98.81	-	4.46

Source: (Donwa, 2006)

- **Develop a strategy for national human resource development**. As tertiary education becomes an important driver of economic growth, governments with constrained financial resources may have but to choose and strategically fund a limited number of priorities (The World Bank, 2008).
- **Reform financing arrangements to offer incentives for attaining policy goals while providing the stability necessary for institutions to plan strategically**. The task of funding tertiary education will become increasingly difficult in the years ahead as social demand increases. Hence, each country will have to devise a financing approach that plays to its economic strengths, its institutional capacities, and its political possibilities. Private sector may also have to increase their contribution towards funding education in the country (The World Bank, 2008). Government of Nigeria should aim at meeting the UNESCO recommended target (26 per cent) for funding education in the country. With this the poor laboratory facilities and practical can be upgraded. There should also be provision for enhancing staff capability in priority areas through an intensive programme of training and re-training and industrial exposure.
- Grant institutional autonomy, buttressed by appropriate accountability mechanisms, in order to increase opportunities for system differentiation and institutional innovation. The combination of autonomy, accountability, and competition within tertiary education systems is necessary in order to foster student learning performance. Autonomy in decision making can ensure institutional managers and governing bodies to act as they see necessary to promote educational achievement. An accountability system can identify and reward good institutional performance. Competition and competition and choice among institutions and academic programmes can lead to student demand creating performance incentives.

Table 2: Research Grant Allocation and Releases from 1987- 2003

S/N	Year of Release	Allocation (N'000,000)	Amount Released (N'000,000)
1	1989	12.78	12.78
2	1988	20.00	17.24
3	1989	20.00	20.00
4	1990	24.00	22.08
5	1991	51.27	16.65
6	1992	14.50	17.47
7	1993	122.18	122.18
8	1994	132.21	98.66
9	1995	155.54	73.97
10	1996	153.84	50.58
11	1997	194.01	122.02
12	1998	215.62	149.99
13	1999	302.74	183.50
14	2000	448.13	612.67
15	2001	206.41	206.41
16	2002	-	-
17	2003	73,44	73.44
	Total	2,146.66	1,799.64

Source: (Okebukola, 2002)

- Encourage diversity in teaching, and learning approaches that facilitate institutional specialisation. There is need to change the traditional pedagogy of teaching from disciplinary to interdisciplinary perspectives; from lectures to flexibility in learning and group work; and from memorisation of facts to problem solving. Others are practical learning (field trips, attachments, internships) as a complement to theory; learning assessment through project work that demonstrates competence instead of multiple choice examinations; communication skills; and computer literacy (The World Bank, 2008).
- **Foster the development of national and regional postgraduate programmes.** This is the best way to increase academic staff numbers and build research capacity. National R&D efforts are more likely to be sustainable when they are grounded in postgraduate programmes and the professional networks that emerge around them.
- **Search for lower-cost delivery alternatives for tertiary education**. Traditional face-to-face models of delivering post-secondary education are expensive and can limit developing countries' capacities for enrollment expansion. Hence, alternative, lower-cost delivery models are needed if educational access is to increase. This could be in form of

lifelong learning, ICT applications to education, online distance education, open source courses, self-paced learning, and so on (The World Bank, 2008).

- Government must be ready to put in place national research priorities and provide supportive policies to assist the tertiary institutions place their roles in the development of qualitative human resource, and generation of research and development (R&D) results that could translate into innovations. Capability for translating the R&D results into commercialisable product should be nurtured through effective linkages between the academia and domestic industry (The World Bank, 2008).
- A model hybrid coalition capable of resolving cultural differences between the academic and the industry has been proposed. The model will create a forum where effective means of communication would be developed and the two sectors would have the opportunity of interaction and exchange of ideas in an atmosphere of mutual trust and respect (Oyebisi, Ilori, and Nassar, 1996). Under this environment, both parties, together with Government, could establish the technological needs of the industry that requires R&D intervention and get involved in joint venture projects. Joint implementation of projects from research, technology development to production and marketing is feasible under this arrangement. This will ensure that only technology or R&D projects that are relevant to and of direct application to the industry are embarked upon (Oyebisi, Ilori, and Nassar, 1996).

- For science and technology (S&T) to succeed in promoting development, formulation and implementation of R&D policy and strategic planning should occupy a central position in the research institutes, universities and other tertiary institutions. The strategic planning should flow out from the National S&T, industrial and other relevant policies. The universities, polytechnics and research institutes should build intellectual capital around their core competencies and seek for opportunities to spin-out new technology-based enterprises arising from their R&D outputs and inventions. They should ensure that all S&T activities are aligned with their strategic directions. The growing changes of global scientific and business environment demand global partnership for future survival of our educational and research organisations. They should therefore reach out to other global institutions and seek opportunity for international projects and partnerships.
- Business units or science and technology parks having strong affiliation to educational and research organisations should be established to promote R&D markets and client industry relationship. Appropriate policy measures need to be put in place to encourage greater investment in local R&D by industry. The contributions of the private sector in support of R&D should be enhanced to be greater than that of Government. Government should put in place policy instruments such as tax incentives for R&D in order to encourage and promote private sector expenditure on R&D. A more robust patenting regime should also be put in place. Provision of adequate infrastructure and standardisation of locally fabricated equipment are necessary for effective operation of the Nigerian Innovation System (Ilori, 2006).
- Tertiary institutions must be ready to be more entrepreneurial and ready to function as networked partners and institutional collaborators. The curriculum revision is also important to streamline it to the dynamic needs of the labour market.

8. CONCLUSION

Both the MDG document and the Nigerian versions recognise the importance of a people-centered and multidisciplinary approach in the achievement of the goals contained in these documents. Also, the documents equally recognised the role of pro-poor growth and efficiency; a focus on inequality, women and marginalised groups; and social, political and civil empowerment in support of human dignity and freedom. This then suggests that any effort at achieving these without making knowledge creation, its dissemination and utilisation as part of its strategy might achieve very little.

REFERENCES

Adeyemi, J.K. and Uko-Aviomoh, E.E., Effective Technological Delivery in Nigerian Polytechnics: Need for Academic Manpower Development Policy. Education Policy Analysis Archives, 12(24), 2004. Retrieved on 6 March, 2009 from http://epaa.asu.edu/v12n24.pdf.

Association of Universities and Colleges of Canada, Higher Education is Key to Achieving MDGs, 2004. Accessed on 4 March, 2009 from http://www.aucc.ca/_pdf/english/publications/upcd_fact_sheets/mdgs_e.pdf.

Caloghirou, Y., S. Ionnides, and N. S. Vonortas, Research Joint Ventures. Journal of Economic Surveys 17(4), 2003, 541-570.

Cervantes, M., Public/Private Partnership in Science and Technology: An Overview. STI Review, No. 23, OECD, 1990, p.4.

Donwa, P.A., Funding of Academic Research in Nigerian Universities, 2006. Accessed on 6 March, 2009 from http://portal.unesco.org/education/fr/files/51642/11634301905Donwa-EN.pdf/Donwa-EN.pdf.

Foray D. and W.E. Steinmueller, On the economics of R&D and technological collaborations: Insights and results from the project. *Economics of Innovation and New Technology*, 12, 2003, 77–91.

Freeman, C., *Technology Policy and Economic Performance: Lessons from Japan*. (London: Pinter Publisher, 1987).

Hagedoorn, J., A. N. Link, and N. S. Vonortas, Research partnerships. *Research Policy* 29, 2000: 567-586.

Ilori, M.O., From Science to Technology and Innovation Management. Inaugural Lecture Series 191, Obafemi Awolowo University, Ile-Ife. (Ile-Ife: Obafemi Awolowo University Press Ltd, 2006).

Ilori, M.O., Oyebisi, T.O. and Nassar, M.L., Models of Technology Transfer from Laboratories to the Industry: Relevance and Implementations for Developing Countries. UNILAG Journal of Business, 1, 1995, 1-8.

Jinma, C.; Disenso, A.; and Bince, A., Forging New Technology Alliances. Cooperation South. 6 2005, pp. 59-71.

Kwanjai, N.N., Applying General Systems Theory to put together NIS Jigsaw-puzzle pieces: A Profile of the Thai National Innovation System. Paper presented at INTECH-CERES WP3 Conference. Maastricht, 17 May, 2000, p. 13.

Lalkaka, R., New Strategies, Skills and Structures for Technological Innovation. Paper presented at XVI IASP World Conference on Technology Parks. Istanbul, September, 1999, p. 8.

Lalkaka, Rustam, National Innovation Systems: Role of Research Organisations and Enterprises. Paper delivered at the IV International Symposium on Environmental Biotechnology, Veracruz, Mexico, June, 2002. Accessed on 2nd March, 2009 from http://www.btds.biz/publications/pdfs/innovation_system.pdf.

Lee, Y. S. and R. Gaertner, Technology Transfer from University to Industry: A Large-Scale Experiment with Technology Development and Commercialization. *Policy Studies Journal*, 22(2), 1994, 384-399.

Lundvall, B., Introduction. In Lundvall, B. (ed.) *National Systems of Innovation: Toward a Theory of Innovation and Interactive Learning*. (London: Pinter Publishers, 1992). Pp 1-18.

Martin, C., High Education and Economic Development: India, China and the 21st Century Stanford Centre for International Development, Stanford University, 2006.

NBTE, Approved Monotechnic, and Polytechnics in Nigeria, 2009. Accessed on 6 March, 2009 from National Board for Technical Education website (http://www.nbte.gov.ng/institutions.html).

Nigerian National Planning Commission, Meeting Everyone's Needs: National Economic Empowerment Development Strategy. Nigeria NEEDS Document published by Nigerian National Planning Commission, Abuja, 2004. Accessed online on 3 March 2009 from http://www.nigerianeconomy.com/downloads/part1.pdf.

NUC, Monday Bulletin Headlines. *A weekly Bulletin of the National Universities Commission*, 2009. Accessed on 6 March, 2009 from http://www.nuc.edu.ng.

OECD, University Research in Transition, OECD: Paris, 1998.

Okebukola, P, Strategies for Stimulating Research and Development in Nigerian Universities. *Nigerian University System Chronicle*, Vol. 12; No. 2, 2004, 17-18.

Okebukola, P., The State of University Education in Nigeria. National Universities Commission, Abuja, Nigeria, 2002.

Oyebisi, T.O., Ilori, M.O. and Nassar, M.L., Industry-Academic Relation: An Assessment of the Linkages between a University and some enterprises in Nigeria. Technovation: The International Journal of Technological Innovation, Entrepreneurship and Technology Management, 16, 1996, 203-209.

Oyelaran-Oyeyinka, B, Manufacturing Response in Systems of Innovation: Evidence from Brewing Firms in Nigeria. UNU/INTECH Discussion Paper No. 2002-3, 2002.

Oyelaran-Oyeyinka, B. and Barclay, L.A., System of Innovation and Human Capital in African Development. UNU/INTECH Discussion Paper No. 2002-2, 2003.

Pavitt, K., The social shaping of the national science base. *Research Policy 27*, 1998, 793–805.

Plonski, G., Science and Technology Innovation and Cooperation in Latin America. Cooperation South 1, 2000, pp. 99-107.

Prusak, L., The Knowledge Advantage". Strategy & Leadership, March/April, 1996.

Saint, William, Achieving the Millennium Development Goals: A Challenge for Global Higher Education, 2004 Accessed on 2nd March, 2009 from http://www.daad.de/de/download/entwicklung/veranstaltungen/2004_dies_saint.pdf

Senkers, J. and Senker, P., Implications of Industrial Relationships for Universities: A Case Study of the U.K. Teaching Company Scheme. *Science and Public Policy*, Vol. 24, No. 3, June, 1997, pp. 173 – 182.

The World Bank, Accelerating Catch-Up: Tertiary Education for Growth in Sub-Saharan Africa. Report of the Development Economics Research Group, Africa Region Human Development Department of World Bank, October, 2008.

Tiftin, S., Building Science and Technology Innovation System in Africa. Paper delivered at the First Regional Workshop on the Restructuring of National Science and Technology System in Africa Regional Program for Technology Management (REPTEM), Lagos, May 12 – 16, 1997.

United Nations Economic and Social Council/Economic Commission for Africa (UNESC/ECA), Assessing Progress in Africa towards the Millennium Development Goals Report 2008. A Report from the Joint Annual Meetings of the African Union (AU) Conference of Ministers of Finance, Planning and Economic Development, held from 31 March – 2 April, at Addis Ababa, Ethiopia, 2008.

Ife Journal of Technology, Vol. 18 (2), 63-71, 2009

Full Paper

A PLATFORM FOR INERTIAL MOTION CAPTURE AND MODELING OF HUMAN MOVEMENT

O.A. Moninuola
Department of Electronic and Electrical Engineering
Obafemi Awolowo University, Ile-Ife, Nigeria

K.P. Ayodele
Department of Electronic and Electrical Engineering
Obafemi Awolowo University, Ile-Ife, Nigeria
kayodele@oauife.edu.ng

L.O. Kehinde
Department of Electronic and Electrical Engineering
Obafemi Awolowo University, Ile-Ife, Nigeria

T.K. Yesufu
Department of Electronic and Electrical Engineering
Obafemi Awolowo University, Ile-Ife, Nigeria

ABSTRACT

In many aspects of medicine, there is a need for methods to convert human locomotion to data in a form that is amenable to mathematical processing and analysis. Most schemes involve the use of motion capture sensors. This paper presents the development of a platform for inertial motion capture and modeling of human movement. The hardware consists of micro sensor nodes and a base station. A sensor network was implemented to make the motion data from all the sensor nodes available at the base station from where it is wirelessly transmitted to a personal computer (PC) for processing. Each sensor has a sampling rate of 625 kHz. Wireless communication between the base station and the PC is achieved using the IEEE 802.15.4 protocol. Data acquired by the platform is processed using time series analysis with an autoregression moving-average model. Analysis of numerical data obtained from the prototype suggests that with calibration step implemented in software, the process of transforming human body motion into data can be done to a high degree of accuracy.

1. INTRODUCTION

Studies of human limb movement are emerging as a very important component in the study, diagnosis and treatment process in many aspects of medicine. The core premise behind these studies is that certain diseases influence the motion of subjects (for example, Fox et al. 2009;, Griffin et al, 1995 and Petrofsky et al , 2005). Certain medications have also been identified as causing movement disorders (Riker et al, 1997). These have led to more acute interest in observing and measuring movements of various parts of the body and linking them to illnesses or drug side effects. For this reason, motion capture has become an increasingly important tool in medicine.

Motion capture comprises of the several techniques which enable the gathering of motion data from human subjects. It is the recording of human body movement for immediate or delayed analysis and playback. Typically, complexity is reduced by tracking only key points like joints. The information captured can be as general as the simple position of the body in space or as complex as the deformations of the face and muscle masses. Motion capture devices are needed to present human body motion in a form much more suitable for mathematical modeling. Mathematical methods can then be employed to establish statistical patterns from which conclusions can be drawn

Early motion capture platforms employed optical sensors in which light reflected from optical markers worn by the human subject is used for digital reconstruction of body motion. In recent years however, there has been a sharp increase in the development and deployment of another class of motion capture systems: inertial motion capture systems. This increased focus has coincided with the maturity of micro-electromechanical (MEMs) techniques for fabricating cheap and highly accurate inertial sensors. Although optical motion capture systems have traditionally had higher precision, MEMs sensors are so cheap and are benefiting from research by having better performance values. The result of this is that inertial sensors are fast replacing other types of motion sensors in all areas of application.

Much of the initial research, development and marketing in this area were for military applications. Presently however, motion capture is used in many application areas such as biomechanics, sport performance analysis, tele-robotics, ergonomics, entertainment and general medicine.

When used in medicine, the purpose of motion capture is often to try to identify digital markers or signatures of various illnesses from body motion data. The possibility of obtaining such digital markers brings the exactness of mathematics into medical diagnosis and augments such traditional techniques as detection and measurement of vital signs.

This paper presents ongoing work on the development of the EEE-OAU09 motion capture platform targeted directly at medical research. This platform has a sensor network of ten tri-axial accelerometers placed at different parts of the human subject. The I2C protocol was used in implementing the sensor network. I2C was chosen because only two wires are needed to run through the different parts of the human subject which ensures that motion is not impeded.

The paper also reports initial attempts to analyze sample acquired data as a precursor to detecting digital markers. There are various statistical methods that can be employed for the data interpretation. These methods seek to establish if there are any statistical patterns that are characteristic of certain diseases. The search for patterns was based on the development of time series analysis and modeling of captured data. Although multivariate analysis was considered - because some interdependence is expected to exist between collected data streams - this paper argues that the data is better modeled with an autoregression moving-average model.

2. MOTION CAPTURE IN MEDICINE

Much of the early use of motion capture in medicine was in the area of medical rehabilitation and was usually limited to the lower limbs in what is called gait analysis. Gait analysis data acquisition is a subset of motion capture. Long-term monitoring of gait in Parkinson's disease is usually used in the long term assessment of patients' response to medications (Moore et al , 2007). However, tremors associated with advanced stages of this disease can only be captured on a full motion capture platform. Recovery of normal gait function after Total Hip Arthroplasty (THA) is usually assessed using gait analysis (Akker-Scheek et al, 2007). The effect of type 1 and type 2 diabetes on movement have also been widely studies with, for example, a study on the effect of the disease sans sensory impairments [3] establishing that the it led to subjects taking more steps both on a linear path and during turns. In addition, a correlation was seen between suffering from diabetes and both the length of time required to walk a given distance, extension and lateral movement at major body joints. Also, gait analysis is usually used extensively in the rehabilitation of patients with chronically arthritic knee, stroke and hallux valgus Zhang et al (2006), Liberson et al (1961), Menz and Lord (2005).

Despite their potential importance however, gait analysis has not enjoyed wide adoption largely because the required instrumentation systems tend to be expensive and as such are not widely available. In addition to this, most gait analysis platforms require teams of trained personnel to operate. They often cannot be used effectively in free-living conditions, and impose constraints that make subjects exhibit slight departures from their normal ambulatory patterns. In recognition of these limitations, Churchill et al. (2002) used a simple inexpensive video-based kinematic analysis for clinical disorders of gait and Hansen et al. (2002) developed a simple method, using the relative positioning of the overall center of pressure and an ankle marker in the direction of forward progression for the determination of "heel-contact" and "toe-off" events. In one of the very few research efforts related to motion capture in Nigeria, (Buriamoh-Igbo et al, 1997), pressure sensors placed in the soles of shoes were used to determine certain aspects of gait asymmetry. While these methods diminished the overall expense of a formal gait lab, they still could not function in a free-living setting (Zhang et al, 2006).

According to (Zhang et al, 2006), the ideal platform in the free-living condition would be small, noninvasive, reliable, sensitive, low cost, and easy to operate and interpret. This has led to the development of a number of low cost alternative systems, with the emphasis in developing low cost systems is shifting to MEMs accelerometers.

Probably at the front line of active research in the field of accelerometer–based motion capture systems is the Sensor Networks and Applications Research Center. Current research efforts include solving the bias and drift problems associated with modern accelerometers, reducing noise level in motion data captured with accelerometers, resolving complications associated with the non-linear nature of human motion and the development of a complete mathematical framework for human body motion capture and analysis.

3. INSTRUMENTATION

3.1. System Requirements

The motion capture system was conceptualized as a number of sensor nodes sensing movement data and sending such to a computer for recording and analysis. A simplified version of the system is shown in fig 1.

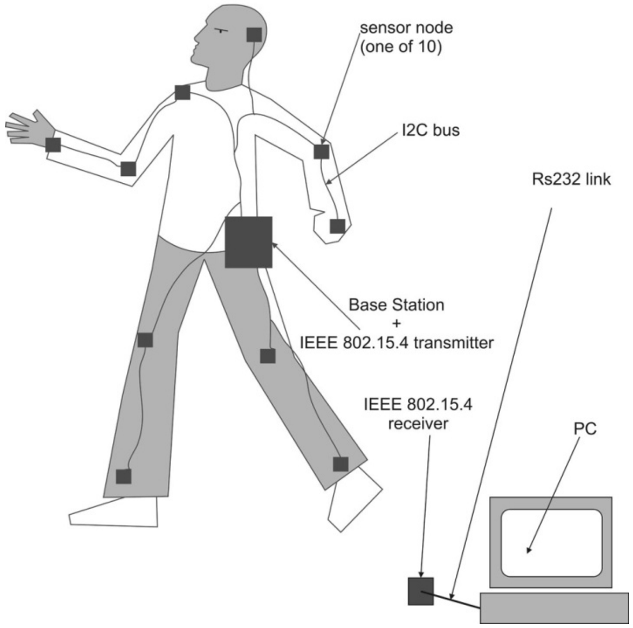

Figure 1: overview of motion capture system

The front ends of the motion capture system consist of MMA7260QT transducers to convert the motion of various body parts to electrical signals. The MMA7260QT micro machined accelerometer features embedded signal conditioning, a 1-pole low pass filter, temperature compensation and g-Select which allows for the selection among 4 sensitivities. Zero-g offset full scale span and filter cut-off are factory set and require no external devices. Sleep Mode feature also makes it ideal for handheld battery powered applications. The fixed offset voltage of around 2V also enables the connection of the accelerometers directly to a microcontroller directly for analog to digital conversion.

The design calls for microcontrollers capable of implementing hardware analog to digital conversion (ADC) and which must in addition, support at least a communication protocol capable of being used for a sensor network. The PIC18F2221 SOIC was chosen as it combines affordability and small size with the meeting of the above requirements. The analog to digital conversion process was achieved using PIC18F2221 capable of 10bit flash ADC, a sampling frequency of 2.4MHz, acquisition time of 0.4us and a voltage reference of 5V.

A sensor network is required to make the motion data from ten sensors available at a base station, which serves as a point at which data from all sensors are combined into a single stream. A wireless network would be ideal for this purpose to minimize obstructions but implementing such is prohibitively expensive for projects like this. I2C (a serial communication type with bus topology) was therefore chosen as only two wires are required for the implementation. This is seen as a good compromise between cost and unobtrusive operation. The bus configuration type was master/slave with a bandwidth of 1.6Kbps.

Communication between the base station and the computer is often achieved using wires. However, the belief in designing this platform was that such tethered systems would affect subjects and cause slight departures from normal movement patterns. Hence, in this design, communication between the base station and the computer is achieved wirelessly using the IEEE 802.15.4 based Zigbee protocol. The Zigbee protocol features simplicity, low latency, very low power requirement and the module are relatively cheap. The Zigbee implementation used has an operating frequency of 2.4GHz, using the Direct Sequence Spread Spectrum (DSSS) and a bandwidth of 250Kbps. The Zigbee transceiver used was the MAXSTREAM Xbee pro Zigbee transceiver (“Xbee”).

3.2. Design Considerations

The I2C protocol limits the allowable bus capacitance to 400pf. To ensure that the bus implemented lies within this limit, the two-wire pair that forms the bus was modeled as a parallel plate capacitor. The equation that relates the capacitance to the geometrical characteristics of the bus is thus

$$C = \frac{k\mathcal{E}oA}{D} \qquad (1)$$

Where

C = bus capacitance
k = dielectric constant
$\mathcal{E}o$ *= permittivity of free space*
D = distance between the two wires.

It can then be deduced that to minimize the bus capacitance, k and A must be minimized while D must be maximized. The dielectric constant was minimized in the design by ensuring that the space between the two I2C wires was air-filled. D was maximized by keeping the wires apart from each other as much as possible.

A trade-off must be made in minimizing A. The resistance of the wires increases as the A is reduced with implies greater signal attenuation. The exact relationship between resistance and the geometrical characteristics of the wire is

$$R = \frac{pL}{A} \qquad (2)$$

Where

R = resistance of the wire
p = resistivity of the wire
L = Length of the wire
A = Cross sectional area of the wire.

Using these two equations as constraints, the Lagrange multiplier method was used to arrive at the optimum surface area.

Another design consideration was the need for offset nulling. Offset-nulling is the process of trimming down to zero the finite output signal that might exist in any system when the input signal is zero (often called zero error correction). At Zero-g, temperature of 25°C and supply voltage, V_{DD} of 3.3 V, the average output voltage of the accelerometers were measured to be as follows:

X- Axis offset voltage: 0.70V
Y-Axis offset voltage: 1.25V
Z-Axis offset voltage: 1.70V

The elimination of these offset voltages was carried out in software. Since the output of the analog-to-digital conversion are discrete numbers, the numeric values corresponding to these offset voltages were measured by simply observing the numeric output when the accelerometers were kept stationary. With the digital values corresponding to these offset voltages recorded, these offsets were subtracted from the readings for each axis in the code written for each sensor to assure accuracy.

4. HARDWARE DESCRIPTION

4.1. The Sustained Counter Torque Soldering Technique

Living in a developing country, one of the problems that often plague Nigerian professionals is the absence of equipment that are considered rudimentary in many developed countries. One such limitation was encountered in this work. Since the design requirements for the project called for small-sized components, surface mount integrated circuit (IC) packages were used where possible. This led to the problem faced by many Nigerian students and professionals: standard pick and place process equipment appropriate for the IC packages was not available. To solve this problem once and for all, a simple soldering technique was developed. This technique is the Sustained Counter-torque Soldering technique (also called the “Spider” soldering method because of the shape that results when it is used.

The spider soldering method was designed specifically for Quad Flat No-Lead (QFN) chips although it can be adapted to other chip designs. The primary motivation for the development of the spider method was the fact that the datasheet for MMA7260QT micro machined accelerometer specifically cautioned against hand soldering. In tests, the spider method achieved hundred percent successes.

The procedure for the spider method is as follows (see figure 2):

1. Permanently position the chip with the pads facing upwards (great care should be taken here as to the numbering of the pads. Conventional numbering assumes that the pad will be soldered down. Thus, the numbering to use in this case should be the lateral inversion of the conventional one).

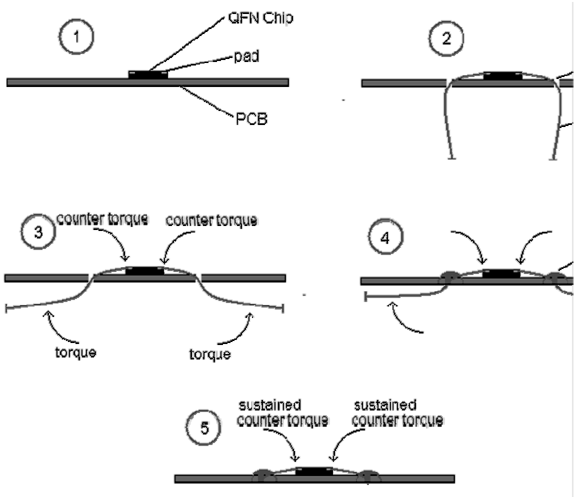

Figure 2: The Sustained Counter Torque soldering technique

1. Low malleability pins of about 2cm should be positioned such that their tips just make contact with the necessary pads on the chip.
2. To ensure that the pins make permanent contact with the pads, a first-class lever should be implemented as follows:
    i. Via holes should be made on the board to which the chip is attached at approximately half length the pins.
    ii. The pins should be bent through via holes such that the tips just touched the pads while the other half length of the pin was on the other side of the board.
    iii. Torque applied to the half-length of the pin beneath the board results in a **counter torque** that presses the pin tips to the pads. The greater the torque applied, the better the pad- pin tip contact.
    iv. To **sustain** this counter torque (which is the force that keeps the pad and pin tips in firm contact), the vias are heavily soldered.
    v. The half-length of pin beneath the pin can now be trimmed off.

An added advantage of using this method (apart from flexibility) is that the nodes the vias that are eventually soldered are typically about 1cm from the chip itself meaning that the heat transferred to the chip itself is minimal. It is also noteworthy that the chip is physically unaltered after the process (the chip can be recovered physically unaltered in any form). This means that the process in non-intrusive. The Spider technique has been described as the socket (non-invasive) form of the popular "dead-bug" soldering technique often used for prototyping.

The advantages of the Spider soldering technique can thus be enumerated as

- Simple equipment requirements
- Flexibility
- Minimal heat transfer (to chip)
- Non-intrusiveness

4.2. Circuit Design and Operation

The block diagram of the system is as shown in figure 3. Each of the accelerometers labeled 1 to 10 is interfaced with a slave microcontroller (the PIC18F2221 or "'2221"). These accelerometers sense the accelerations in three dimensional axis of each location they are attached. Three channels of the analogue to digital converter (ADC) module of the '2221s are used to digitize the accelerometer analogue outputs. Each slave '2221 stores the values of digitized accelerometer output value in its memory awaiting request from master '2221.

The master '2221 controls the operation of all the slaves and coordinates the data transfer of the system. The master places a request and destination address on I2C for data and the corresponding slave responds by placing its current reading on the network. The master '2221 receives and sends the readings of each accelerometer via serial communication using the RS232 protocol to the Xbee (transmitter, Tx) for wireless transfer. Xbee sends the data out and it is received by the second Xbee (receiver, Rx) interfaced to the computer through MAX 232 level translator. The output of the Xbee (Rx) is TTL and is converted to RS 232 using a MAX232 chip. RS232 communication settings were 9600 baud, 8 data bits, with no parity check or flow control.

This data is interpreted by the software on the computer for human motion modeling. Figure 4 shows the terminal circuitry of an MMA7260QT micro machined accelerometer while Figure 5 shows the sensor network with one master, a slave and the ADC inputs.

5. SOFTWARE AND DATA COLLECTION

CCS C was used for the program development. This is the de facto standard high level programming language for PIC microcontrollers as Microchip optimized most PIC's for CCS C programming. The base station (corresponding to the master in the network) requests for data from each of the sensors in turn. This is achieved by a program which instructs it to transmit the address of each slave (sensor) in turn to the I2C bus and to store in memory whatever the replying slave transmits. This is the data that the base station transmits to the PC wirelessly. The program written for the ten sensors (which correspond to slaves in network) are similar except for the address of each. The main program in each slave instructs it to carry out analog to digital conversion continuously in an indefinite while loop. An interrupt is triggered whenever an address match is received by any slave. The program branches out of the while loop into an interrupt service routine where the results of the most recent conversion are transmitted to the base station.

The algorithm is as follows:

Master code

```
Define the address of each slave
While (true)
{
            Transmit the address of slave1 to the I2C bus
     Read and store the reply from slave1
            Transmit the address of slave2 to the I2C bus
     Read and store the reply from slave2
     ...
            Transmit the address of slave10 to the I2C bus
     Read and store the reply from slave10
     Transmit whole data to Zigbee module
```

Slave Code

```
Assign slave address
Enable I2C activity interrupt
If address match is received
{
  Transmit latest ADC results to the master
}
Else
{
Continue ADC
}
```

The transmitted data can be viewed using any universal synchronous-asynchronous receiver-transmitter (USART) terminal software or read straight into MATLAB.

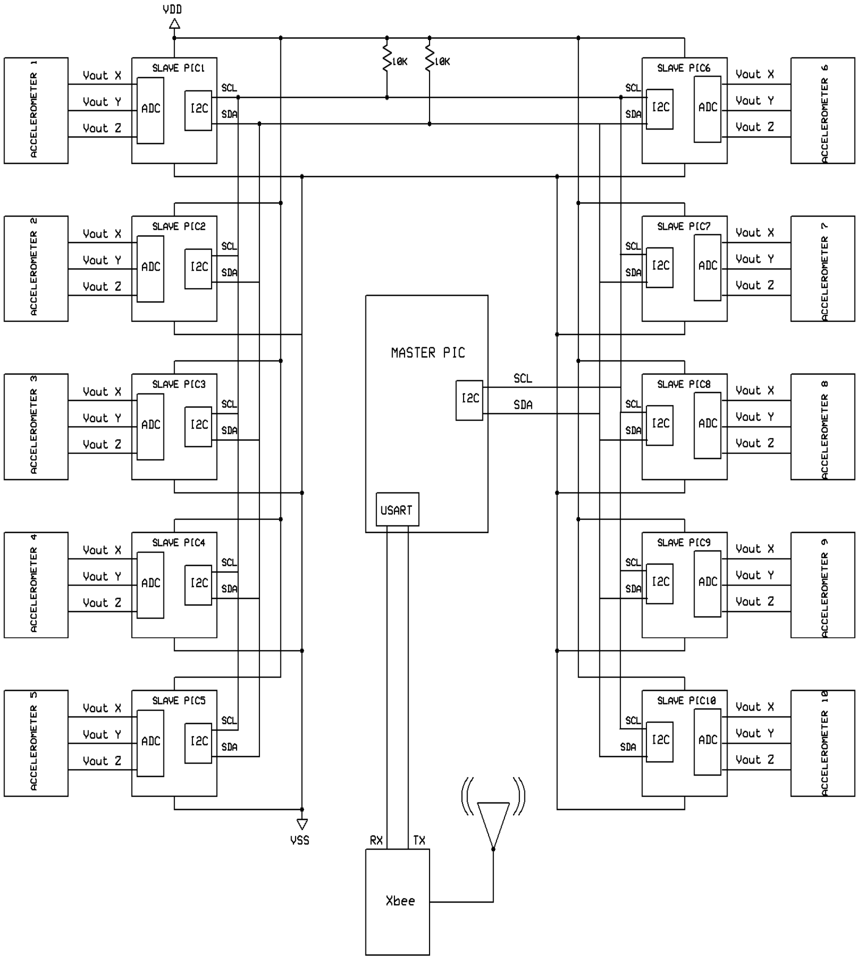

Figure 3: Block diagram of the EEE-OAU09 motion capture system

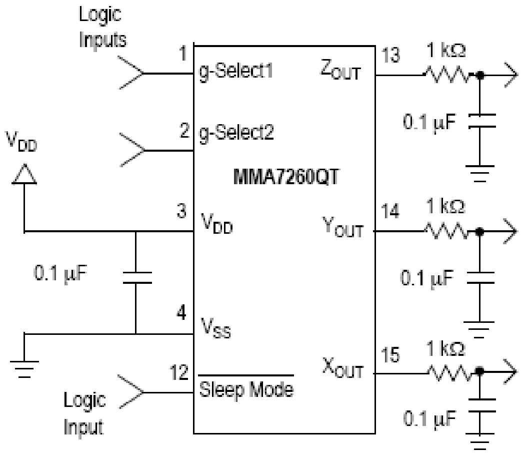

Figure 4: MMA7260QT micro machined accelerometer Terminal Circuitry

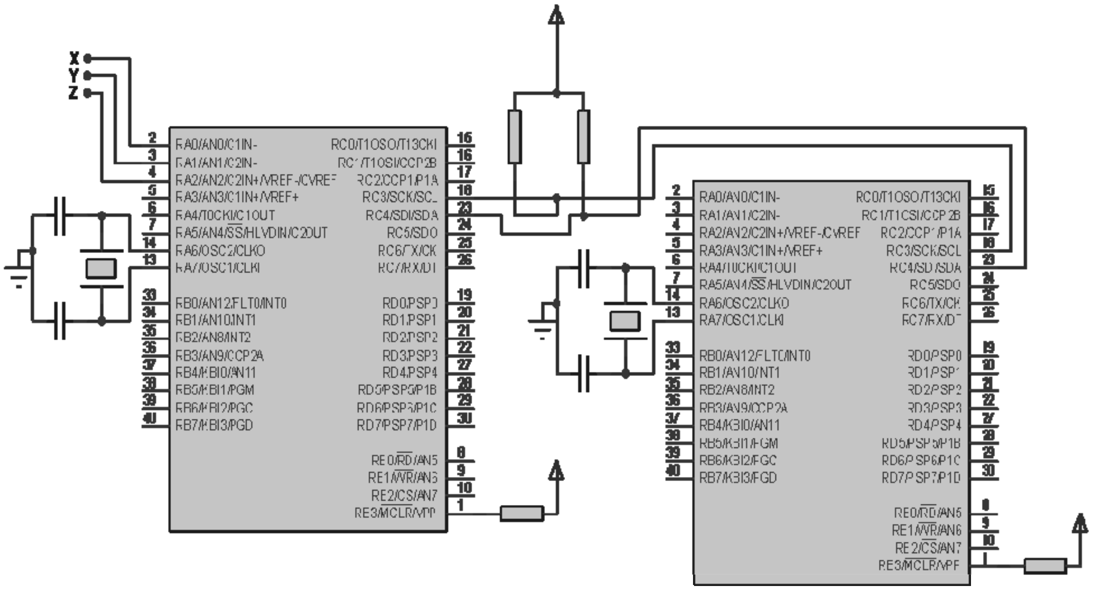

Figure 5 Sensor network with one master, a slave and the ADC inputs.

6. MODEL DEVELOPMENT BASED ON TIME-SERIES ANALYSIS

Motion is easier to observe than measure. Converting accelerometer readings to motion data with minimal errors was a big challenge. Accelerometer offset voltage, noise in the analog signal from the accelerometer to the '2221 were major sources of error. These were dealt with using software offset-nulling by minimizing the distance between the accelerometer and the microcontroller respectively.

With motion data converted to acceleration, it becomes feasible to carry out analysis on them by assuming that the data represent time series. Time series are data values sampled over time, in order and usually at equal intervals (Palit and Popovich, 2005). Time series analysis is concerned with identifying patterns, modeling patterns and forecasting values. Dedicated MATLAB functions and interactive tools perform time series analysis. Standalone MATLAB packages (executable) can be created so that users do not need to have the whole MATLAB software installed.

The steps involved in the analysis are given in figure 6:

6.1. Collecting and Formatting Time Series Data

For now, time series analysis cannot be performed in real time using any of the dedicated MATLAB functions and interactive tools. The motion data has to be stored for post-processing. Delayed processing of the motion data offers some flexibility; it can be stored in any format and the data can be arranged such that member time series in the motion data are evident. A screen capture of the PC data acquisition utility, displaying some data from the motion capture platform is shown in figure 7, while table 1 shows part of the same data, with each column of data forming a member time series.

Storing the motion data in a format in which the member series are distinct is crucial. The base station (master '2221) sends motion data to the PC using the format above and most USART terminals preserve this format.

6.2. Development of Time Series Models

The determination of the best time series representation for the motion data collected is an ongoing effort. The analysis of time series consists of a mathematical description of component variations present in the data.

There are a number of classes of time series models. These include regression models, time domain models and frequency domain models. The regression models adopted in engineering include autoregression model (AR), moving-average model (MA), autoregression moving-average model (ARMA), autoregression integrated moving-average model (ARIMA), and control autoregression integrated moving-average model (CARIMA). In addition, for systems which also have inputs from outside the system itself, there are model classes usually distinguished by the addition of an "X" to their names, with the said X representing "exogenous inputs" (or sometimes "auxiliary input"). Therefore, ARX models are autoregression models with exogenous inputs and so on.

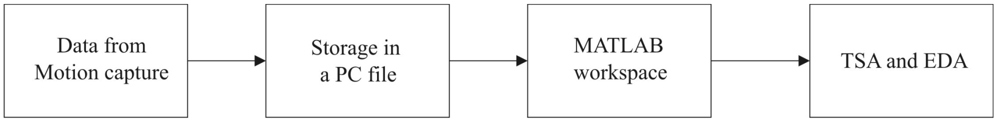

Figure 6: Steps involved in the data analysis

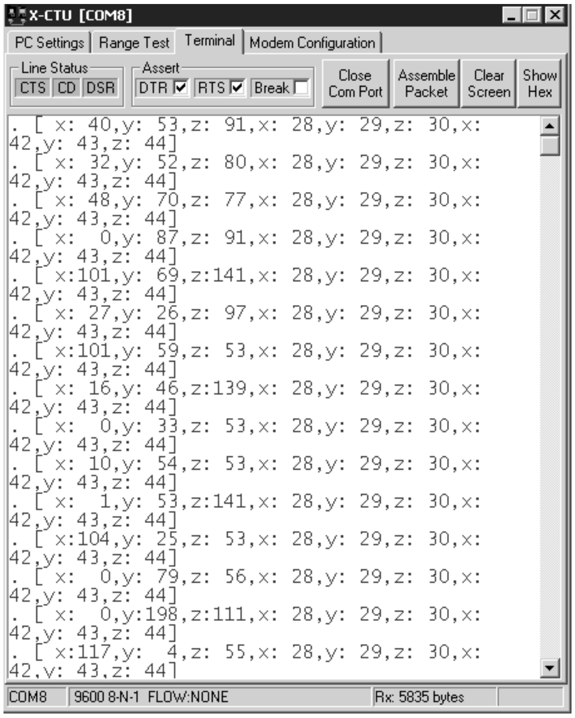

```
. [ x: 40,y: 53,z: 91,x: 28,y: 29,z: 30,x:
42,y: 43,z: 44]
. [ x: 32,y: 52,z: 80,x: 28,y: 29,z: 30,x:
42,y: 43,z: 44]
. [ x: 48,y: 70,z: 77,x: 28,y: 29,z: 30,x:
42,y: 43,z: 44]
. [ x:  0,y: 87,z: 91,x: 28,y: 29,z: 30,x:
42,y: 43,z: 44]
. [ x:101,y: 69,z:141,x: 28,y: 29,z: 30,x:
42,y: 43,z: 44]
. [ x: 27,y: 26,z: 97,x: 28,y: 29,z: 30,x:
42,y: 43,z: 44]
. [ x:101,y: 59,z: 53,x: 28,y: 29,z: 30,x:
42,y: 43,z: 44]
. [ x: 16,y: 46,z:139,x: 28,y: 29,z: 30,x:
42,y: 43,z: 44]
. [ x:  0,y: 33,z: 53,x: 28,y: 29,z: 30,x:
42,y: 43,z: 44]
. [ x: 10,y: 54,z: 53,x: 28,y: 29,z: 30,x:
42,y: 43,z: 44]
. [ x:  1,y: 53,z:141,x: 28,y: 29,z: 30,x:
42,y: 43,z: 44]
. [ x:104,y: 25,z: 53,x: 28,y: 29,z: 30,x:
42,y: 43,z: 44]
. [ x:  0,y: 79,z: 56,x: 28,y: 29,z: 30,x:
42,y: 43,z: 44]
. [ x:  0,y:198,z:111,x: 28,y: 29,z: 30,x:
42,y: 43,z: 44]
. [ x:117,y:  4,z: 55,x: 28,y: 29,z: 30,x:
42,y: 43,z: 44]
```

COM8 | 9600 8-N-1 FLOW:NONE | Rx: 5835 bytes

Figure 7: Screen shot of utility for receiving data from motion capture platform

Table 1: Motion data as a collection of time series

Time	Axis (node)					
	X (1)	Y (1)	Z (1)	X (2)	Y (2)	Z (2)
1	40	53	91	28	29	30
2	32	52	80	28	29	30
3	48	70	77	28	29	30
4	0	87	91	28	29	30
.	.	.	.	.	.	.
.	.	.	.	.	.	.
.	.	.	.	.	.	.
15	117	4	55	28	29	30

Since the underlying system could be modeled as linear or non-linear, there are also non-linear versions for all the models mentioned above (hence, NARX, NARIMA and so on).

Time domain models of time series include transfer function models and state space models. Transfer function models are very similar to regression models, with the distinction that the system transfer function, which is the relationship between the input and the output, is integrated into the model. State space models also factor in the inputs into the model, but differ from transfer function models by having two sets of equations representing each series. While the first set of equations represents the state of the system, the other set models the system output based on a number of factors.

Frequency domain models use various frequency domain techniques to model time series as series of sinusoids with noise superimposed. Although interest in frequency domain models has surged again in recent decades, time domain and autoregression models are still more popular.

Another large set of models are grouped under multivariate time series model. These are required when there are multiple time series which may have some relationship with one another. According to Palit and Popovich (2005) "*model building of multivariate time series is required when the values of one variable of an individual time series are dependent on the values of variables in other related time series*".

Since the movement data of the elbows for example would also influence that of the wrist (just like some other body coordinates would influence various other parts), it stands to reason that multivariate analysis may be the most appropriate tool to use, at least in some measure. The downside however is that multivariate series models are usually harder to develop. For this reason, other models will be tested first and multivariate analysis would be avoided unless the developed models fail to deliver satisfactory performance.

For this work, regression models have been identified as the best fit. Since the motion capture system is most easily modeled as having no exogenous inputs, X-class models, transfer function and state space models are disregarded. In addition, the system is assumed to be linear, as is the usual trend in model development. Only after linear models fail are systems modeled as non-linear. Finally, univariate analysis is adopted (assuming that there are different independent streams of data because the possible gains in accuracy would probably not be worth the added complexity of multivariate analysis.

The specific model class being adopted and tested is the ARMA model. The ARMA model is a combination of the AR and MA models.

For the AR model (mathematical development motivated by Palit and Popovich , 2005),

$$\phi(B)\tilde{Z}_t = a_r \qquad (3)$$

Where $\tilde{Z}_t$represents deviations from the mean, a_r is a white noise component, and the autoregression operator, $\phi(B)$ is defined as

$$\phi(B) = 1 - \phi_1 B - \phi_2 B^2 - \phi_3 B^3 - \cdots - \phi_p B^p \qquad (4)$$

μ, $\phi_1, \phi_2, \phi_3, \ldots, \phi_a, \sigma_a^2$ are unknown parameters to be identified from collected data.

In moving average models,

$$\tilde{Z}_t = \Theta(B) a_t \qquad (5)$$

where the moving average operator, $\Theta(B)$, is defined as $\Theta(B) = 1 - \Theta_1 B - \Theta_2 B^2 - \Theta_3 B^3 - \cdots - \Theta_q B^q$ (6)

and again, the parameters μ, $\Theta_1, \Theta_2, \Theta_3, \ldots, \Theta_a, \sigma_a^2$ are to be estimated from collected data.

Combining eq [3] and [5] to form an ARMA model yields

$$\tilde{Z}_t = \phi_1 \tilde{Z}_{t-1} + \phi_2 \tilde{Z}_{t-2} + \ldots + \phi_p \tilde{Z}_{t-p} + a_t - \theta_1 a_{t-1} - \theta_2 a_{t-2} - \ldots - \theta_q a_{t-q}.$$

Which can be rearranged as

$$\tilde{Z}_t - \phi_1 \tilde{Z}_{t-1} - \phi_2 \tilde{Z}_{t-2} - \ldots - \phi_p \tilde{Z}_{t-p} = a_t - \theta_1 a_{t-1} - \theta_2 a_{t-2} - \ldots - \theta_q a_{t-q}$$

Subsequently,

$$(1 - \phi_1 B - \phi_2 B^2 - \ldots - \phi_p B^p)\tilde{Z}_t = (1 - \theta_1 B - \theta\ B^2 - \ldots - \theta_q B^q) a_t$$

To arrive at the standard form:

$$\phi(B)\tilde{Z}_t = \theta(B) a_t \qquad (7)$$

where B is the delay operator. This model contains (p+Q+2) unknown parameters and the process of developing time series models from motion capture data would simply consist of determining these parameters for each subject.

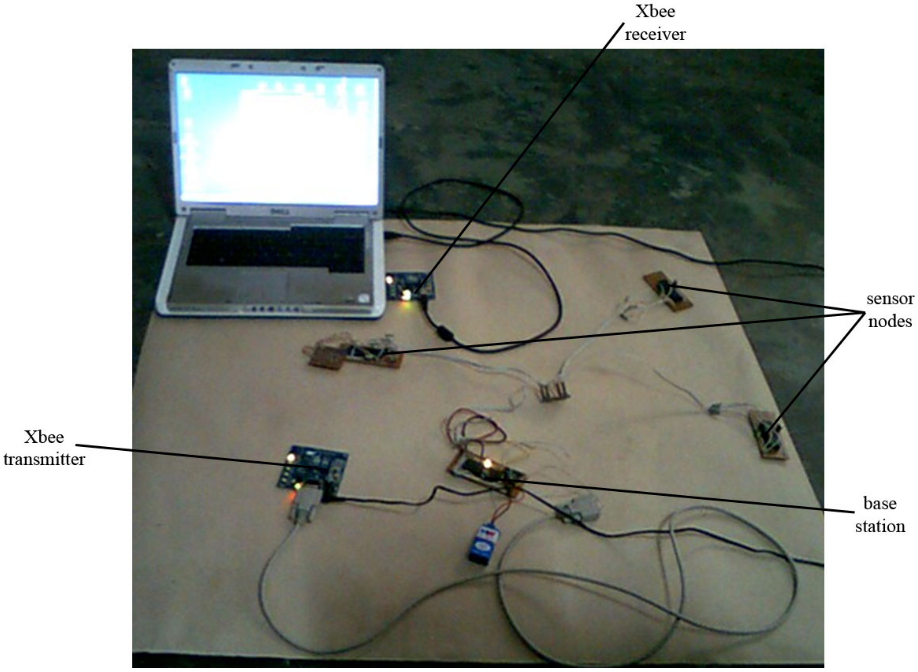

Figure 8: Prototype implementation of the EEE-OAU09 motion capture system featuring three sensor nodes

7. TESTING AND RESULTS

The prototype consisting of three slaves and the master was tested. Figure 8 shows the prototype setup. It was tested by powering up the sensor network using a 9V battery, the Xbee transmitter was powered using the adapter provided while the Xbee receiver is powered through the USB connection it has with the PC.

The sensors were tested by observing the numerical readings on the PC screen when the sensors are moved in various directions and with varying speeds. It was observed offset nulling was not able to completely remove accelerometer offset. Finite (although small) readings were obtained when the sensors were stationary. The effect of noise was also observed, as reading changed often rapidly when the sensors were kept stationary.

The Xbee module worked as expected with good reception at the receiving end as distances in excess of 10m.

One important consideration in developing instrumentation devices for human subjects is the health implications of the system. The EEE-OAU09 platform is completely non-invasive and the radiation generated by the IEEE 802.15.4 transceivers is very much within standards.

Observation of numerical data obtained from the prototype has suggested that with a calibration step implemented in software (say a lookup table), the process of transforming human body motion into statistical data can be done to a high degree of accuracy

The need for a better implementation of software offset-nulling and further noise reduction measures are the most important points being looked at. Although the general class of models has been picked, detailed model generation and data analysis proper was not carried out on this prototype. That will be done when the final version is ready

8. CONCLUSION

A platform for motion capture using MEMs accelerometers has been described. The platform has ten MMA7260QT whose analog outputs are converted to digital form and transmitted to a central base station using I2C. The base station then transfers the data to a computer using IEEE 802.15.4. Data on the computer can then be analyzed using any suitable technique. For this work, motion capture data are modeled such that human movement is seen as an ARMA system. The platform has been tested and the results so far have been positive.

During course of work, a new soldering technique was developed. The new technique can be used in places where sophisticated soldering stations are not available.

REFERENCES

Akker-Scheek I.,Stevens M., Bulstra S.K., Groothoff J.W., Horn J.R., and Zijlstra W. (2007): "Recovery of gait after short-stay total hip Arthroplasty". Arch Phys Medical Rehabilitation. No 88:pp 361–367.

Buriamoh-Igbo, L.A., Olaogun, M.O.B., Jubril, A.M. (1997): "Measurement of ground-foot reaction force to determine gait asymmetry using a computer-based telemetry system", *Journal of Rehabilitation Research and Development*, vol. 34, no. 2, pp 53-55.

Churchill A.J., Halligan P.W., and Wade D.T. (2002): "A Simple Video-based Kinematic Analysis for Clinical Disorders of Gait". *Computer Methods Programs Biomed*. 69:197–209.

Fox S.H., Chuang R., and Brotchie J.M. (2009): "Serotonin and Parkinson's disease: on movement, mood, and madness. *Movement Disorders*, Vol. 24, No. 9, 2009, pp. 1255–1266

Griffin, M., Olney, S., and McBride, I. (1995)" "Role of asymmetry in gait performance of stroke subjects with hemiplegia". *Gait Posture* 1995(3): 132–142.

Hansen A.H., Childress D.S. and Meier M.R. (2002): "A Simple Method for Determination of Gait Events". *Jour. Biomech*.35: 135–138.

Liberson W.T., Holmquest H.J., Scott D., Dow A., (1961): "Functional Electrotherapy: stimulation of the peroneal nerve synchronized with the swing phase of the gait of hemiplegic patients", *Arch. Phys. Med. Rehab*. 42, 101-105.

Menz H.B., and Lord S.R. (2005): "Gait Instability in older people with Hallux Valgus". *Foot & Ankle International*, Vol. 26, No. 6.

Moore S.T., MacDouglas H.G., Gracies J.M., Cohen H.S. and Ondo W.G. (2007), "Long-term monitoring of gait in Parkinson's disease". *Gait Posture* ; 26:200–7.

Palit, A.K. and Popovic, D. (2005): Computational Intelligence in Time Series Forecasting: Theory and Engineering Applications. Springer-Verlag limited, London.

Petrofsky J., Macnider M., Navarro E., and Lee S. (2005): "Motor Control and Gait Characteristics in people with Type 1 and Type 2 Diabetes without sensory impairment in the foot". *Basic Applied Myol.*, 15 (2): 75-86.

Riker RR, Fraser GL, Richen P. (1997): "Movement disorders associated with withdrawal from high-dose intravenous haloperidol therapy in delirious ICU patients". *Chest* 1997;111: pp 1778–1781.

Zhang K., Gorijan A. and Lester K.D. (2006) "Gait change after local anesthetic of chronically arthritic knee". *Journal of Long-Term Effects of Medical Implants.* 16(3):223–234 (2006)